UNIVERSITÀ DI PARMA

UNIVERSITÀ DEGLI STUDI DI PARMA

DOTTORATO DI RICERCA IN
SCIENZE DEL FARMACO, DELLE BIOMOLECOLE E DEI PRODOTTI PER LA SALUTE

CICLO XXXI

Nasal powders for delivery of disease modifying agents in early treatment of Alzheimer's disease: formulation and characterization

Coordinatore:
Chiar.mo Prof. Marco Mor

Tutore:
Chiar.mo Prof. Gaia Colombo

Dottorando: Laura Tiozzo Fasiolo

Anni 2015/2018

INDEX

CHAPTER 1 – INTRODUCTION Pag. 6

1.1 NASAL DRUG DELIVERY 6

1.1.1 Anatomy and physiology of the nasal cavity 6

1.1.2 Relevant factors for nasal deposition of the formulation, drug absorption and clearance 11

1.1.3 Commercial nasal drug products 13

1.1.4 Nasal powders 15

1.1.4.1 Manufacturing methods 21

1.1.4.2 Delivery devices for powder insufflation 27

1.2 ALZHEIMER'S DISEASE 31

1.2.1 Neuroinflammation 33

1.2.1.1 Flurbiprofen 35

1.2.2 Impairment in brain responsiveness to insulin 37

1.2.3 Combination therapy 44

AIM OF THE RESEARCH 46

CHAPTER 2 – DESIGN, CONSTRUCTION AND CHARACTERIZATION OF FLURBIPROFEN NASAL POWDERS 47

2.1 MATERIALS AND EQUIPMENT 48

2.2 METHODS 48

2.2.1 HPLC-UV method for flurbiprofen determination 48

2.2.2 Particle and agglomerate manufacturing 49

2.2.3 Physico-chemical characterization of spray-dried microparticles and agglomerates 53

2.2.4 Biopharmaceutical characterization of spray-dried microparticles and agglomerates 55

2.2.5 Data analysis 57

2.3 RESULTS AND DISCUSSION **57**
2.3.1 Spray-dried flurbiprofen microparticles 58
2.3.1.1 Manufacturing: yield, size, morphology and drug content 58
2.3.1.2 Microparticle physical state characteristics 65
2.3.1.3 Biopharmaceutical characterization of flurbiprofen microparticles 69
2.3.2 Agglomerates of spray-dried microparticle powders 75
2.3.2.1 Manufacturing: yield and drug content 75
2.3.2.2 *In vitro* flurbiprofen dissolution and *ex vivo* transport across nasal mucosa from agglomerates 84
2.4 CONCLUSIONS 85

CHAPTER 3 – *IN VIVO* ADMINISTRATION OF FLURBIPROFEN POWDERS 87
3.1 MATERIALS AND EQUIPMENT **88**
3.2 METHODS **88**
3.2.1 Preparation of flurbiprofen formulations for nasal administration 88
3.2.1.1 Flurbiprofen aqueous solution 88
3.2.1.2 Flurbiprofen nasal powders 88
3.2.2 *In vivo* experiments 89
3.2.3 Extraction of flurbiprofen from serum and brain samples 91
3.2.4 HPLC-FLD method for flurbiprofen determination 93
3.2.5 Non-compartmental PK analysis 94
3.2.6 Data analysis 95
3.3 RESULTS AND DISCUSSION **96**
3.3.1 Nasal drug powders manufacturing and combination with the insufflator device 96
3.3.2 Flurbiprofen serum pharmacokinetic 99
3.3.3 Flurbiprofen brain levels 101
3.3.4 Nose-to-brain drug delivery 103
3.4 CONCLUSIONS 106

CHAPTER 4- *IN VITRO* AND *EX VIVO* STUDY OF AN INSULIN NASAL POWDER 108

4.1 MATERIALS AND EQUIPMENT 109

4.2 METHODS 109

4.2.1 HPLC-UV method for insulin determination 109

4.2.2 Preparation of insulin spray-dried microparticles 110

4.2.3 Physico-chemical characterization of the insulin spray-dried microparticles 110

4.2.4 Biopharmaceutical characterization of insulin spray-dried microparticles 111

4.2.5 Data analysis 112

4.3 RESULTS AND DISCUSSION 112

4.3.1 Physico-chemical characteristics of insulin spray-dried microparticles 112

4.3.2 Biopharmaceutical characteristics of insulin spray-dried microparticles 114

4.4 CONCLUSIONS 119

CHAPTER 5 - COMBINATION OF FLURBIPROFEN AND INSULIN MICROPARTICULATE POWDERS FOR NASAL DELIVERY 120

5.1 MATERIALS AND EQUIPMENT 122

5.2 METHODS 122

5.2.1 HPLC-UV method for insulin and flurbiprofen determination 122

5.2.2 *In vitro* study of insulin and flurbiprofen compatibility 123

5.2.3 *Ex vivo* transport of insulin and flurbiprofen across rabbit nasal mucosa 124

5.2.4 Manufacturing of agglomerates of flurbiprofen and insulin spray-dried microparticles with excipients spray-dried microparticles 125

5.2.4 Data analysis 125

5.3 RESULTS AND DISCUSSION 125

5.3.1 Chemical stability of insulin in the presence of flurbiprofen 125
5.3.2 *Ex vivo* drug transport across rabbit nasal mucosa 130
5.3.3 Agglomerates of insulin and flurbiprofen spray-dried microparticles 134
5.4 CONCLUSIONS 135

FINAL CONCLUSIONS **136**

BIBLIOGRAPHY **138**

LIST OF THE ABBREVIATIONS AND CODES

Abbreviation	Meaning
AD	Alzheimer's Disease
API	Active Pharmaceutical Ingredient
AUC	Area under the concentration
BBB	Blood Brain Barrier
CNS	Central Nervous System
COX	Cyclooxygenase
CSF	Cerebrospinal Fluid
DSC	Differential Scanning Calorimetry
DTE	Drug Targeting Efficiency
DTP	Direct Transport Percentage
Et	Ethanol
FB-COOH	Flurbiprofen acid
FB-COONa	Sodium flurbiprofen
HPLC	High Performance Liquid Chromatography
i.n.	Intranasal
iPr	Isopropanol
i.v.	Intravenous
ML	Mannitol/Lecithin
NSAIDs	Non-steroidal anti-inflammatory drugs
PBS	Phosphate Buffered Saline
PXRD	Powder X-ray Diffraction
rT	Retention time
SD	Spray dryer
SEM	Scanning Electron Microscopy
SEM	Standard Error of the Mean

CHAPTER 1 - INTRODUCTION

1.1 NASAL DRUG DELIVERY

The currently available drug treatments and most of those under clinical study for brain disorders exploit the systemic (oral and parenteral) route of administration. This could reduce the efficacy of the therapy, especially because it limits the access of the active molecule to the central nervous system (CNS) from the blood. Extensive research claims that the intranasal route (i.n.) for drug delivery to the brain could overcome the limitations of systemic drug delivery, offering at the same time advantages in terms of effect onset or non-invasiveness (Illum et al., 2002; Chapman et al., 2013; Hirlekar and Momin, 2018; Sood et al., 2014; Sonvico et al., 2018). Currently, the challenges in nasal drug delivery (e.g., rapid drug clearance from the nasal cavity and low drug transport across the nasal barriers) have made this route of administration envisaged mainly for potent drugs (Fortuna et al., 2014; Illum, 2002; Pires and Santos, 2018; Ugwoke et al., 2005). The knowledge of the nasal anatomy and physiology is therefore necessary to understand how the nasal route may be exploited for the brain-targeting. Then, in the development of the nasal preparation, the drug formulation and its combination with a nasal device must be studied together, to address both the efficacy of the therapy and acceptability by the patient (Dalpiaz and Pavan, 2018).

1.1.1 Anatomy and physiology of the nasal cavity

The nasal cavity is the upper respiratory structure that filters, humidifies and warms the air before it reaches to the lower airways. Moreover, olfaction starts exactly inside the nasal cavity. In humans it is symmetrically divided by the septum into two cavities extending approximately 12-14 cm in length from the nostril to the nasopharynx, having a volume of 15-20 cm^3 and a total surface area of approximately 150-180 cm^2 due to the three bony structures called *turbinates*. Both cavities are anatomically and histologically characterized by four different areas: the nasal vestibule, atrium, respiratory region and olfactory area (Dhakar et al., 2011; Lochhead and Thorne, 2012; Pires et al., 2009).

The **respiratory region** comprises 80-90% of total surface in humans (approximately 130 cm^2) (Pires et al., 2009). It is covered by a pseudo-stratified secretory epithelium. Small extensions, known as *microvilli*, stand on the apical surface of the epithelial cells

enlarging the respiratory surface, while other fine projections called *cilia* are essential to transport the nasal secretion - the mucus - toward the nasopharynx, where it is either swallowed or expectorated (mucociliary clearance). The nasal mucus moves through the nose at an approximate rate of 8 mm/min and is removed every 15-20 minutes. It is 5 μm thick and consists mostly of water (95%), mucine glycoproteins (2.5-3%), electrolytes (2%) and small amounts of proteins, lipids, enzymes, antibodies, sloughed epithelial cells and bacterial products (Ozsoy et al., 2009). The mucus' pH ranges between 5.5 and 7.5 and is physiologically indispensable for the humidification and warming of the inhaled air, and for the physical and enzymatic protection of the nasal epithelium against pathogens (Colombo et al., 2015; Dhakar et al., 2011; England et al., 1999; Lochhead and Thorne, 2012; Pires et al., 2009).

Below the nasal respiratory epithelium there is the *lamina propria* where nerves, glands and immune cells are located. The nasal respiratory epithelium is innervated by branches of trigeminal nerve, whose axons are directed into the brainstem at the level of the pons, where they finally synapse with neurons in the brainstem area. Fibers of trigeminal nerve convey chemosensory, nociceptive, temperature and tactile information. The nasal respiratory mucosa is richly supplied with blood vessels, mainly branches of the ophthalmic, maxillary and facial arteries. Drainage from nasal cavity occurs preferentially via the jugular vein, which is accompanied by other minor veins. Nasal capillaries are fenestrated with porous basal membranes (Lochhead and Thorne, 2012; Ugwoke et al., 2001).

The **olfactory region** comprises less than 10% of total the surface of the nasal epithelium in humans (<15 cm^2) (Pires et al., 2009). It is located in the roof of the nasal cavity and extends a short way down the septum and lateral wall. The olfactory epithelium is pseudo-stratified and contains specialized cells involved in smell perception. These cells are bipolar neurons having odorant responsive receptors in the plasma membrane of their olfactory cilia and unmyelinated axons converging into bundles, called *fila olfactoria*, enclosed by ensheathing cells (Lochhead and Thorne, 2012). These glial cells have a particular structural arrangement around the neurons enabling regeneration, regrowth or remyelination of neuronal axons in the olfactory bulb both for natural turnover and after injury (Field and Raisman, 2003; Dhuria et al., 2010). Ensheathing cells are further enclosed by olfactory nerve fibroblasts. All together, olfactory sensory neurons, glial cells and fibroblasts constitute the olfactory nerve that projects directly the olfactory bulb into the brain without the "filter" of the

blood brain barrier (BBB) (Dhuria et al., 2010; Djupesland, 2013; Chaturvedi et al., 2011; Illum, 2003 and 2002; Lochhead and Thorne, 2012).

Pathways for nasal transport

Thinking about drug administration via the nose, the respiratory region is suitable for systemic drug absorption due to the thin epithelium, large surface area (i.e., presence of *microvilli*) and rich vascularization (Fig. 1.1A). Drugs deposited in the nasal cavity may be disperse/dissolve in the nasal mucus and cross the nasal epithelium *via* intracellular and extracellular pathways. In addition, the innervation of the respiratory and the olfactory region by trigeminal and olfactory nerve, respectively, is interesting for targeting the brain since the drug can be transported along the nerve into the CNS bypassing the BBB (Fig. 1.1B-E) (Agrawal et al., 2018).

The **intracellular pathway** across the respiratory epithelium includes the endocytosis into peripheral trigeminal nerve processes located near the epithelium surface and following intracellular transport to the brainstem. A second possibility is the transcytosis across the epithelial cells to the *lamina propria*. The intracellular pathway across the olfactory epithelium includes the endocytosis into the olfactory sensory neurons and subsequent intraneuronal transport to the olfactory bulb, and the transcytosis across sustentacular cells to the *lamina propria*. Intracellular pathways are generally reserved to small lipophilic drugs: either passive diffusion, receptor/carrier-mediated or vesicular mechanisms can occur, based on the specific drug properties. The **extracellular pathway** is a paracellular diffusion movement across either the olfactory or the respiratory epithelia to the underlying lamina propria. Tight junctions between nasal epithelia cells usually hinder the molecule's paracellular permeability. Thus, the paracellular route is exploited by water soluble compounds with low molecular weight (<1000 Da). Indeed, the main way of transport for peptides and proteins is the endocytosis through the respiratory or olfactory epithelium (Jadhav et al., 2007; Lochhead and Thorne, 2012).

Active compounds crossing the nasal epithelium until the lamina propria may enter into the systemic circulation, through which they reach the BBB. The passage depends on both physiological factors and drug characteristics. Cerebral blood flow, influx and efflux transporters, binding to plasma proteins, elimination from the circulation, sequestration within the BBB, are some examples of the first (Banks, 2009). In addition, disease-related alterations of the BBB can occur, impacting on drug passage.

Concerning the drug molecule, molecular weight and lipophilicity are the major determinants in case of passive diffusion. In addition, the drug chemical structure determines the affinity toward active transporters of the BBB, enabling carrier-mediated transport (Pardridge, 2012). Several drugs (e.g. levodopa, gabapentin, etc.) and also peptides are reported to cross the BBB by active transporters in the barrier. However, these transporters are saturable and sensitive to a number of different factors, potentially limiting the brain availability of the compounds (Banks et al., 2009). Concerning drug transport to the CNS, more commonly the olfactory and trigeminal pathways allow for the direct passage from the nose to the brain. In the case of the olfactory pathway, drugs are transported intracellularly (inside the olfactory neurons or the epithelial supporting cells) and/or extracellularly (first in the open intercellular cleft of the epithelium, then in the perineural space of the lamina propria and beyond), heading to the olfactory bulb. Once inside the brain the active molecules distribute to their target regions via either extra- or intraneuronal pathways (Fig. 1.1D) (Agrawal et al., 2018; Hallschmid et al., 2008; Meredith et al., 2015)

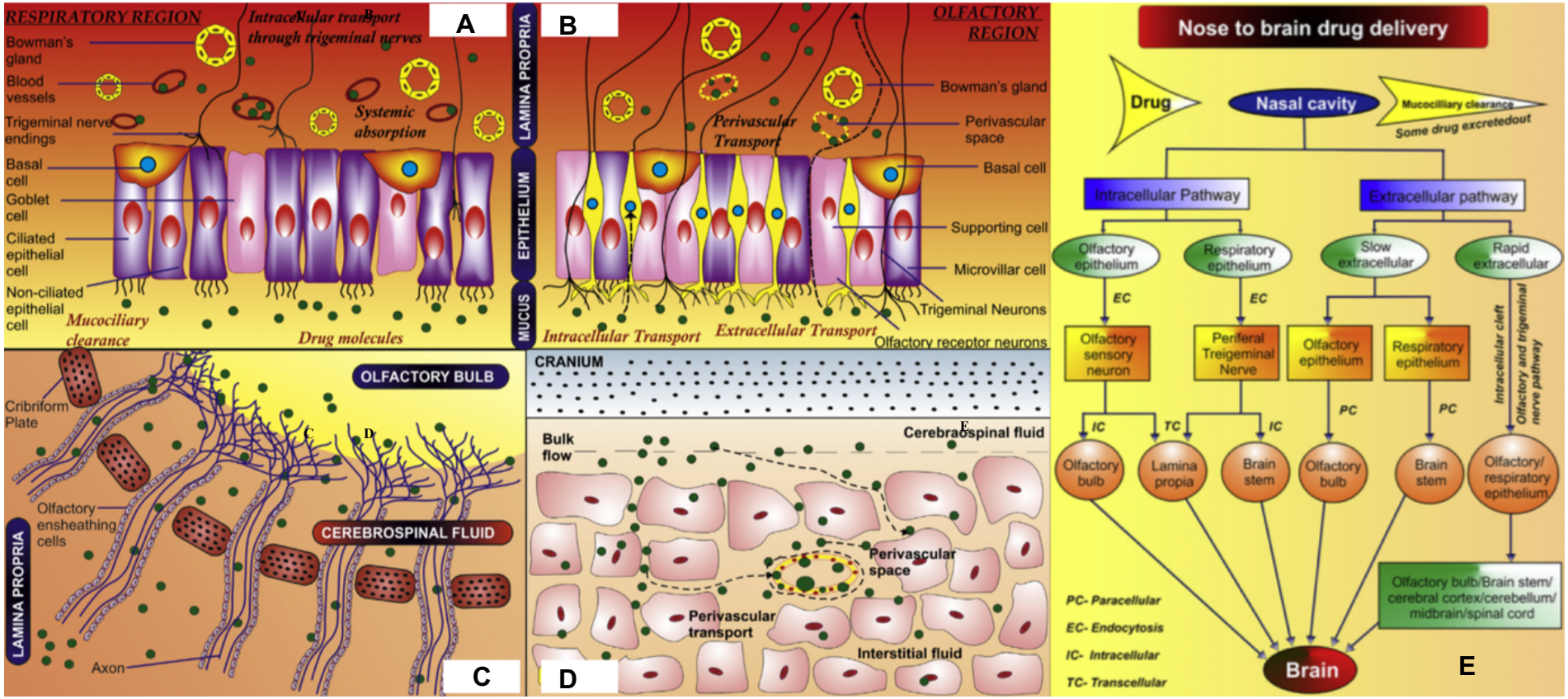

Figure 1.1. *Left: Nasal histology and pathways of intranasal drug transport to the brain. (A) Respiratory region, mucociliary clearance, systemic absorption and trigeminal nerve transport. (B) Olfactory region and drug transport pathways. (C) Drug transfer from the lamina propria to the cerebrospinal fluid and olfactory bulb via olfactory nerve pathway. (D) Distribution of drug throughout the cerebrospinal fluid and brain region. Right: (E) Summary of cellular transport mechanisms in drug delivery from the nasal cavity to the brain (reproduced with permission from Agrawal et al., 2018).*

1.1.2 Relevant factors for nasal deposition of the formulation, drug absorption and clearance

The anatomical and physiological features of the nasal cavity make the i.n. drug administration attractive. However, the design, construction and development of the nasal product faces a number of challenges to attain successful therapeutic outcome (Agrawal et al., 2018; Fortuna et al., 2014; Jadhav et al., 2007; Pardeshi et al., 2013; Ugwoke et al., 2001). Such challenges exist both for systemic drug delivery and direct nose-to-brain transport, and may be more difficult to be overcome in the latter case. In particular, they are:

(1) the **deposition** of the formulation on the nasal epithelium.

Drug deposition and distribution inside the nasal cavity is key to elicit the intended effect, local or systemic. If deposition does not occur at all or occurs elsewhere, the drug bioavailability will be modified. The deposition site determines the subsequent drug passage across the nasal barriers:

- if the formulation is deposited into the anterior region of the nasal cavity, the drug tends to enter into the systemic circulation;
- if the formulation is deposited into the posterior and upper region of the nasal cavity, the drug is absorbed to the olfactory region and directed to the brain (Scheibe et al., 2008).

The technique of nasal administration contributes to the efficient drug deposition. For example, the supine position of the subject with head angle at 70° or 90° seems to enhance the olfactory deposition of the drug dose (Dhuria et al., 2010). In addition, the mechanism of function and technical characteristics of the device (e.g., tip dimensions, depth of insertion of the tip inside the nose, actuation pressure, etc.), the type and properties of the drug formulation and the amount of formulation administered, are fundamental to confront the resistance to the airflow provided by the nasal mucosa and secretions, eventually affecting the deposition pattern of the drug inside the nasal cavity (Djupesland et al., 2006; Dong et al., 2018). For example, in liquid products a delivery volume of 0.2-0.4 ml administered in 100 µl aliquots may favor the drug deposition in the olfactory area (Hirlekar and Momin, 2018). Finally, a suitable combination between the delivery device and the nasal formulation may contribute to place the drug in the appropriate region in nasal cavity, allowing the drug to be address its therapeutic target (Pardeshi et al., 2013; Agrawal et al., 2018).

(2) the **passage** of the drug across the nasal barriers.

As illustrated in Fig. 1.2, the nasal drug passage across the nasal barrier depends on both the drug and the formulation, not disregarding the anatomical and functional features of the nasal structures. Concerning the nasal formulation, the pH and osmolarity of the liquid forms and their viscosity impact on drug absorption. pH affects the solubility of ionizable drugs as well as the formulation's tolerability. Viscosity can favor the retention of the formulation in the nasal cavity, also considering the mucociliary clearance. For suspensions and powders, the drug dissolution rate in the mucus is another variable to consider. Thus, the choice of the drug dosage form is determinant for absorption, also as a function of the excipients (Jadhav et al., 2007). As soon as the drug molecules are available for absorption, generally, lipophilic compounds are easily allowed to penetrate the tissue *via* transcellular pathway compared to hydrophilic ones. In fact, they can partition within the cell membrane and cross the cytoplasm. Non-ionized species are facilitated compared to ionized species because they are more lipophilic. The hydrophilic molecules pass through the aqueous pores in between the epithelial cells (paracellular pathway). This pathway is available to low molecular weight drugs (<1000 Da). There are other physiological factors affecting the drug passage across nasal barriers. For example, enzymes like cytochrome P450 monooxygenases and carboxylesterases in the olfactory mucosa, metabolize and inactivate the drug deposited in this region, reducing the amount of drug available for entering the brain (Hirlekar and Momin, 2018).

Moreover, multidrug resistance proteins and multidrug resistance-associated proteins efflux transporters are localized both in the respiratory and in the olfactory mucosae. Wioland et al. (2000) reported that the P-glycoprotein efflux transporter and the multi-resistance associated protein 1 and 2 are expressed in the epithelium and nasal glands of the human nasal respiratory mucosa, while Graff and Pollack (2003; 2005) reported that presence of P-glycoprotein in the murine olfactory mucosa. Kandimalla and Donovan (2005b) demonstrated by immunohistochemistry that the expression of P-glycoprotein is higher in the olfactory epithelium compared to the respiratory epithelium. Such efflux proteins hinder the access of drugs into the blood circulation and their brain uptake after i.n. administration (Oliveira et al., 2016). For example, Kandimalla and Donovan (2005a and b) showed that etoposide, chlorpheniramine and chlorcyclizine were effluxed by P-glycoprotein from the bovine nasal mucosa *ex vivo* and the efflux was higher in the olfactory compared to the respiratory epithelium. Conversely, [^{3}H]-verapamil distribution into the brain after i.n. administration to mice

was enhanced when rifampin, a P-glycoprotein efflux inhibitor, was administered i.n. with the drug (Graff and Pollack, 2005).

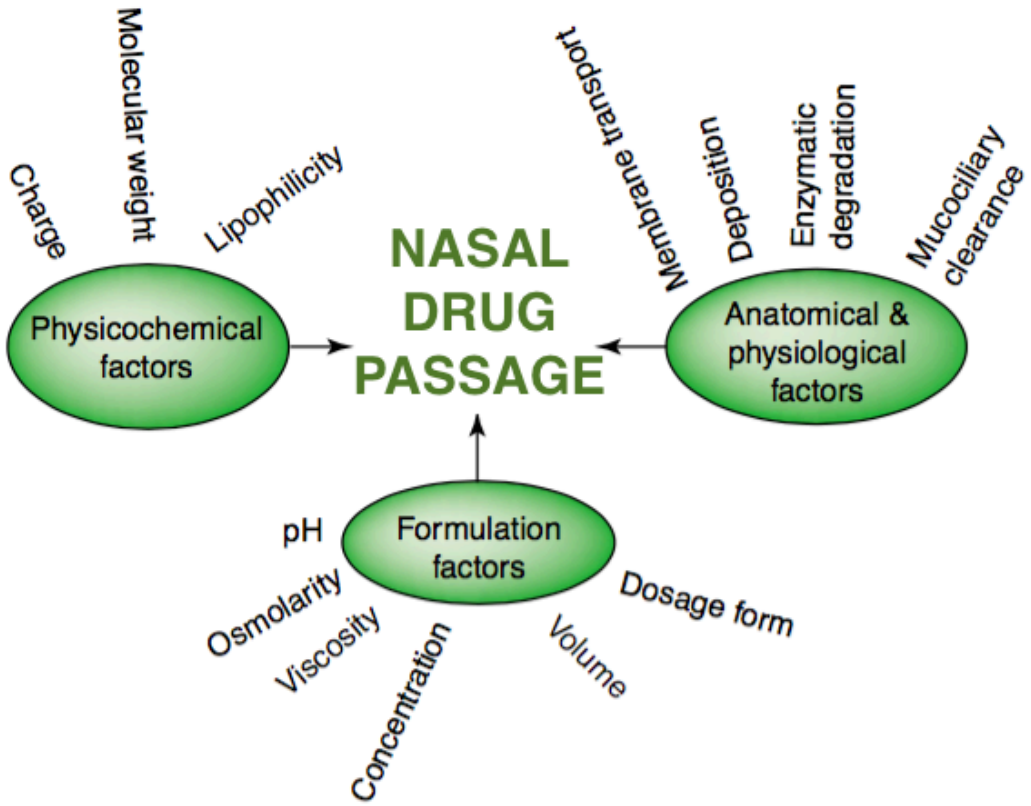

Figure 1.2. *Factors affecting drug passage across nasal barriers (adapted with permission from Illum et al., 2002).*

(3) the **clearance** of the formulation from the nasal cavity.

The mucociliary clearance removes the drug rapidly from the site of deposition/absorption. In particular, if the formulation is deposited to the floor of the nasal cavity, it is prone to a more rapid elimination by this defense mechanism (Agrawal et al., 2018). Hence, the site of deposition requires to be controlled by means of the combination "formulation-device", while the type of formulation and excipients should favor the longest possible retention of the drug inside the nasal cavity against the physiological clearance mechanisms.

1.1.3 Commercial nasal drug products

When it comes to nasal drug formulation, product design generally focuses on simple formulation strategies and convenience of the delivery system. Nasal preparations can

be liquids (solutions, suspensions and emulsions) or solids, like powders. Nasal drugs can be also formulated as micro- and nanoparticulate delivery systems, which can be presented as liquid or solid preparations. The majority of nasal products, both under research level and on the market, are liquids administered by spray or drops, independently of the therapeutic indication and population age. Nasal liquid sprays have been used for the administration of small and large molecules (including peptides, proteins and vaccines) and different therapeutic indications. A non exhaustive list of commercial liquid sprays for systemic action (including a vaccine) is the following (Sonvico et al., 2018):

- FluMist® Quadrivalent (Astra Zeneca, Wilmington DE, USA), live attenuated influenza vaccine;
- Fortical® (Upsher-Smith, Maple Grove MN, USA), salmon calcitonin for postmenopausal osteoporosis;
- Imigran® (GSK, Brentford, UK), sumatriptan for migraine;
- Intstanyl® (Takeda, Japan and Pecfent/Lazanda®, Archimedes Pharma Ltd., Reading, UK), fentanyl for pain management;
- Nicotrol® NS (Pfizer, New York City, NY, USA), nicotine for smoke cessation;
- Suprecur® (Sanofi-Aventis, Paris, France), buserelin for prostate cancer;
- Synarel® (Pfizer, New York City, NY, USA), nafarelin for endometriosis.

Regarding nasal powders, the only approved product for systemic action is Onzetra® Xsail® (Avanir Pharmaceuticals Inc., Aliso Viejo, CA, USA), containing sumatriptan for migraine (approved by the Food and Drug Administration, FDA, in January 2016). In Europe, Rhinocort® Turbuhaler® (budesonide, AstraZeneca, London, UK) is marketed for topical treatment of seasonal and perennial allergic and vasomotor rhinitis and of nasal polyps. Other two locally-acting products, Rhinocort® Teijin (beclomethasone dipropionate, Teijin, Tokyo, Japan) and Erizas® (dexamethasone cipecilate, Nippon Shnyaku, Kyoto, Japan), are commercially available in Japan (Tiozzo Fasiolo et al., 2018).

Chemical and microbiological instability, the relatively high formulation's volume required to ensure the drug dosage and the rapid clearance from the nasal cavity are significant drawbacks of nasal liquids. When it comes to peptide and protein delivery, nasal liquid formulations need additives and stabilizing agents, and proper storage conditions to assure the intended shelf life. Moreover, when administered in solution,

the absorption of some drugs across the nasal barrier was demonstrated low and variable, with bioavailability not exceeding 10% for small molecular weight drugs such as alniditan and morphine, and <1% for peptides such as insulin and leuprolide (Illum et al., 2002; Costantino et al., 2007; Dong et al., 2018; Ozsoy et al., 2009). Djupesland et al., 2014 report that in general the drug reaching the brain through the nose-to-brain transport is <1% of the administered dose and even as low as 0.1% or less.

It is known that solid dosage forms, which for i.n. administration are mainly represented by powders, are more stable than liquids. Formulation-wise, powders denote a simpler composition in excipients (if any) (Buttini et al., 2012), even though one has to use a dedicated manufacturing process such as spray drying, for example. They allow for the administration of larger drug doses and also facilitate the formulation of poorly water-soluble compounds (Pozzoli et al., 2016; Tiozzo Fasiolo et al., 2018; Vasa et al., 2015). Moreover, nasal powder dosage forms can enhance drug diffusion and absorption across the mucosa, thus improving drug bioavailability at the site of action compared to liquids (Vasa et al., 2017). Focusing on nose-to-brain transport, the effective brain delivery of the drug by nasal powders depends on the characteristics of both the drug formulation and the device. Formulation aspects include size, shape, density, dissolution, wettability, aerodynamic diameter and surface properties of drug particles, while the device is crucial for determining the deposition of the formulation in the olfactory region of the nasal cavity, the local drug concentration and residence at the site of deposition (Dong et al., 2018).

1.1.4 Nasal powders

Although defined in the European Pharmacopoeia (Ph. Eur, 9th Ed.) as “powders for insufflation into the nasal cavity by means of a suitable device”, nasal powders comprise a number of dosage forms spacing from the pure active pharmaceutical ingredient (API) raw material to microparticulate powders, where the API can be formulated alone or with excipients (Colombo et al., 2016; Dalpiaz et al., 2015; Gavini et al., 2006). Moreover, both the raw material and microparticulate powders can be the building blocks to produce new structures, named soft or chimera agglomerates (Balducci et al., 2013).

It is noteworthy that composition and manufacturing method influence the structure and fundamental properties of the powder’s particles. The combination of the fundamental properties of a powder, i.e., particle size and shape, then determines the

powder derived properties: packing, apparent density, and flow. Fine tuning of fundamental and derived properties of a powder is required as they impact on the manufacturing process and biopharmaceutical behavior of the finished nasal product, ultimately determining the therapeutic outcome (Fig. 1.3).

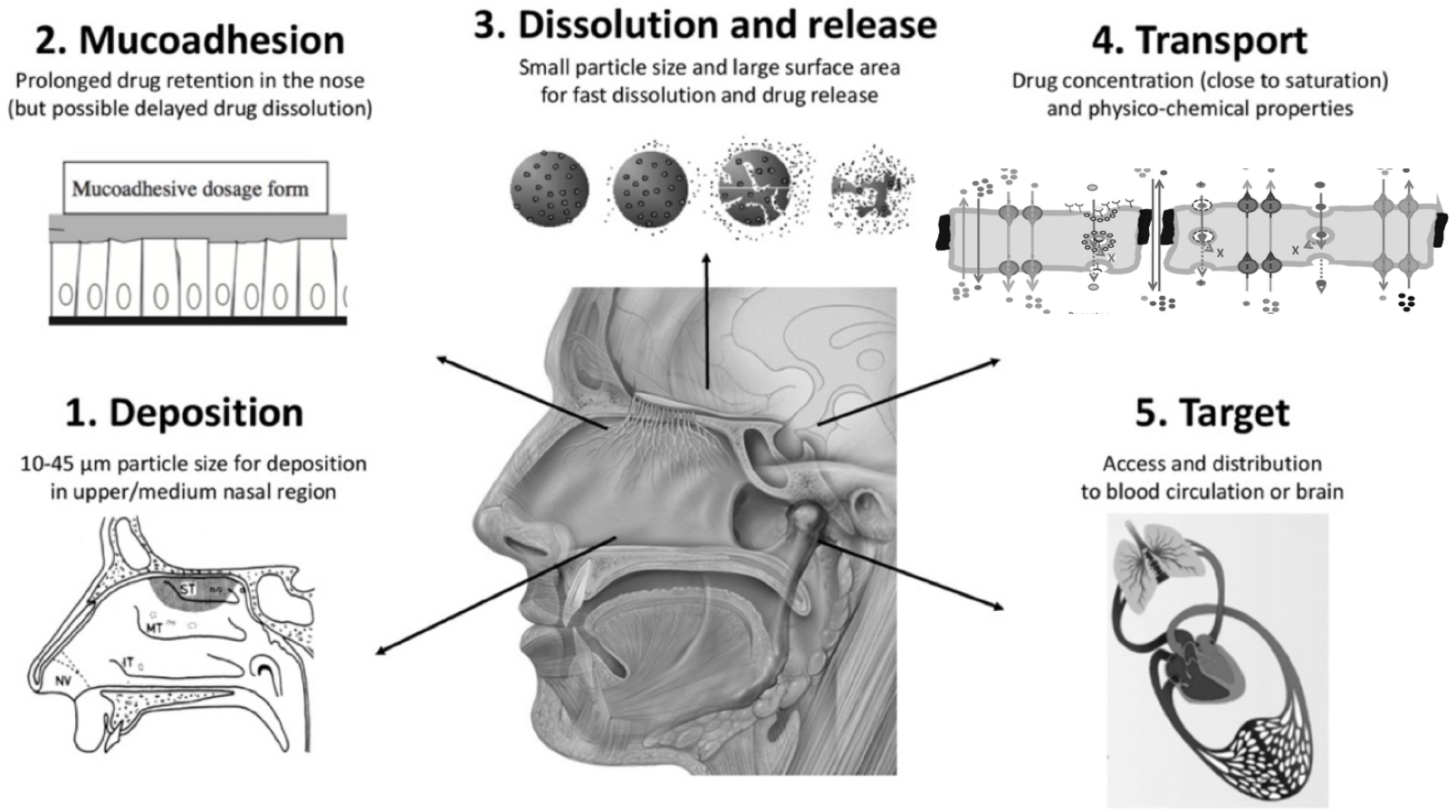

Figure 1.3. *Biopharmaceutics of nasal powders, from insufflation to effect. The therapeutic outcome depends sequentially on steps (1) to (5). Steps 1-3 are influenced by the powder properties. Steps 4 and 5 involve drug molecules with their characteristics of lipophilicity, ionization, molecular weight, etc. (Adapted with permission from Tiozzo Fasiolo et al., 2018; Smart, 2005; De Lange, 2014; Agrawal et al., 2018*).

API raw material

In most cases, the API raw material in powder form cannot be proposed as a solid nasal dosage form *per se*. One reason is that the micromeritics of the unprocessed solid APIs can be unsuitable in light of the need for the powder to be combined with the device, deposit in the nasal cavity and release the drug for absorption/transport. Micromeritics refers to size and shape of the particles in the powder (Testa et al., 2007). These fundamental properties determine the powder packing and flow properties. In particular, powder flow is favored by coarse particle size and spherical shape. Coarse particle size combines with lower specific surface area per unit mass of powder, which makes the powder less prone to moisture adsorption. Low flowability makes it difficult to meter the powder in the insufflator device during the "manufacturing phase" of the nasal drug product and deliver it quantitatively during the "administration phase". To get the proper flow properties, the API raw material requires a process, which refines the unfavorable powder particles' properties, including not only shape and size, but also density, surface properties, hygroscopicity. A second reason is related to the API biopharmaceutical properties, such as the mucoadhesion and dissolution rate, the latter also depending on particle properties like size. Moreover, the drug raw material may be susceptible to degradation in the nasal cavity.

Lyophilized powders have been proposed as nasal products since the '80s when Tsuneji and colleagues first applied the use of dry powders to the nasal delivery of insulin for diabetes (Tsuneji et al., 1984). Being very porous and fast-dissolving in contact with the nasal fluid, lyophilized powders allow for prompt drug release and diffusion across the mucosa. The *in vivo* data (dogs) by Tsuneji and co-workers allowed to estimate that an insulin-Carbopol 934 co-freeze-dried powder gave the same hypoglycemic effect at 3-fold the i.v. dose. This result is a positive evidence of the benefit of the lyophilized nasal powder, even though Carbopol 934 may have positively contributed to powder retention time into the nose, ultimately affecting insulin bioavailability. In fact, Carbopol 934 could have provided the powder with mucoadhesive properties (Lee and Chien, 1996; Patel and Chavda, 2009). However, nowadays lyophilized powders for nasal drug delivery have been largely overcome, due to limitations of lyophilization as manufacturing method and the introduction of alternative powder manufacturing technologies like spray drying (Rassu et al., 2015). Even more relevant is the fact that lyophilization for powder manufacturing does not

allow to control the powder size and morphology of the resulting powder. As discussed, particle size and shape are key factors for the insufflation, deposition and dissolution of the nasal powder in the nasal cavity (Zeng et al., 2003).

The use of the API as raw material is certainly relevant in research, to carry out preliminary studies before developing the actual nasal drug formulation. Typically, these experiments aim to characterize *in vitro* the drug powder dissolution profile in simulated nasal fluid or compare the diffusion across a barrier (artificial or biological) between a liquid formulation of the drug *versus* its solid form. For example, ribavirin, a drug candidate for the treatment of viral neurological disorders in dogs, was nose-to-brain delivered in rats as aqueous solution and as powder raw material to investigate whether its brain distribution was affected by the physical state. Differences in brain drug accumulation were found, with 3-fold higher drug levels in the olfactory bulb with ribavirin powder compared to the solution: the stronger and longer contact between powder and mucosa and the higher concentration gradient across the mucosa explained the increased drug absorption and brain bioavailability detected with drug powder. In fact, *ex vivo* permeation experiments of ribavirin across rabbit nasal mucosa confirmed that the drug permeated from the powder was significantly higher than from the solution at the same applied dose (5 mg, of which 85 ± 2% and 34 ± 4% permeated across the tissue in 4 h of experiment from the powder and the solution) (Colombo et al., 2011).

Microparticulate powders

These are powders composed of “microparticles”, which is a general word identifying particles in the micrometer size range (1-1000 μm). They can be manufactured by different methods. Milling is the main “top-down” method for their manufacturing. “Bottom-up” methods include spray drying, spray freeze-drying, supercritical fluid assisted spray drying (Fig. 1.4). Spray-dried and spray freeze-dried drug microparticles can be in certain cases excipient-free. Microparticles can be called “microspheres” if they have spherical shape and matrix structure.

Microparticulate powders represent the majority of nasal solid formulations studied so far in the literature. In fact, microparticles are interesting for reasons including fast dissolution in the nasal mucus when they are made of soluble excipients for the majority of their composition. This favors nasal transport and bioavailability leading to

rapid therapeutic effect. Moreover, microparticulate powders can be made of polymers encapsulating the drug active in a matrix structure (Gavini et al., 2005; Illum et al., 2001). In this case, they may sustain drug release over prolonged time. Lipids may also be used as matrix formers (Martignoni et al., 2016). Microparticulate powders allow for adequate nasal deposition if the particle size falls in the range 10-45 μm. On the other hand, they can show difficult handling during manufacturing (e.g. cohesiveness, adhesiveness and moisture-sensitivity). For patients, the risk of lung inhalation during administration exists if the powder contains a significant fraction of particles below 10 μm in diameter.

Microparticle agglomerates

Agglomeration is a technological strategy to counteract the drawbacks of microparticulate powders (poor flow, moisture sensitivity, cohesiveness) preserving their positive features in terms of dissolution rate. It is a way to have, although transiently, bigger and easy-flowing structures for improved handling during manufacturing of the dosage form, particularly when it comes to powder metering inside the device. Similarly, dose delivery from the device, aerosolization and nasal deposition benefit from the size-increase produced by agglomeration. In fact, the agglomeration process consists in forming soft clusters of the microparticles composing the microparticulate powder. These clusters form because weak bonds are established between adjacent microparticles. Such weak bonds may be the result of a number of concurrently acting forces or mechanisms developing between the microparticles, including van der Waals, electrostatic, capillary forces, solid bridges and mechanical interlocking. The prevalence of a force over the others depends first on the physico-chemical properties of the interacting particles (electrical properties, hygroscopicity), morphology (size, shape, surface texture) and their crystal form (such as crystallinity and polymorphism). Moreover, external conditions including environmental relative humidity and processing conditions may determine the development of the inter-particulate forces. For example, electrostatic forces occur between charged particles *per se* or being charged because of handling. Dispersion forces (van der Waals) are established between uncharged particles. When a powder is hygroscopic or contains same residual humidity as result from the manufacturing process or storage, water condensation may happen on the solid-solid interfaces and capillary forces may arise from the surface tension of the adsorbed liquid layer.

Mechanical interlocking between particles is common when particles are irregularly shaped or with rough surfaces (Zeng et al., 2003).

Agglomerates have size larger than the original microparticulate powders, measuring tenths to hundreds of microns in diameter and are free-flowing. The bonds between the microparticles are strong enough for the agglomerates to sustain the mechanical stress of the handling processes. At the same time, they allow the agglomerates to be fragmented during insufflation. The size of these fragments is suitable for nasal deposition and makes lung inhalation unlikely. The original microparticles are "released" from the fragments due to the dispersing action of the nasal fluid, after deposition on the mucosa. The released primary microparticles dissolve in the nasal mucus (Balducci et al., 2013; Russo et al., 2006 and 2004; Sacchetti et al., 2002).

1.1.4.1 Manufacturing methods

Nasal powders can be manufactured by means of various techniques, the choice of which also depends on the type of formulation envisaged. For example, chitosan-based microspheres were produced by emulsification-cross linking (Patil et al., 2010; Varshosaz et al., 2004), spray drying (Gavini et al., 2005 and 2011; Martinac et al., 2005), precipitation (Abdel Mouez et al., 2014) or solvent evaporation processes (Jain et al., 2004; Lim et al., 2000; Nagda et al., 2011). Any method should work to obtain a powder whose size falls in the suitable range for nasal delivery. Physico-chemical methods based on solvent evaporation (e.g. spray drying) or sublimation (e.g. freeze drying) (Fig. 1.4A-D) are frequently proposed in the literature. One reason is that these exploit well-established technologies, whose industrial scale-up is feasible (freeze drying) or is being studied (Masters, 1994; Zbicinski, 2017).

Having elected spray drying as the technique to manufacture the nasal powders under investigation in this thesis, a brief description follows.

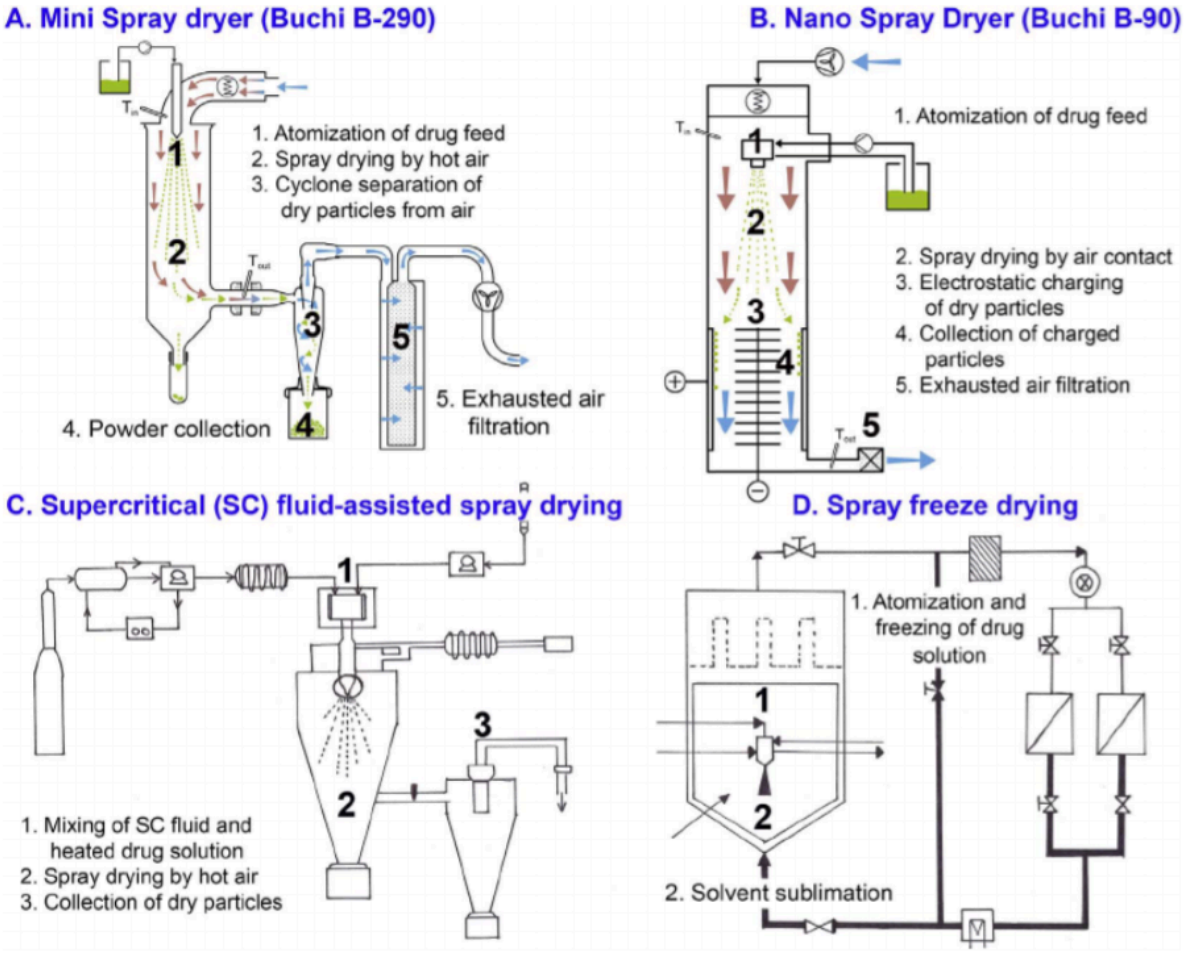

Figure 1.4. *Manufacturing methods of nasal microparticles (adapted with permission from Büchi Labortechnic, 2017, Cho et al., 2015 and Ishwarya et al., 2015).*

Spray drying

This is a widely applied technology, not only in the pharmaceutical field (Fig. 1.4, A-B). A feed liquid system containing the API dissolved or dispersed in a vehicle (both alone or in the presence of excipients), is sprayed and converted into a dried particulate upon evaporation of the vehicle. Nasal drug powder formulations made by spray drying include those produced for the delivery of carbamazepine (Gavini et al., 2006), cyanocobalamin (Garcia-Arieta et al., 2001), deferoxamine (Rassu et al., 2015), desmopressin (Balducci et al., 2013), diltiazem (Kulkarni et al., 2016), doxylamine (Katsarov et al., 2018), gentamicin (Hascicek et al., 2003), insulin, metoprolol tartrate, salmon calcitonin, somatotropin (Coucke et al., 2009), lorazepam (Zhao et al., 2012), metoclopramide (Gavini et al., 2005), morphine (Russo et al., 2006), ondansetron (Mahajan et al., 2012; Mahajan and Gattani, 2010; Suryawanshi et al., 2015), pyridoxine (Katsarov et al., 2018), repaglinide (Elmowafy et al., 2014), rokitamycin

(Gavini et al., 2011), ropinirole (Karavasili et al., 2016), tacrine (Saladini et al., 2013), tramadol (Belgamwar et al., 2011), valsartan (Pardeshi et al., 2012) and zidovudine (Dalpiaz et al., 2015).

The principal advantages of the technique are:

- processing of both drug solutions and disperse systems, at different total solid concentration;
- multiple options with respect to the liquid feed composition, spacing from aqueous to volatile organic solvents, the latter being not always suitable to be used in other processes;
- possibility to tune process parameters such as feed rate and evaporation temperature, according to the drug to process (e.g. lower temperature for temperature-sensitive APIs).

Spray drying allows for the optimization of particle characteristics like size, shape and density (Pilcer and Amighi, 2010). For example, both nozzle design and mechanism of atomization influence the droplet size of the spray, enabling to control the particle size distribution of the final product. For instance, aiming to realize dry powders for nasal deposition, caffeine microparticles were spray-dried using a 1 mm nozzle diameter (Sacchetti et al., 2002).

However, the technique does not go beyond 50-60% as production yields due to powder sticking to the equipment's parts (nozzle, drying chamber, cyclone, filter or collector vessel wall). This could be a drawback of the method, especially when the process variables are not controlled and the parameters concerning both the spray dryer and the feed formulation have not been optimized (Walters et al., 2014). Different spray drying equipment may also impact on the yield. A recent study has shown low yields (maximum 70%) in laboratory scale production using spray dryer models such as the Mini spray dryers B-190 or B-290 by Büchi (Flawil, Switzerland) (Fig. 1.4A), which are very common spray dryers in laboratories (Haggag and Faheem, 2015). Compared to the Mini spray dryers by Büchi, the recent Nano spray dryers B-90 or B-90HP by the same producer (Fig. 1.4B) enabled to process minimal quantities of liquid samples (few ml) into dry powder at high yields (up to 90%) (Aquino et al., 2014; Del Gaudio et al., 2017). In particular, there are three main claims in the patented technology: (1) a laminar airflow to decrease sample loss with minimal dead volume; (2) a spray head system to produce small particles with very narrow size distribution; (3) an electrostatic particle collector to obtain high yields and recover even the smallest

particles (Burki et al., 2011; Sosnik and Seremeta, 2015). Until now the Nano spray dryer has found application in the field of powders for inhalation that are produced with high nano (>300 nm) - low micrometer size (<5 μm) (Büchi Labortechnic, 2017) round shape, good aerodynamic properties. Nevertheless, it could also be applied for spray drying microparticles to be agglomerated for nasal delivery. As one part of this thesis focused on the comparison of nasal microparticulate powders produced by two spray dryers by Büchi, namely the Mini B-191 and the Nano B-90, their key features are reported in table 1.I. Mini B-290 is presented in the table instead of Mini B-191, because it is the currently available model of Mini spray dryer replacing the B-191 equipment. B-191 and B-290 work based on the same principles, but the latter has a bigger evaporation chamber and incorporates the automatic nozzle purging system.

Table 1.I. *Comparison between Mini B-290 and Nano B-90 spray dryers (Büchi Labortechnic, 2017).*

	Mini B-290	**Nano B-90**
Main advantage	For traditional spray drying, established process	For small quantities, fine particles, high yield
Max. Inlet temperature	220 °C	120 °C
Water evaporation	1.0 kg/h, higher for organic solvent	Max 0.2 kg/h, higher for organic solvent
Nozzle types	Two fluid nozzle, ultrasonic nozzle	Piezoelectric driven nebulizers
Particle size	2-60 μm	0.2-5 μm
Particle separation	Cyclone, dependent on particle mass	Electrostatic particle collector, independent of particle mass
Typical yield	50-70%	Up to 90%
Min. sample volume	30 ml	3 ml
Max. sample viscosity	300 cps	5 cps

Regarding other techniques for “bottom-up” manufacturing of microparticulate powders, supercritical fluids-assisted spray drying and spray freeze drying are the most innovative. The supercritical fluid-based processes (Fig. 1.4, C) exploit the specific properties of a gas in supercritical conditions, such as the modulation of the solubilizing power, large diffusivity, solvent-less or organic solvent-reduced operation. These processes have emerged as a promising technique for the production of powders for inhalation delivery, as they enable to control particle size and size distribution of the powder (Cho et al., 2015). On the other hand, spray freeze drying is a three-step process, consisting of dispersion of a bulk liquid (drug solution/dispersion) into droplets, droplet freezing and drying by sublimation of the frozen liquid (Fig. 1.4, D). It has been developed aiming to combine the advantages of spray drying and freeze-drying techniques (Ishwarya et al., 2015).

Agglomeration of microparticulate powders

In principle, any microparticulate powders is suitable to construct agglomerates as the final nasal dosage form. Agglomeration occurs spontaneously in powders when particle size goes below 100 μm due to the high surface area to volume ratio and increased cohesive forces. As previously detailed, the interaction between the microparticles relies on the establishment of weak bonds like van der Waals, electrostatic, capillary, interlocking forces (Zeng, 2003). These interparticulate interactions develop when the microparticulate powders are subjected to tumbling or mechanical vibration on sieves. In a study to construct agglomerates of pantoprazole gastro-resistant microparticles, Raffin et al. showed that the agglomeration method affected the morphology of the agglomerates, but not their mechanical properties (Raffin et al., 2007). With the sieving method, agglomerate formation may depend on the size of microparticulate powders with respect to the sieve’s mesh size: particles in the lower micrometer range (e.g. <5 μm particle size) could require sieve’s mesh <100 μm to make sure that the first agglomerated nuclei are retained on the sieve and can further enlarge.

If the original (or primary) microparticulate powders to be agglomerated are made of pure drug, they may be not cohesive enough *per se* and lead to fragile agglomerates. The cohesiveness of the microparticles is affected by their composition. In this regard, it has been shown that soybean lecithin acted as binder in the agglomerate’s construction, increasing its mechanical resistance (Russo et al., 2004; Raffin et al.,

2007). The binder can be either embedded in the structure of the primary drug microparticulate powder or be included in the composition of a second microparticulate population (referred to as “excipient microparticles”) to be blended with the drug microparticulate powder before agglomeration (Fig. 1.5). In addition, moisture presence in the microparticles and relative humidity can have an effect on microparticle cohesion (Kim et al., 2016). Nasal agglomerates of spray-dried microparticles have been described for both low molecular weight active molecules (caffeine and morphine) and a small peptide (desmopressin) (Balducci et al., 2013; Russo et al., 2006; Sacchetti et al., 2002).

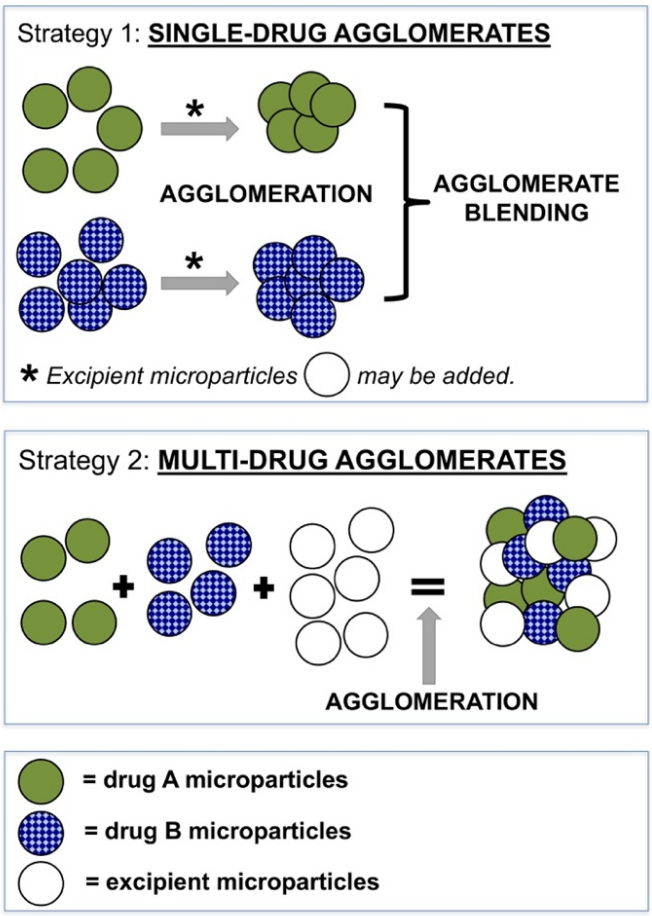

Figure 1.5. *Strategies for microparticulate powders’ agglomeration: 1) single-drug agglomerates. One-drug agglomerates can be blended with agglomerates of another drug in a combination nasal product. 2) multi-drug agglomerates. Microparticulate powders of different APIs (with excipient microparticles, as required) can be firstly blended and then agglomerated to obtain multi-drug agglomerates. Both strategies could be used to prepare nasal products for drug combined therapy (e.g. synergism of drugs for the same disease, multi-drug therapy in patients suffering from different disease, etc.).*

1.1.4.2 Delivery devices for powder insufflation

According to the Ph. Eur. definition of nasal powders, the formulation must be combined with a device for nasal insufflation for use. In a nasal drug product, the device represents the container closure system. It is responsible for 1) containing and protecting the drug formulation, 2) dosing the formulation (unless the dose is pre-metered) and 3) presenting the formulation to the administration site (the nasal cavity) in a suitable form for nasal deposition. The joint effect of nasal powder properties and device design and mechanism of insufflation is largely responsible for the nasal drug bioavailability, due to the influence on particle deposition in the nasal cavity. The effect of the delivery device on drug bioavailability has been studied by Pringels and co-workers using a freeze-dried powder formulation of insulin with starch and Carbopol (Pringels et al., 2006). Three insufflators were selected, namely Monopowder (Valois, Marly-le-Roi, France) (Fig. 1.6A), Pfeiffer system (Pfeiffer, Radolfzell, Germany) and an experimental device composed of a polyethylene tube filled with the nasal powder formulation. When the device allowed the formulation to deposit in the anterior part of the nasal cavity of the rabbit, slower mucociliary clearance and increased insulin bioavailability were observed.

The pharmaceutical development of nasal drug products requires that the delivery device is developed in combination with the designed formulation (Colombo et al., 2013). This evaluation starts early during product development, even to drive the selection of the optimal device for the subsequent clinical trials. Some aspects of the device's development derive from the general pharmaceutical development strategy of any drug product. In particular, the container closure system must be suitable for product storage and transportation, guaranteeing protection of and compatibility with the formulation. Compatibility includes the major aspect of "extractables and leachables" (E&L), i.e., any chemical passing from the device into the formulation, which may be potentially harmful for the patient. E&L assessment is not required by the EMA for nasal powder devices because the likelihood of chemical interaction between the solid formulation and the container components is low. Specific development requirements for nasal devices include the verification of dose delivery, particle size distribution of the emitted powder, plume geometry, all impacting on drug deposition and absorption.

As some parts of the device (e.g. cap or nozzle) will come into direct contact with the nasal mucosa during product's use, the device and/or its composing material may

require a biocompatibility assessment, particularly if the device is new or modified. In this regard, the FDA has recently developed a guidance document (Food and Drug Administration, CDRH, 2016) to assist industry in the evaluation of the potential for adverse responses resulting from device's component materials in contact with the body. The attention to the biocompatibility issue is further witnessed in the literature: *in vitro* cytotoxicity and *in vivo* skin sensitization and irritation tests were carried out on the polypropylene resin used for the delivery device of a glucagon nasal powder (Reno et al., 2016).

Based on their mechanism of function, Djupesland (2013) classifies the nasal devices for powder insufflation are classified in breath-actuated inhalers, powder sprayers and insufflators.

Figure 1.6. *Delivery devices for insufflation. (A) Monopowder®; (B) Prohaler®; (C) UDS (Unit Dose System) and D) Bi-Directional Breath Powered*

Breath-actuated powder inhalers

Devices activated by patient's breath work based on a passive mechanism of powder emission that may be suitable to limit powder dispersion in the environment. If the device is single-dose, the powder is contained in a blister or a capsule that is emptied as the subject inhales through with the nose.

Prohaler® by Aptar (Fig. 1.6B) is a blister-based pre-metered multi-dose powder inhaler. Powder delivery is triggered by the patient inhalation act with minimal dependence of product performance on airflow. It is claimed to have a patient-friendly design to improve patient adherence to therapy.

Powder sprayers

They produce a plume of particles when a compressible compartment containing the formulation is pressed and then released. For example, Monopowder® (Fig. 1.6A), originally developed by Valois and today acquired by Aptar (Crystal Lake, IL, USA), is a reservoir-based system allowing to spray the drug powder into the nose when a plunger is pressed and creates a positive pressure that breaks a membrane in the powder reservoir. In the already mentioned study by Pringels, low bioavailability of an insulin powder delivered by the Monopowder® was reported in comparison to that obtained when the same powder was conveyed by an experimental active device (6.6% and 14.4% absolute bioavailability for Monopowder® and the experimental device, respectively). In the same paper, an *in vitro* deposition study in a human nose silicon model showed that Monopowder allowed the powder to deposit in the upper turbinate region and the nasopharynx, close to the exit of the nasal cavity. This deposition pattern was related to the lower bioavailability in vivo compared to the other devices (Pringels et al., 2006).

Another powder sprayer is UDS (Unit Dose System) (Fig. 1.6C), which contains pre-loaded cartridges and generates an aerosolizing air jet upon mechanical actuation. It is designed for targeting the drug to the olfactory region for the nose-to-brain delivery. BDS (Bi Dose System) is similar, but delivers two nasal shots or two half-doses (when used for i.n. vaccination) (AptarGroup, 2017). Recently, Lewis et al. (2015) combined the UDS with a powder formulation of human growth hormone (5 mg hGH) formulated with a novel absorption enhancer called CriticalSorb™. Compared to the hormone's subcutaneous injection (1 mg hGH), the nasal powder produced a relative bioavailability of 3%, which was 3-time as higher as compared to the bioavailability produced by a reference liquid i.n. product (without the absorption enhancer). Despite the i.n. powder product was superior to the nasal solution in terms of bioavailability due to the dosage form and formulation composition, the Authors considered the measured bioavailability possibly biased by the blowback/powder loss effect produced by the UDS device.

Nasal powder insufflators

Insufflators are made of two pieces fluidly connected, named mouthpiece and nosepiece. Similar to breath-actuated inhalers, they are activated by the patient, who in this case blows into the mouthpiece producing an airflow through the system that

makes the powder particles enter the nose via the nosepiece. This system was designed to exploit the fact that the act of blowing naturally causes the soft palate to close. In this way, during powder delivery, there is no possibility for the powder to pass from the nose to the deeper airways. Bi-Directional Breath Powered (Fig. 1.6D), developed by OptiNose® (Yardley, PA, USA), is based on this concept. Djupesland proved that this device has the potential for the nasal delivery of systemic active compounds, since it broadens the powder deposition in the nasal cavity allowing for fast and efficient drug absorption. Deposition studies *in vivo* in humans with gamma scintigraphy imaging, showed that the OptiNose® Breath Powered device broadly deposited a lactose powder covering the posterior and superior areas of the nasal cavity, whereas a traditional liquid spray concentrated most of the dose (around 60%) in the lower areas of the nasal cavity. Nasal delivery of a low dose of sumatriptan by OptiNose® device in pharmacokinetic studies confirmed the large lining of nasal mucosa surface by drug formulation was associated with high rate and efficiency of drug absorption (Djupesland, 2013). Currently, Bi-Directional is the device combined with the sumatriptan succinate powder in Onzetra® Xsail®, indicated for migraine relief. In the COMPASS comparative efficacy trial, Onzetra® Xsail® loaded with 22 mg sumatriptan succinate was compared with oral administration of 100 mg sumatriptan. The nasal administration produced earlier onset of action with a lower dose and fewer adverse effects. Onzetra® Xsail® product produced faster absorption also *versus* a conventional sumatriptan liquid nasal spray (20 mg), with an earlier and significantly higher peak plasma concentration and a 61% higher systemic sumatriptan exposure in the first 30 minutes (Tepper and Johnstone, 2018). Moreover, Onzetra® Xsail® is now under clinical evaluation for delivery of fluticasone propionate for the treatment of chronic rhinosinusitis (Djupesland, 2013; Hansen et al., 2010). Shin Nippon Biomedical Laboratories (SNBL, Tokyo, Japan) has recently developed µco® System, a nasal delivery technology composed of a combination of a mucoadhesive powder drug carrier and a nasal delivery device. Milewski and collaborators prepared the first intranasal oxytocin dry powder formulation combined with a device exploiting the SNBL technology for the treatment of post-partum hemorrhage in the developing world. Pharmacokinetic studies in monkeys have revealed good in vivo absorption rate of oxytocin from the dry powder of the active with µco® carrier, rapid onset of the effect and reasonable nasal bioavailability (12% of intramuscular bioavailability) (Milewski et al., 2016).

1.2 ALZHEIMER'S DISEASE

Pathogenesis and epidemiology

Alzheimer's Disease (AD) is a CNS disorder. At the biological level, it is a progressive degeneration of the cerebral neurons, which is reflected, on the behavioral side, in loss of cognitive performance, memory impairment and disturbance in daily routine activities (i.e., brushing, bathing, eating, drinking, communicating, reading, writing, etc.), overall disturbing the thinking ability and causing mental illness. Although AD is age-dependent and mainly affects older adults, in modern lifestyle it seems to touch also people at an early age (younger stage AD) (Agrawal et al., 2018).

The pathogenesis of AD is multifactorial and not yet completely known. In the early '90, the amyloid cascade hypothesis reported the deposition of amyloid-β proteins (Aβ) as the causative agent of AD (Fig. 1.7 Top). Amyloid-β is a peptide consisting of 37-43 amino acids, which is produced from the cleavage of the amyloid precursor protein (APP) in the cellular plasma membrane by different secretase enzymes. Among the other isoforms, the 1-42 amyloid peptide is the most toxic. It produced by a cut in the γ-site of the APP by the γ-secretase enzyme and secreted in the extracellular space where it acquires β-pleated sheet configuration, aggregate and accumulate in amyloid plaque due to its hydrophobic nature (Sanabria-Castro et al., 2017). While in healthy people, the concentration of amyloid-β42 is balanced between generation and clearance, in AD patients a clearance abnormality leads to the accumulation of amyloid-β in the brain. As a direct result, neurofibrillary tangles formation, cell loss, vascular damage and dementia happen.

Recent evidence suggests that AD pathogenesis is even more complex and numerous metabolic conditions including aging, oxidative stress, impaired synaptic functions, neuroinflammation, etc., interplay to each other, ultimately resulting in late onset of AD (Fig. 1.7) (Pimplikar, 2014).

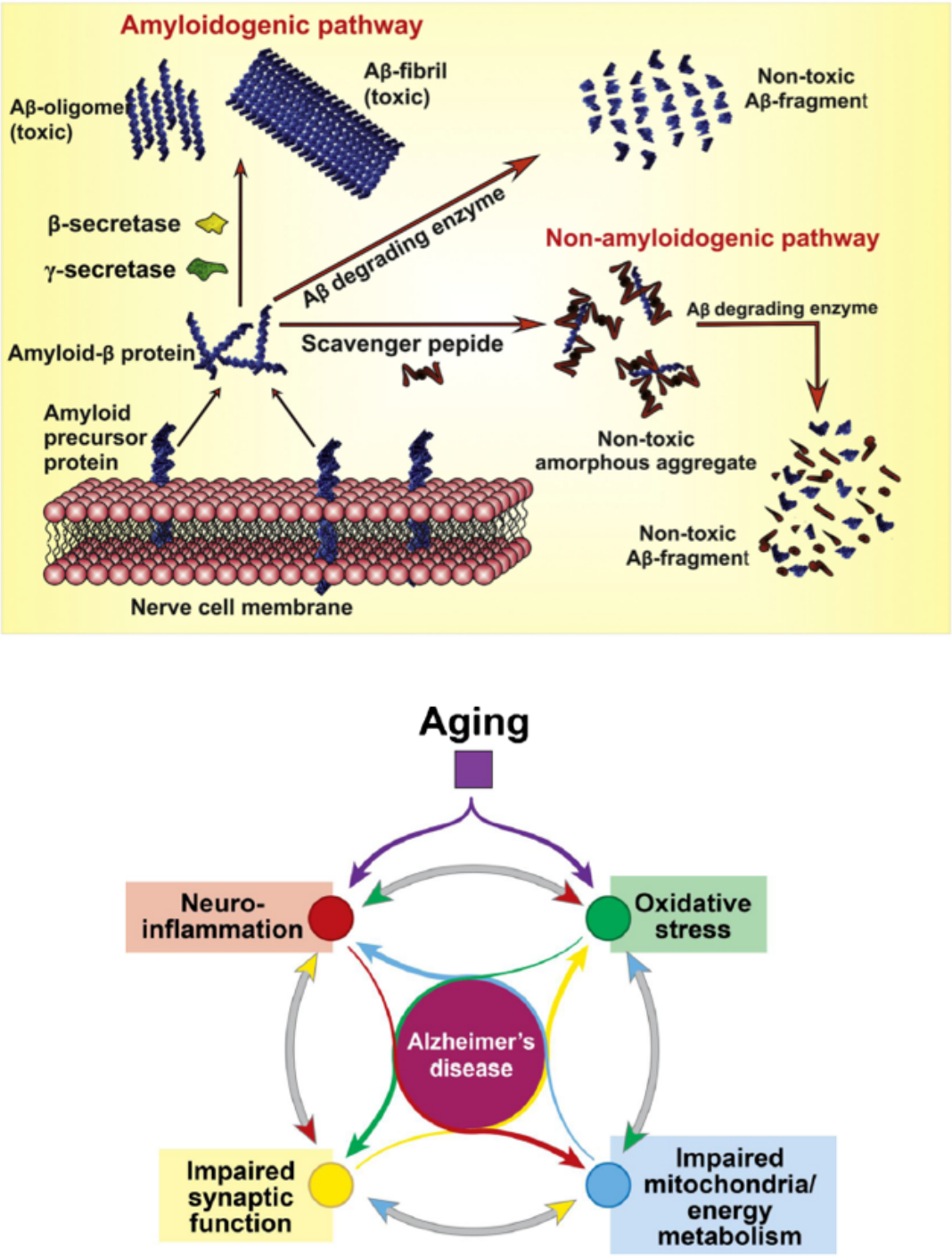

Figure 1.7. *AD pathogenesis. Top: Aβ plaques formation according to the amyloid hypothesis of AD. Bottom: multifactorial pathogenesis of AD, with different pathological factors interplaying. Specifically, during aging, the brain is naturally more subjected to neuroinflammation and more exposed to the effect of oxidative stress. Neuroinflammation and oxidative stress sustain and worsen each other, while they inhibit synaptic transmission, causing synaptic dysfunction, or alter mitochondria and energy metabolism (reproduced with permission from Agrawal, 2018 and Pimplikar, 2014).*

According to the Alzheimer Association report (2018), presently AD affects over 47 million people worldwide, being the most common form of dementia (60-80% of all cases). However, the number is estimated to increase dramatically by 2050 (up to 131 million). The statistics indicate that in the last 15 years, AD has increased as cause of mortality in the US, in comparison with other death causes like heart disease, cancer, and many more. Only in the US the total cost of AD treatment is approximately 259 billion USD, expected to rise by 1 trillion by 2050 (Agrawal et al., 2018).

Even though it may not be the only reason, such numbers may be the consequence of the lack of effective therapy. In fact, few drugs are approved for AD, which mainly act on some of its clinical manifestations like the acetylcholinesterase enzyme inhibitors (rivastigmine, galantamine, donepezil) and memantine. Actual AD-modifying therapeutic strategies, namely drugs acting on the specific site or physiological factor of the AD, are therefore required (Geldenhuys and Darvesh, 2015). Considering the difficulties encountered to identify a drug alone able to address the disease, a multi-target approach (drug combination therapy), could be more appropriate targeting different pathological mechanisms (Fan and Chiu, 2014). Nevertheless, the drug availability in CNS is of primary importance for neurological disease as AD, thus convenient approaches to deliver efficiently the drugs to the brain have to be investigated as well (Cuello, 2017).

1.2.1 Neuroinflammation

Based on the evidence that the deposition of Aβ fragments in AD brain induces a marked neuro-inflammatory response, researchers hypothesized that neuroinflammation could be a target of drug therapy (Rubio-Perez et al., 2012). The hypothesis was reasonable also in light of various observational studies on patients with rheumatoid arthritis evidencing the association between long-term exposure to non-steroidal anti-inflammatory drugs (NSAIDs) and reduced risk and delayed onset of AD (Zhang et al. 2018). Hence, clinical trials were started in which different NSAIDs (e.g. ibuprofen, celecoxib, R-flurbiprofen, aspirin, etc.) were administered to symptomatic AD patients (Gupta et al., 2015; Miguel-Álvarez et al., 2015). Regrettably, the overall outcomes were not as positive as expected, with a substantial lack of efficacy of NSAIDs in patients that were already cognitively impaired. One current opinion about this failure is that the late inflammation in the CNS of AD patients may

have a beneficial “protective” function as the disease progresses (Cuello, 2017). Thus, an anti-inflammatory therapy would worsen the pathological condition.

Nevertheless, new hopes raised from more recent studies reporting that inflammation in the CNS begins much earlier and likely before the formation of amyloid plaques (Fig. 1.8) (Cuello, 2017). This early inflammation was observed in studies with transgenic animal models, as human markers have yet to be identified. Provided it can be detected in asymptomatic individuals, early inflammation could become the target of a NSAID-based therapy. Several reports show that the conventional cyclooxygenase-inhibition mechanism of action of NSAIDs could be effective before the clinical signs appear (Heneka et al., 2015; McGeer et al., 2018).

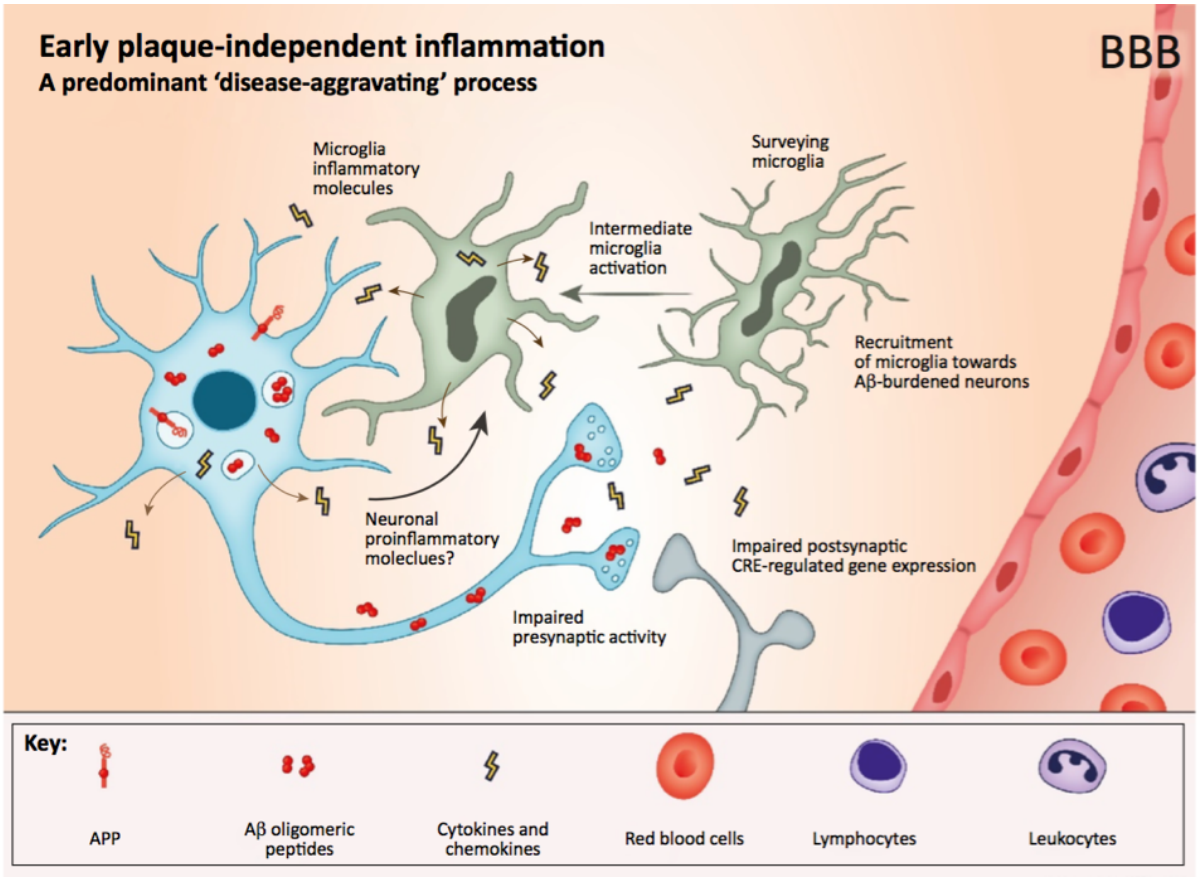

Figure 1.8. *Early CNS inflammation in AD. Aβ-burdened neurons are likely to act as initiators of the inflammatory process inducing the activation of microglia and their mobilization towards Aβ-burdened neurons. Both cell systems produce a disease-aggravating process in which the release of proinflammatory cytokines and chemokines predominates (reproduced with permission from Cuello, 2017).*

1.2.1.1 Flurbiprofen

Mechanism of action and potential use in AD

Flurbiprofen ($C_{15}H_{13}FO_2$, Fig. 1.9) is a chiral molecule, derivate of propionic acid.

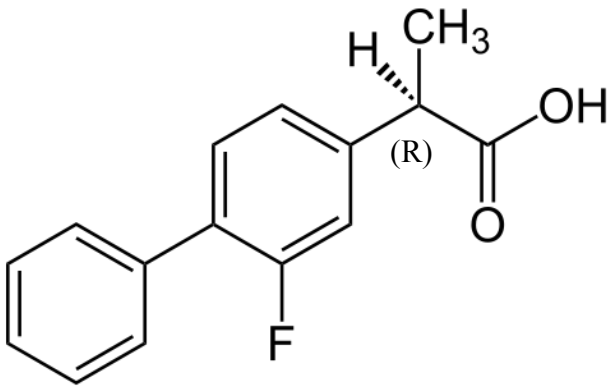

Figure 1.9. *Flurbiprofen. The chemical structure of the R-enantiomer of flurbiprofen.*

It belongs to the NSAIDs. In particular, the anti-inflammatory activity of flurbiprofen is attributed to its S-enantiomer, which non-selectively inhibits the cyclooxygenase enzyme (COX). Compared to other NSAIDs, flurbiprofen is more potent and has 12.5 times the power of ibuprofen to block the formation of prostaglandin E2 from the arachidonic acid. The R-enantiomer of flurbiprofen is devoid of any anti-cyclooxygenase activity, but it is a selective $A\beta_{42}$-lowering agent. In fact, it has been shown *in vitro* and *in vivo* to modulate the γ-secretase enzyme and reduce the $A\beta_{42}$ production in favor of shorter and less toxic forms of Aβ (e.g., $A\beta_{38}$ and $A\beta_{37}$). Pre-clinical studies reported that the R-flurbiprofen prevented learning and memory deficits in a transgenic AD model mouse (Aisen, 2008; Eriksen et al., 2003; Meister et al, 2013; Green et al., 2009; Lehrer, 2014).

Although until now no anti-inflammatory drug has been recommended for AD, S-flurbiprofen could be suitable as anti-inflammatory for AD due to its higher potency. Moreover, based on the amyloid cascade in AD brain, R-flurbiprofen appears interesting as well for AD. In the last few years, Myriad Genetics conducted extensive research and clinical trials to investigate the efficacy of R-flurbiprofen as an anti-AD drug targeting the amyloid deposition. In particular, a phase-II clinical trial (Wilcock et a., 2008) in 80 patients receiving an oral dose of 400 and 800 mg R-flurbiprofen twice daily, depicted a significant improvement in the memory and cognition without affecting the routine activities. However, the phase-III clinical trial (1700 patients with mild AD,

800 mg R-flurbiprofen twice daily *per os*) (Green et al., 2009) did not show any further improvement in thinking and learning ability of the patients. Due to the non-satisfactory results, Myriad decided to dismiss the project in 2008 (Myriad Genetics Reports, 2008). Several reasons have been proposed to explain the unsuccessful outcomes of R-flurbiprofen during this phase-III trial, including the poor brain permeation and weak pharmacological activity of the drug (Cummings et al., 2018; Imbimbo et al., 2009; Sanz-Blasco et al., 2018). Indeed, it is known that flurbiprofen has low brain penetration after systemic administration (i.e., cerebrospinal fluid to plasma ratio of 1-5% in rodents) and low brain concentrations (≈2 μM) (Parepalli et al., 2006; Zheng et al., 2014). Moreover, addressing only amyloid plaques in AD brain could be insufficient (Holmes et al., 2008). The S-enantiomer's anti-inflammatory activity was not considered in the failed phase-III clinical trial, thus it cannot be excluded that S-flurbiprofen may improve, by synergism, the effect of the R-enantiomer.

Thus, provided that the drug bioavailability in the brain is properly enhanced, e.g. by an alternative route of administration than the systemic one, the use of the racemic flurbiprofen could be still worth of investigation as a therapeutic approach in AD based on its action against both the cyclooxygenases and the γ-secretase enzyme.

Formulations for nasal delivery in AD

In order to favor the brain uptake of flurbiprofen exploiting a direct brain targeting in AD, nasal delivery may be proposed (Parepally et al., 2006).

Indeed, low molecular weight lipophilic drug could be readily transported across the mucosal barrier to the CNS. Flurbiprofen belongs to the Class II of the Biopharmaceutical Classification System of drugs, because it has low aqueous solubility and high permeability. A chemical modification of the drug structure involving its acidic moiety, could be used in order to increase the drug water solubility and dissolution rate, possibly favoring its transport across the mucosa (Pignatello et al., 2007; Zheng et al., 2016). Moreover, in nasal drug administration, technological approaches are available to further ameliorate the drug delivery to and bioavailability in the brain by a dedicated dosage form. An example is offered by a recent research by Muntimadugu and co-workers, who developed two nanocarrier systems for i.n. administration of R-flurbiprofen in brain disorders. The first system consisted in polymeric nanoparticles, prepared by emulsification solvent diffusion method with surfactant and poly(lactide-co-glycolide) copolymer. The second formulation were solid

lipid nanoparticles, prepared by emulsification solvent evaporation method using soybean lecithin, glyceryl monostearate, and stearic acid as lipid phase. *In vitro* release studies proved the sustained release of R-flurbiprofen from polymeric nanoparticles and solid lipid nanoparticles in comparison with the pure drug, indicating prolonged residence time of the drug at targeting site. The *in vivo* data in rats showed improved drug pharmacokinetic by the nasal nanocarriers than the reference solution/suspension. Moreover, the i.n. route was reported advantageous over the oral route of administration in terms of drug brain availability (Muntimadugu et al., 2016).

1.2.2 Impairment in brain responsiveness to insulin

Recent studies in animals and humans have suggested that the early course of AD is mediated by an impairment in brain responsiveness to insulin, glucose utilization and energy metabolism, leading to increased oxidative stress, inflammation and worsening of insulin resistance in the late AD. Exogenous insulin administration could have significant therapeutic potential in the early AD treatment (Bedse et al., 2015; Claxton et al., 2015; Willette et al., 2015).

Mechanism of action and potential use of insulin in AD

Human insulin is a globular protein of 51 amino acids (molecular weight: 5808 Da), chemically composed of two polypeptide chains joined by two disulphide bonds (Fig. 1.10).

Figure 1.10. *Human insulin. Primary amino acid sequence (Ph. Eur., 9th Edition).*

Physiologically, insulin regulates brain energy metabolism, but also plays an important role in learning and memory. In the brain, insulin levels can reach 10- to 100- fold greater than in plasma, especially in hippocampus, hypothalamus, cortex, olfactory bulb, substantia nigra and pituitary gland. Insulin receptors are abundantly expressed in neurons, but they are located also in glia cells. In the normal brain insulin signaling is important for neuronal growth, synaptic maintenance and neuroprotection. In contrast, in AD the number of insulin receptors in various brain regions is significantly reduced, while the remaining receptors become resistant to insulin. Although the exact pathogenic mechanism is not fully understood, aberrant brain insulin metabolism and signal correlate to increased accumulation of Aβ, phosphorylated tau, reactive oxygen/nitrogen species, pro-inflammatory and pro-apoptosis molecules (Fig. 1.11). Nevertheless, reduced insulin levels in the cerebrospinal fluid have been observed in AD.

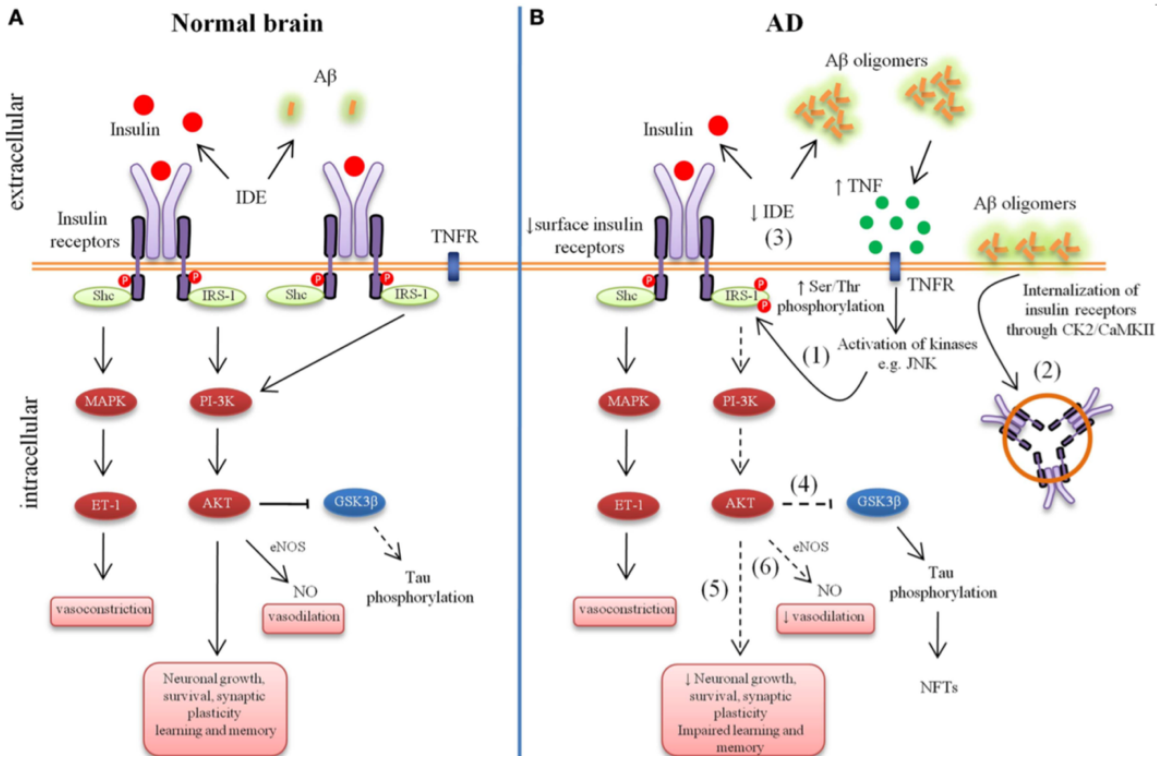

Figure 1.11. *Neuronal insulin signaling in the normal brain (A) and AD brain (B). Under physiological conditions, insulin binding to its receptor (IRs) produces a biological response resulting in downstream cellular events that facilitate neuronal growth and survival, synaptic plasticity, learning and memory. Activation of the IRs mediates both vasodilatation and vasoconstriction to regulate the metabolic requirements of various tissues. In AD, accumulation of Aβ oligomers leads to inhibition of IRs activation (1) or IRs removal form the cell surface and redistribution to cell bodies (2). Insulin resistance*

lowers the expression of Aβ-degrading insulin degrading enzyme (IDE) (3). Other events associated to aberrant insulin signal produce abnormal tau phosphorylation (4), impairment in nerve growth, synaptic plasticity, learning and memory (5) or imbalance of vascular function (6) (reproduced with permission from Bedse et al., 2015).

Based on common pathophysiological changes and signaling pathways between type-1 and type-2 diabetes and AD, AD was named "type-3 diabetes". Indeed, the direct analysis of post-mortem human brains with documented AD have shown that AD-neurodegeneration was associated with abnormalities in the expression of genes encoding insulin, insulin-like growth factor 1 (IGF-1) and insulin-like growth factor 2 (IGF-2), their receptors and downstream signaling mechanisms. Such abnormalities have been detected in the early stages of disease and found to worsen as the disease progressed. *In vitro* and *in vivo* data reported that neuronal and glial cell survival and function were related to the integrity of insulin and IGF signaling mechanisms in the brain. Impairments in insulin/IGF signaling led to deficits in energy metabolism with attendant increased oxidative stress, mitochondrial dysfunction, proinflammatory cytokine activation, and expression of amyloid precursor protein. It was remarkable that an experimental animal model was developed with brain diabetes with features closely mimicking the molecular, biochemical and neuroanatomical feature of AD, by intracerebral delivery of streptozotocin, commonly used to induce type 1 or type 2 diabetes (De la Monte et., 2008).

Formulations for insulin nasal delivery in AD

Based on these premises, enhancing brain insulin appears a valid pharmacologic strategy to address AD. For insulin administration to AD patients, the oral route would end with insulin enzymatic degradation in the gastrointestinal tract, while injection may cause peripheral side effects, such as hypoglycemia and induction/exacerbation of peripheral insulin resistance. Instead, nasal administration was suggested to produce therapeutic brain insulin levels avoiding peripheral effects. It is interesting that the early investigations about nose-to-brain drug delivery focused on insulin for the treatment of AD. Nasally delivered, insulin was found available in the brain and confirmed the existence of the nose-to-brain pathway (Agrawal et al., 2018). Moreover, systemic absorption and metabolic effects after nasal administration were not evidenced. As reported in an update review of the literature on i.n. insulin by Schmid et al., (2018), 40 UI nasal dose of insulin did not produce in human significant changes in circulating

insulin levels. Again, up to 4-time higher nasal drug dose (until 160 UI) produced limited and not concerning insulin absorption in the systemic bloodstream.

Based on the evidences on the effectiveness of i.n. insulin in humans, the National Institute of Health chose i.n. insulin administration as one of the two therapeutic strategies for AD treatment receiving substantial funding as part of the National Alzheimer's Plan in the US (Bedse et al., 2015; Benedict et al., 2004 and 2008; Reger et al., 2006 and 2008; Stein et al., 2011; Claxton et al., 2013). Among others, a remarkable clinical research by Craft et al. (2012) studied i.n. insulin treatment for AD and examined its efficacy on more than 100 human volunteers (mild and moderately AD) for 4-year period. It was found that a 20 IU dose of insulin was effective to significantly improve memory, and to increase cognitive and behavioral functions. These findings were matched with a reduction in Aβ and Tau level after insulin treatment. Due to some limitations in the study (i.e., age of the subjects, dose tested, period of study), other follow-up trials are further under way including one registered at clinical trials.gov as NCT01767909. This 4-years study is examining the effects of i.n. insulin administered in form of a solution (20 UI, twice-a-day) on cognition, entorhinal cortex and hippocampal atrophy, and cerebrospinal fluid biomarkers in totally 240 amnestic mild cognitive impaired or mild AD subjects. Results will be available soon since the study is going to be completed in 2018.

It is interesting to note that in clinical trials on nasal insulin, the peptide was administered as a solution, despite the liquid form resulted in less than 1% insulin nasal absorption (Illum, 2002). Modern technological strategies could lead to a more efficient delivery system to further improve insulin brain availability and drug efficacy. One such innovative approach, recently investigated by Picone et al. (2018), was a specially designed nanocarrier system consisting in a nanogel (10 to 100 nm), synthetized by e-beam irradiation alone, to which insulin was covalently attached. Tested *in vivo*, the nasal nanogel-insulin formulation was biocompatible, able to protect insulin from enzymatic degradation and offering better insulin activation as compared to free insulin. The nanogel-insulin significantly reduced the Aβ toxicity in neurons.

In addition to nanocarriers, solid formulations like powders, could be another approach to consider for nasal delivery of insulin (Tab. 1.II). Indeed, the first and most extensively studied protein for nasal delivery by powder formulations has been insulin to be administered in diabetic patients. The majority of the studies were conducted between the late '80s and the first decade of the years 2000s, likely comparing the research on

insulin delivery by pulmonary inhalation. In the last years, the number of studies has decreased, as if somehow the “holy grail” of non-invasive insulin administration had faded away with the commercial “failure” of the first approved human insulin product for pulmonary administration. In fact, Exubera® by Pfizer, a dry powder inhaler approved in the US in January 2006 for the pulmonary administration of insulin was withdrawn from the market 18 months later. Similarly, another insulin powder for inhalation registered more recently (Afrezza®) is costing more to produce than it returns. Beside this, it is worth highlighting that in many of the reported studies (Tab. 1.II), the simple concept of increasing insulin bioavailability by using a solid product instead of a liquid (to create a higher concentration gradient) proved not effective enough. Absorption-enhancing strategies had to be adopted to impact significantly on insulin bioavailability compared to liquid formulations. Mucoadhesion, tight-junction modulation, use of surfactants, cyclodextrins or anionic resins are some of the strategies proposed (Illum et al., 2002; Krauland et al., 2006; Pringels et al., 2008; Varshosaz et al., 2004).

Table 1.II. *Examples of powder formulations for insulin nasal delivery.*

Formulation	Excipient(s)	Manufacturing method	Ref.
Lyophilized powder	Water-insoluble cellulose derivatives	Freeze-drying	Tsuneji et al., 1984
Lyophilized powder	Carbopol® 934	Freeze-drying	Tsuneji et al., 1984
Lyophilized powder	Dimethyl-β-cyclodextrin	Freeze-drying	Schipper et al., 1993
Lyophilized powder	dried waxy maize starch with Carbopol® 974P; maltodextrins and Carbopol® 974P	Freeze-drying	Callens and Remon, 2000; Callens et al., 2003
Microparticles	Amioca®, Carbopol® 974P	Spray drying	Coucke et al., 2009
Powder blend	Starch and poly(acrylic acid) with $Ca(OH)_2$ powder	Physical mixture	Pringels et al., 2008
Microparticles	Thiolated chitosan-4-thiobutylamidine	Emulsification solvent evaporation	Krauland et al., 2006

Microspheres	Starch, lysophosphatidylcholine	Emulsion polymerization	Farraj et al., 1990
Microspheres	Starch with lysophosphatidyl choline; Starch with glycodeoxycholate; Starch with sodium taurodihydroxyfusidate	Freeze drying	Illum et al., 2001
Microspheres	Hyaluronic acid ester	Emulsification solvent	Illum et al., 1994
Microspheres	Dextran microspheres	Emulsion polymerization	Pereswetoff-Morath et al., 1995
Microspheres	Chitosan	Emulsification-cross linking	Varshosaz et al., 2004
Microspheres	Aminated gelatin		Wang et al., 2006
Microspheres	Thiolated carbopol–cysteine	Emulsification solvent evaporation	Nema et al., 2013

1.2.3 Combination therapy

The concept of combination therapy is becoming key in the development of therapies for metabolic, cardiovascular, autoimmune, neurological infectious and many other diseases. It means to treat patients with multiple drugs for a single disease, or even combination of a drug and immunotherapy or non-medical treatments. The concept of combination also includes the association between a drug formulation and a device for its administration. Currently more than 10000 ongoing clinical trials are registered in the US and even more preclinical investigation on combination therapies (https://www.nature.com/articles/nm.4426). The contemporary use of different approaches could take benefit from drug synergism *in vivo* or from contemporarily targeting a broad range of pathological factors with drugs and non-drug molecules.

In particular, combination therapy is reasonable for AD that has many underlying pathogenetic causes changing as it progresses. The medications approved by the US Food and Drug Administration (FDA) for the treatment of mild-to-moderate AD are all symptomatic and, when used as monotherapy, modestly effective. Trials in humans studying the combinations of the anti-AD drugs already approved have shown to benefit patients with moderate-to-severe AD dementia more than the monotherapy (Atri et al., 2008; Cheng et al., 2017; Fan and Chiu, 2014; Hartmann et al., 2003; Howard et al., 2012; Lopez et al., 2009; Porsteinsson et al., 2008; Schneider et al., 2011; Tariot et al., 2004). Recently (2014), FDA approved the first combination therapy of donepezil and memantine, named Namzaric® (a capsule for oral use), which still remains a symptomatic medication (https://www.namzaric.com). Moreover, combination of donepezil or memantine with anti-apoptotic or neuroprotective factors, nerve growth factor-stimulators or even food supplements like vitamins and folate, have a chance as possible disease-modifying therapy for AD (Annweiler et al., 2011 and 2012; Cano-Cuenca et al., 2014; Connelly et al., 2008; Lundbeck 2013; Rich et al., 2017). Cerebrolysin, a neurotrophic compound, was found to improve cognitive performance in mild-to-moderate AD patients when associated to donepezil (Alvarez et al., 2011). The administration of memantine with vitamin D for 6 months in AD patients led to relevant gain in cognition compared to each drug alone (Annweiler et al., 2011). Folic acid supplementation for 6 months in AD patients improved the response to cholinesterase inhibitors (Connelly et al., 2008).

Currently, the Alzheimer's Drug Discovery Foundation and the Alzheimer's Association are collaborating to jointly fund ($1.85 million) a phase II clinical trial to test a new

combination therapy for AD sponsored by Amylyx Pharmaceuticals Inc. The drug is AMX0035, consisting in a combination of sodium phenylbutyrate and tauroursodeoxycholic acid, which in preclinical studies protected brain cells from both inflammation and oxidation. The trial began at the end of August 2018 and enrolled 50 volunteers with late mild cognitive impairment or early dementia due to AD. The study will evaluate the safety, tolerability, drug target engagement and neurobiological effects of treatment with AMX0035 over 24 weeks (https://clinicaltrials.gov/ct2/show/NCT03533257).

In summary, encouraging outcomes compared to the monotherapy came from clinical trials on combination therapy for AD. Thus, combination therapy appears worth of investigation, provided that the drugs are properly identified and the route of administration guarantees sufficient brain availability of the selected compounds.

AIM OF THE RESEARCH

The presence of anti-inflammatory flurbiprofen and insulin in the brain could be protective on AD progression. A multi-target drug approach, i.e., by combination of flurbiprofen and insulin, appears worth of investigation to contemporarily target two pathological mechanisms of AD (Fan and Chiu, 2014). Nasal administration may enable these drugs to access the CNS by direct nose-to-brain transport along the olfactory and trigeminal nerve terminations exposed in the nasal cavity. Formulation-wise, nasal powders increase drug retention in the nasal cavity and drug diffusion across the mucosa.

The present work aimed to design, study and construct a combined powder dosage form of flurbiprofen and insulin for nose-to-brain delivery, proposed for early AD management. In particular, the work was carried out in 4 phases:

- **Phase 1 (chapter 2)**: design, construction and characterization of flurbiprofen nasal powders;
- **Phase 2 (chapter 3)**: study of plasma pharmacokinetic and brain distribution profile of flurbiprofen after *in vivo* administration of flurbiprofen nasal powders;
- **Phase 3 (chapter 4)**: construction and characterization of an insulin nasal microparticulate powder;
- **Phase 4 (chapter 5)**: flurbiprofen and insulin combination for nasal powder delivery.

CHAPTER 2
DESIGN, CONSTRUCTION AND CHARACTERIZATION OF FLURBIPROFEN NASAL POWDERS

One of the hypotheses made to explain the unsuccessful oral administration of R-flurbiprofen in the phase III clinical trial on AD patients was that the drug poorly accessed the brain *via* the systemic route (Imbimbo, 2009). Therefore, the aim underlying the work described in this chapter was to design and construct a solid formulation suitable for the nose-to-brain delivery of flurbiprofen to reach effective concentrations at the site of action. Several flurbiprofen powder formulations were manufactured by means of two different spray dryer equipment to see possible differences in the physico-chemical properties and biopharmaceutical behavior of the spray-dried microparticles or yield of production. Then, the flurbiprofen spray-dried microparticles were used as building blocks to construct agglomerates (i.e., soft pellets) with excipient spray-dried microparticles. The agglomerates represent the dosage form for flurbiprofen for the nasal product.

2.1 MATERIALS AND EQUIPMENT

Materials

Flurbiprofen acid (coded FB-COOH) raw material (batch n° T17121044) was kindly donated by Recordati S.p.A. (I-Milano). This drug substance was used for the preparation of the HPLC analytical standards and also as reference powder in the *in vitro* dissolution and *ex vivo* transport experiments. Mannitol (Ph. Eur.) was supplied by Lisapharma S.p.A. (I-Erba) and lecithin (Lipoid® S45) by Lipoid AG (CH-Steinhausen). HPLC-grade acetonitrile and isopropanol were supplied by Sigma-Aldrich® (St. Louis, MO, USA). All other reagents and solvents were analytical grade.

Equipment

- Gibertini Crystal 500CAL analytical balance (max weight 510 g, d=1 mg)
- Kern ALS 120-4 analytical balance (max weight 120 g, d= 0.1 mg, reproducibility =0.2 mg, linearity = +/- 0.2 mg)
- Mini Spray Dryer B-191 (Büchi Labortechnik, CH-Flawil)
- Nano Spray Dryer B-90 (Büchi Labortechnik, CH-Flawil)
- Zetasizer Nano S90 (Malvern Instruments Ltd., Malvern, UK) for Photon Correlation Spectroscopy analysis
- Branson 2510 Ultrasonic Bath (Emerson, St. Louis MO, USA).

2.2 METHODS

2.2.1 HPLC-UV method for flurbiprofen determination

Flurbiprofen quantification was carried out by reverse phase high performance liquid chromatography (HPLC) with UV-Vis detection (Agilent 1100 series, Santa Clara, CA, USA). Isocratic elution was carried out with a NaH_2PO_4 20 mM:CH_3CN (40:60) mobile phase (pH 3.0 $\pm$ 0.1) at room temperature. The detection wavelength was set at 244 nm. The stationary phase was a Zorbax Eclipse XDB column (C18, 5 µm, 4.6 x 15 mm; Agilent, Santa Clara, CA, USA). The flow rate was 0.8 ml/min. The injection volume was 20 µl (auto-sampler). In these conditions, the retention time of flurbiprofen was 4.6 min (Fig. 2.1). The method was developed in-house and validated with respect to linearity range (concentration range 0.13 - 4.2 µl/ml, y=112.6x - 0.1506, R^2=1; n=3), repeatability (0.089% RSD for peak area, n=6 injections) and limit of quantification (LOQ, 6.2 ng/ml).

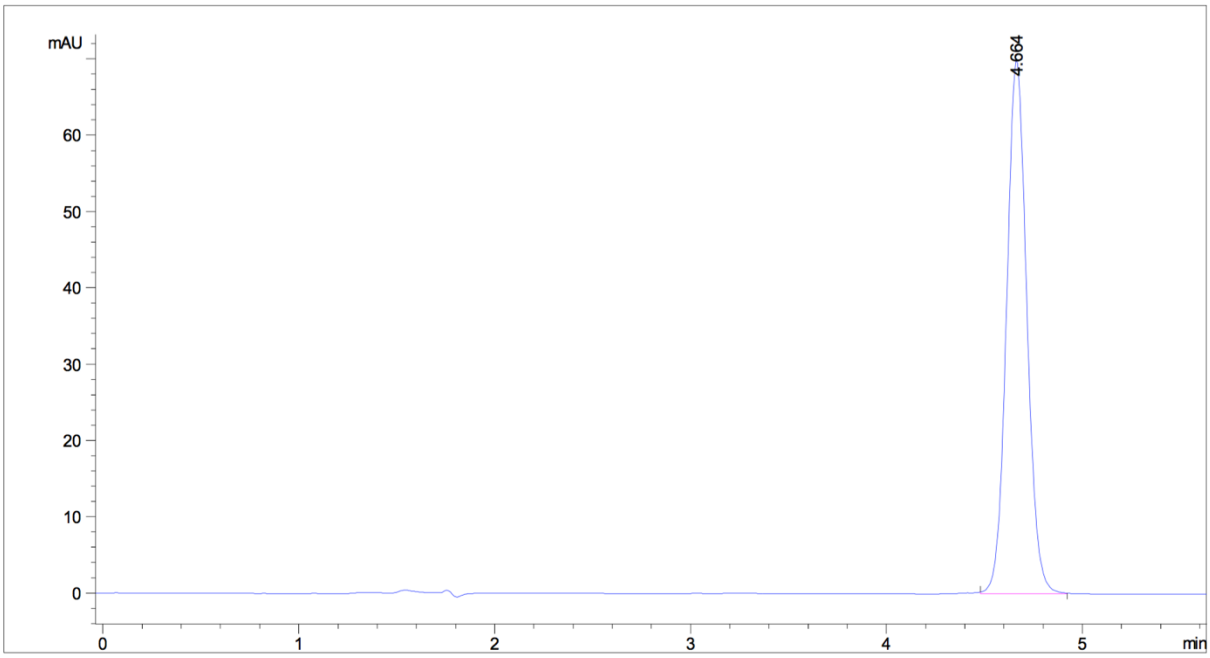

***Figure 2.1**. HPLC-UV chromatogram of flurbiprofen.*

The analytical standard solution was prepared from a 0.2 mg/ml stock solution of FB-COOH dissolved in methanol. This stock solution was prepared and stored at 2-8 °C for up to one month. On each day of analysis an aliquot of stock solution was diluted with the mobile phase to a final drug concentration of about 4 μg/ml, which was within the method's linearity range.

The concentration of flurbiprofen (as FB-COOH) in the sample (C_{sample}) was calculated according to the proportion:

$$A_{std} : C_{std} = A_{sample} : C_{sample} \qquad \text{Eq. 2.1}$$

where:

- A_{std} is the area under the flurbiprofen peak in the chromatogram of FB-COOH standard solution;
- C_{std} *i*s the concentration of FB-COOH in the standard solution;
- A_{sample} is the area under flurbiprofen peak in the chromatogram of the sample.

2.2.2 Particle and agglomerate manufacturing

Manufacturing of flurbiprofen and excipient spray-dried microparticles

Spray drying was carried out using both the Mini (B-191) and the Nano (B-90) spray dryers (Büchi Labortechnik, CH-Flawil). Microparticulate powders of flurbiprofen acid (FB-COOH) or its sodium salt (FB-COONa), were prepared by spray drying the drug, alone or together with lecithin (ratio 92:8 w/w, respectively), keeping the total solid

concentration at 2% (w/v) in all cases. For FB-COOH microparticles, the liquid feed was a hydro-alcoholic suspension of FB-COOH (water/isopropanol or water/ethanol 70:30 v/v). First, FB-COOH was dissolved in the alcohol, then this solution was added to water. For FB-COONa microparticles, FB-COOH was dispersed in water (2% w/v), then NaOH 1M was added until a solution was obtained (final pH 7.4), according to Manniello et al. (2016).

Finally, for the drug spray-dried microparticles embedding lecithin, the phospholipid was preliminarily solubilized in isopropanol or ethanol at 2% (w/v) concentration, together with FB-COOH, then the solution was added to water. To produce FB-COONa/lecithin microparticles, lecithin was dissolved in isopropanol and this solution added to the FB-COONa aqueous solution. Two water/alcohol ratios in the resulting hydroalcoholic solution were considered, namely 95:5 or 92:8 (v/v).

Table 2.I summarizes the operative conditions applied as well as the liquid feed composition. 100 ml of each liquid feed were processed by the Mini B-191 in the following operating conditions: drying air flow 500 L/min, aspiration rate 100%, air pressure 6 atm, liquid feed flow 5 ml/min, inlet temperature 90 or 120 °C, nozzle diameter 0.7 mm. Outlet temperatures are reported in Table 2.I. With the Nano B-90, the operating conditions were the following: drying air flow 100 L/min, liquid feed flow 1.5 ml/min, relative spray rate 100%, inlet temperature 40 or 70 °C, spray cap 7.0 µm. Outlet temperatures are reported in Table 2.I.

Mannitol/lecithin microparticles were prepared by spray drying as well according to Balducci et al. (2013). Separately, mannitol was dissolved in water, whereas lecithin was solubilized in ethanol. These two solutions were mixed to obtain the feed with a 92:8 water/ethanol ratio (v/v) and total solid concentration of 2% (w/v). The same feed was spray-dried with both apparatuses. The operating conditions were the same applied for the drug particles, with the exception of the inlet temperature (Table 2.I).

Table 2.I. *Spray-dried microparticle composition and spray drying conditions that were varied in the study (equipment type, liquid feed composition and drying temperature). (FB-COOH: flurbiprofen acid; FB-COONa: sodium flurbiprofen; iPr: isopropanol; Et: ethanol; ML: Mannitol/Lecithin).*

Powder Code	Spray Dryer	Spray-dried microparticle composition (% w/w)				Liquid feed composition (% v/v)			Drying temperature (°C)	
		FB-COOH	FB-COONa	Mannitol	Lecithin	H_2O	iPr	Et	Inlet	Outlet
F2	Mini B-191	100	-	-	-	70	30	-	90	56-60
F3		-	100	-	-	100	-	-	120	65-68
Mini ML_Et		-	-	92	8	92	-	8	90	42-44
Mini ML_iPr		-	-	92	8	92	8	-	90	40-42
F13_70	Nano B-90	-	100	-	-	100	-	-	70	33-34
F13_40		-	100	-	-	100	-	-	40	29-30
F15_70		-	92	-	8	95	5	-	70	30-33
Nano ML_Et		-	-	92	8	92	-	8	40	22-24
Nano ML_iPr		-	-	-	8	92	8	-	40	22-23

Agglomerate Manufacturing

The spray-dried drug (FB-COOH or FB-COONa) microparticles were manually blended with spray-dried mannitol/lecithin microparticles at a drug to excipient mass ratio of 10:90 and 50:50 with a spatula in a 5 ml glass vial. The blending action was applied for 15 min, executing approximately 60 spatula movements per min. Before agglomeration, the blends were sampled (5 mg samples, randomly collected on the top, center and bottom of the vial, n=3) to assess homogeneous drug distribution by the HPLC-UV method described in paragraph 2.2.1.

Two methods were employed to agglomerate manufacturing, namely:

1) Vibration method (Fig. 2.2, left). A weighed amount (0.5 – 1 g) of spray-dried microparticles was loaded on top of a pile of two analytical sieves (10 cm diameter) of 850 μm and 106 μm mesh size. The pile was vibrated on a sieve shaker (Octagon Digital, Endecotts Limited, London, UK) at fixed intensity (amplitude 6) for 10 min. Vibration caused the microparticles to aggregate and progressively form agglomerates with varying sizes. After the first cycle, the agglomerates retained on the smaller sieve were collected, whereas the non-agglomerated powder was reprocessed for further 2 cycles. As the size fraction of interest was the one above 106 μm, a pooled yield was calculated from the amount of agglomerates collected on each sieve divided by the total weight of microparticles processed per cent.

Figure 2.2. *Agglomeration methods of spray-dried microparticles. Left: powder on sieve after vibration; right: powder in glass pan for tumbling.*

2) Tumbling method (Fig. 2.2, right). A weighed amount (0.5 – 1.0 g) of spray-dried microparticles was tumbled in a 100 ml glass pan having deflected walls (DISA, IT-

Sesto San Giovanni). The pan was fixed with a 90° angle to the rotating arm of a tablet friability tester and rotated at 25 rotations per minute for 40 min. Agglomerates were then manually sieved (106 µm mesh) to collect the fraction >106 µm. The yield was calculated as for the vibration method.

2.2.3 Physico-chemical characterization of spray-dried microparticles and agglomerates

Drug content

Drug content was determined by HPLC after dissolving an accurately weighed amount of powder (5.0 ± 0.5 mg for the spray-dried microparticles and 10 ± 0.5 mg for the agglomerates) in methanol or phosphate buffered saline pH 7.4 1M (PBS; KCl 0.2 g/l; NaCl 8 g/l; Na_2HPO_4 1.15 g/l; KH_2PO_4 0.2 g/l), depending on whether the powder contained FB-COOH or FB-COONa. The obtained solutions were diluted with mobile phase before injection. For each batch, measurements were performed in triplicate. Data are reported as mean ± standard deviation.

Morphology

The morphology of raw material and spray-dried microparticles was evaluated by scanning electron microscopy (SEM). Sample preparation and operating conditions were as reported elsewhere (Aquino et al., 2014). A Carl Zeiss EVO MA 10 microscope was used with a secondary electron detector (Carl Zeiss SMT Ltd., Cambridge, UK) equipped with a LEICA EMSCD005 metallizer to deposit a 200–400 Å thick gold layer. Analyses were conducted at 17 keV.

Particle size analysis

The size distribution was determined for FB-COOH raw material and the various FB-COOH and FB-COONa spray-dried microparticles by laser light diffraction with an apparatus equipped with a 45 mm focal lens (Mastersizer X, Malvern Instruments Ltd, Worcestershire, UK). The FB-COOH spray-dried microparticles and raw material were suspended in water (Ph. Eur, 9th Ed.), whereas FB-COONa spray-dried microparticles were suspended in dichloromethane at a concentration of 0.9 mg/ml (solid concentration >> drug solubility in each medium). Each suspension was sonicated in an ultrasonic water bath at room temperature for 5 min for homogeneous particle dispersion. The water bath prevented any temperature increase of the sample due to

sonication, to avoid changes of the drug solubility. Then, the suspension was diluted dropwise in 100 ml of the same vehicle until proper obscuration was reached. Size data are expressed as $d_{v,10}$, $d_{v,50}$ and $d_{v,90}$ (n=3 samples *per* batch). The SPAN value was calculated according to Equation 2.2:

$$Span = \frac{[d_{v,90} - d_{v,10}]}{d_{v,50}} \qquad \text{Eq. 2.2}$$

Mannitol/lecithin spray-dried microparticles were analyzed as described for drug spray-dried microparticles, but using acetonitrile as suspending vehicle. Data are reported as mean ± standard deviation.

Thermal analysis

Differential Scanning Calorimetry (DSC) analysis was carried out on the FB-COOH raw material and drug spray-dried microparticles (DSC 822e, Mettler Toledo, Columbus, OH, USA). 10.0 ± 0.5 mg of sample were weighed in a 40 µl aluminum pan (MTS Mettler Toledo microbalance, Columbus, OH, USA), sealed and pinholed. Samples were heated up to 350 °C at a scanning rate of 10 °C/min in a single cycle of measurement (Sansone et al., 2013).

For FB-COONa spray-dried microparticles, which bore two water molecules in the crystal habit, preliminary dehydration was carried out to remove the bound water, heating the samples up to 130 °C at a scanning rate of 10 °C/min and leaving them at 130 °C for 15 min. Then, they were heated as reported above.

Powder X-ray diffraction analysis

Powder X-ray diffraction (PXRD) patterns of raw material and drug spray-dried microparticles were recorded on a BRUKER AXS D8 Advance diffractometer (Brucker, Billerica, Ma, USA), equipped with a curved graphite crystal, using Cu Kα radiation (λ = 1.5406 Å). The scanning rate was 2θ/θ; 3°≤ 2θ ≤ 50°; Step 0.02°; Step time 2 s.

2.2.4 Biopharmaceutical characterization of spray-dried microparticles and agglomerates

In vitro flurbiprofen dissolution

Vertical Franz-type diffusion cells with a diffusion area of 0.58 cm^2 (Vetrotecnica, I-Padova) were used to measure *in vitro* the dissolution rate of FB-COOH and FB-COONa from the raw material, spray-dried microparticles and agglomerates. A regenerated cellulose membrane (one layer, cut from a dialysis tubing having MW cut-off 12,000–14,000 Da, width 32–34 mm, nominal dry wall thickness 20 μm; Dexstar Visking, Medicell International Ltd, London, UK) separated donor and receptor compartments. The receptor compartment was filled with 5 ml of PBS pH 7.4. About 5.0 mg of API raw material or spray-dried microparticles or 10.0 mg of agglomerates were introduced in donor compartment. Each powder was weighed on a piece of silicon foil. Then, the foil was folded to form a cone to facilitate controlled powder sliding into the donor and deposition on the surface of the membrane, avoiding the adhesion to the donor's wall. Care was payed to avoid non-homogenous distribution of the particles. The powder in the donor was wet by adding 100 μl of PBS pH 7.4 on top of it. Assembled Franz cells were maintained at 37 °C in a water bath and under magnetic stirring. 100 μl samples of receptor solution were withdrawn at pre-determined time points up to 4 h. Experiments were performed in triplicate. With this experimental set up, sink conditions were guaranteed at least for the first 60 min.

At the end of the experiment, aiming to calculate the mass balance (sum of the amounts of FB-COOH recovered from receptor, donor and membrane), the residual drug in the donor compartment was quantitatively recovered with PBS pH 7.4. The membrane was rinsed by sonication in 5 ml of PBS pH 7.4 for 10 min. The rinsing solution were analyzed by HPLC-UV method. Data are reported as mean ± SEM.

Ex vivo flurbiprofen transport across rabbit nasal mucosa

The *ex vivo* transport of flurbiprofen across excised rabbit nasal mucosa was studied using the same Franz-type cells of the dissolution experiments (0.58 cm^2). Rabbit nasal mucosa was extracted from rabbit's heads supplied by a local slaughterhouse (Pola S.r.l., Finale Emilia, Italy) on the day of the experiment and transported to the laboratory in a refrigerated box. The extraction procedure, completed within 2 h from the animal's death, is described elsewhere (Balducci et al., 2013). The diffusion cells were assembled with the tissue's mucosal side facing the donor compartment. The

receptor compartment was filled with 5 ml of PBS pH 7.4. The assembled cells were equilibrated for 20 min at 37 °C before introducing the formulation. As for the dissolution studies, about 5.0 mg of FB-COOH spray-dried microparticles or FB-COONa spray-dried microparticles or 10.0 mg of agglomerates + 100 µl of PBS pH 7.4 were loaded. FB-COOH raw material (5 mg + 100 µl PBS) and a FB-COOH saturated solution in PBS pH 7.4 (1.5 mg/ml, 0.5 ml) were tested for comparison purposes. The saturated solution was prepared by adding an excess amount of a FB-COOH raw material to 6 ml of PBS pH 7.4 and letting the suspension under magnetic stirring at 37 °C for 24 h. Then, the supernatant was separated by centrifugation (6000 x g, 5 min) and used as donor after determining the drug concentration by HPLC-UV method. It was decided to test only the FB-COOH saturated solution with the excised nasal mucosa because this research focused on the powder formulations. This test allowed to assess the drug partition in and diffusion across the nasal mucosa independently of the dissolution of the drug, which occurs with the powders. The FB-COONa saturated solution in PBS pH 7.4 was not tested, because partition and diffusion involve the non ionized form of the molecule.

Experiments lasted 4 h (Colombo et al., 2016). The receptor medium was sampled at the beginning of the experiment (time 0) and then every h. At the end of the experiment the residual drug in the donor compartment was quantitatively recovered by rinsing with fresh PBS. Drug accumulated within the tissue thickness was extracted by comminuting the mucosa with a surgical blade and homogenizing it in 5.0 ml of water with Ultra-Turrax® IKA homogenizer (T10 basic model, IKA® Werke GmbH & Co. KG, D-Staufen) for 3 min. Two milliliters of methanol were then added and homogenization continued for further 30 s to disrupt the cell membranes and complete the extraction. The homogenates were centrifuged (7500 x g, 10 min) and the obtained supernatant was diluted with mobile phase for injection. The mass balance was calculated as seen. The minimum number of replicates was 5.

The transport parameters, i.e., steady-state flux (J_{SS}) and permeability of FB-COOH across the mucosa, were calculated (Bortolotti et al., 2009) according to the steady-state solution of Fick Equation (Eq. 2.3):

$$J_{SS} = \frac{dM}{dt*A} = P_e * C \qquad \text{Eq. 2.3}$$

where P_e is the apparent permeability coefficient of diffusant (cm s^{-1}), C is the initial donor concentration and J_{SS} is the flux at steady-state (mg cm^{-2} s^{-1}); dM is the amount of drug (mg) transported through the membrane during the infinitesimal time dt and A is the diffusion area (cm^2). The steady state flux across the mucosa was calculated from the slope of the linear part of the line obtained by plotting the mass transported per unit area against time. Data are reported as mean ± SEM.

2.2.5 Data analysis

Statistical analysis of data was performed by applying unpaired two-tailed Student's test. Significance was accepted at $P < 0.05$.

2.3 RESULTS AND DISCUSSION

The FB-COOH raw material is a powder unsuitable for the purpose of nasal administration due to its low aqueous solubility and powder micromeritics (Testa et al., 2007) (Tab. 2.II). Considering that for all nasal formulations the residence time is short (though longer for powders than for liquids), the dissolution rate in aqueous fluids should be as high as possible to provide sufficient drug concentration on site.

Here, the equilibrium solubility of FB-COOH at 37 °C was experimentally determined using the raw material and resulted equal to 0.029 ± 0.004 mg/ml and 1.5 ± 0.1 mg/ml in deionized water (pH 5.4) and in phosphate buffered saline (PBS) pH 7.4, respectively (mean ± standard deviation, n=3). The higher solubility in the buffer was due to the chemistry of FB-COOH, which is a weak acid with pH-dependent solubility. Thus, it was decided was to exploit the presence of the acidic moiety to improve the drug aqueous solubility, while increasing the dissolution rate by particle size reduction via spray drying. In particular, FB-COOH solubility was determined in PBS pH 7.4 because this medium was used as wetting liquid and dissolution medium in the subsequent *in vitro* and *ex vivo* experiments. The choice is reasonable also as formulation strategy to favor the local drug concentration after solid particle deposition on the mucosa. The optimal pH of nasal liquid preparations for tolerability reasons, falls in the range 5.5 – 7.5 (Colombo et al., 2015). The normal pH of nasal secretions in adults ranges from 5.5 to 6.5 (Chien et al., 1989). A more recent study in human volunteers indicates a baseline human nasal pH of 6.3 (Washington et al., 2000). These authors also observed that the administration of 100 µl of an isotonic saline solution pH 7.2 increased the nasal pH to 7.06 only, but in the anterior part of the nose.

2.3.1 Spray-dried flurbiprofen microparticles

2.3.1.1 Manufacturing: yield, size, morphology and drug content

Firstly, microparticulate powders were produced by spray drying the drug without excipients, either in acid form (FB-COOH) or as sodium salt (FB-COONa), the latter to increase the drug aqueous solubility. Secondly, aiming to agglomerate the drug spray-dried microparticles into coarse soft clusters to improve their flow properties, the particle composition was modified by adding 8% (w/w) of soybean lecithin. The effect of lecithin on the agglomeration of spray-dried microparticles was investigated by Raffin et al. (2007). They prepared mannitol/lecithin spray-dried microparticles containing different amounts of lecithin (10-12.5-15% w/w). These spray-dried microparticles were agglomerated with enteric pantoprazole-Eudragit® S100 spray-dried microparticles. The characteristics of the mannitol/lecithin spray-dried microparticles investigated by SEM, atomic force microscopy and X-ray microanalysis, were correlated to the yield of agglomeration and tensile strength of the agglomerates, also as a function of the quantity of lecithin in the spray-dried microparticles and its location in the particle structure. Specifically, larger yield and higher tensile strength were found for the agglomerates containing particles richer in lecithin. In these microparticles, lecithin was located on the surface allowing to establish solid bridges between particles. The fact that lecithin conveys binding properties to the spray-dried microparticles and mechanical resistance to the agglomerates was observed again with agglomerates made on spray-dried microparticles composed of mannitol, lecithin and the antidiuretic hormone desmopressin (Balducci et al., 2013). In this study, it was observed that the removal of lecithin from the composition of the spray-dried microparticles hindered the formation of agglomerates or eased their breaking during handling. “Stickiness” in lecithin-containing spray-dried microparticles compared to the lecithin-free ones was evident also from the macroscopical observation of the powder, as the formulation without lecithin appeared more powdery (Balducci et al., 2013).

Spray drying is a widely used technique for microparticle manufacturing, drying the liquid feed continuously and relatively fast (Belotti et al., 2014 and 2015; Tiozzo Fasiolo et al., 2018). Here, two spray dryers were used, namely the Mini B-191 and Nano B-90 equipment by Büchi (CH-Flawil), also aiming to assess the equipment’s impact on the relevant characteristics of the dried product. In particular, the Nano B-90 apparatus exploits a newer technology for laboratory scale production requiring minimal volumes of liquid feed to obtain microparticulate powders with high yields (Aquino et al., 2014;

Del Gaudio et al., 2017; Lee et al., 2011). Moreover, the two differ for droplet generation, drying airflow and temperature and mechanism of particle collection.

As shown in Tab. 2.I, the composition of the liquid feed was not the same for all the spray-dried microparticles. It first depended on whether the drug should be spray-dried as FB-COOH or FB-COONa. For the FB-COOH, a hydro-alcoholic feed (isopropanol or ethanol) was necessary to form a homogeneous suspension easier to spray. FB-COONa was obtained starting from an initial coarse suspension of the raw material in water, which was dissolved by adding NaOH 1M (final pH 7.4).

Yields of production did not exceed 40% using the Mini B-191 equipment and were particularly low in the case of FB-COONa (Tab. 2.II). Several unsuccessful attempts were made to increase this low yield, mainly by modifying the liquid feed (data not shown). Modifications included doubling of the total solid concentration (from 2% to 4% w/v), increasing the percentage of organic solvent when spraying FB-COOH or adding 10-20% (v/v) of isopropanol when spraying FB-COONa. In all cases, the critical step was the droplet evaporation, with major losses of liquid feed sticking on the wall of the evaporation chamber.

Aiming to increase the yields, the same liquid feeds containing FB-COOH or FB-COONa, were processed with the Nano B-90 spray dryer. This apparatus is equipped with an electrostatic particle collector where particle separation is expected to be independent of particle mass as in standard cyclones. The Nano B-90 spray dryer did not allow to obtain spray-dried microparticles of FB-COOH. This was due to the fact that the liquid feed droplets are generated by a piezoelectric system, vibrating a thin membrane which can only process solutions or very diluted suspensions. As seen, the FB-COOH liquid feeds were concentrated suspensions. In addition, a thin layer of solid material adhered to the collector's walls and could not be collected.

In contrast, the drying process was quite efficient for FB-COONa and yields were significantly improved compared to the Mini spray dryer, even when the inlet temperature was 40 °C. Considering the composition of feed solution was exactly the same for the Mini B-191 and Nano B-90 equipment, a low evaporation temperature (and corresponding outlet temperature) is an additional advantage of the Nano B-90 spray dryer with respect to drug thermal stability, even though it prolongs the duration of the drying phase.

When lecithin was included in the spray-dried microparticle composition, it was necessary to add the organic solvent (isopropanol or ethanol) to the liquid feed also

when processing FB-COONa. Barely no powder was obtained when spray drying FB-COOH and lecithin on the Mini spray dryer: the liquid feed's droplets stuck to the evaporation chamber's glass wall and did not evaporate. In contrast, some powder was formed with the salt, but the yield was very low (<10%). The outlet temperature above 60 °C, resulting from the high inlet temperature necessary to dry the aqueous feed (120 °C), could have interfered with the hardening of lecithin, negatively affecting the yield.

Neither the Nano spray dryer was able to process FB-COOH together with lecithin as well, again because the liquid feed was a concentrated suspension.

With FB-COONa, similarly to what happened with the case of the drug alone, the Nano spray dryer increased the yield also in presence of lecithin (drug to lecithin ratio 92:8). At 70 °C, using 5% (v/v) isopropanol as organic solvent, the yield was almost 60%. The isopropanol percentage in the feed was increased from 5% to 8% (v/v) aiming to work at lower inlet temperature (40 °C), without substantial improvements of the yield (data not shown). However, the use of ethanol as alternative organic solvent, maximized the powder yield (data not shown). Ethanol is more volatile than isopropanol (Paudel et al., 2013) and the volatility of the solvent positively affects the solid production yield (Patel et al., 2015).

Table 2.II. *Yield, drug content as FB-COOH, and size distribution data of drug spray-dried microparticles and mannitol/lecithin spray-dried microparticles (n=3 batches). Drug content as FB-COONa can be calculated based the molecular weights of FB-COOH (244.26 g/mol) and FB-COONa (266.26 g/mol), considering that FB-COONa precipitates as a dihydrate salt (302.26 g/mol). (FB-COOH: flurbiprofen acid; FB-COONa: sodium flurbiprofen; ML: Mannitol/Lecithin; iPr: isopropanol; Et: ethanol). Data are reported as mean ± standard deviation.*

Code	**Spray Dryer**	**Yield (%)**	**Particle size (μm)**			**SPAN**	**Drug content as FB-COOH (% w/w)**
			$d_{v,10}$	$d_{v,50}$	$d_{v,90}$		
API raw material	-		3.30 ± 0.41	16.27 ± 4.64	44.15 ± 5.09	2.58 ± 0.41	-
F2	Mini B-191	34.8 ± 1.8	4.49 ± 0.65	14.16 ± 1.51	35.43 ± 4.23	2.18 ± 0.02	99.3 ± 2.5
F3		27.3 ± 10.2	2.09 ± 0.42	10.43 ± 1.18	28.00 ± 7.06	2.46 ± 0.43	81.3 ± 0.3
Mini ML_Et		29.2 ± 9.2	1.45 ± 0.05	3.03 ± 0.16	6.30 ± 0.71	1.60 ± 0.13	-
Mini ML_iPr		45.0 ± 2.4	1.83 ± 0.05	3.56 ± 0.06	7.54 ± 0.43	1.61 ± 0.08	-
F13_70	Nano B-90	76.3 ± 4.2	1.20 ± 0.10	5.69 ± 0.36	23.16 ± 7.59	3.84 ± 1.29	80.3 ± 1.8
F13_40		78.7 ± 6.4	1.62 ± 0.04	4.31 ± 0.44	10.84 ± 1.33	2.13 ± 0.08	78.7 ± 1.2
F15_70		45.6	7.42 ± 0.99	21.99 ± 1.72	49.84 ± 5.02	1.93 ± 0.11	77.1 ± 0.3
Nano ML_Et		54.2 ± 3.3	1.54 ± 0.06	4.54 ± 0.29	10.30 ± 0.76	1.93 ± 0.10	-
Nano ML_iPr		61.2 ± 5.2	3.10 ± 0.07	9.85 ± 0.27	20.24 ± 0.99	1.74 ± 0.05	-

SEM micrographs of Mini and Nano spray-dried powders are shown in Fig. 2.3. Using the Mini B-191 spray dryer, the morphology of FB-COOH spray-dried microparticles (F2) (Fig. 2.3B) did not change substantially compared to the raw material (Fig. 2.3A). The spray drying reduced the particle size at a certain extent and narrowed the size distribution (Tab. 2.II). This size reduction and morphology may be explained by considering that during the preparation of the liquid feed for F2, FB-COOH was initially dissolved in the organic solvent. Then, the mixing of the organic phase with water caused the drug precipitation due to an antisolvent effect with the formation of new, but smaller particles due to recrystallization.

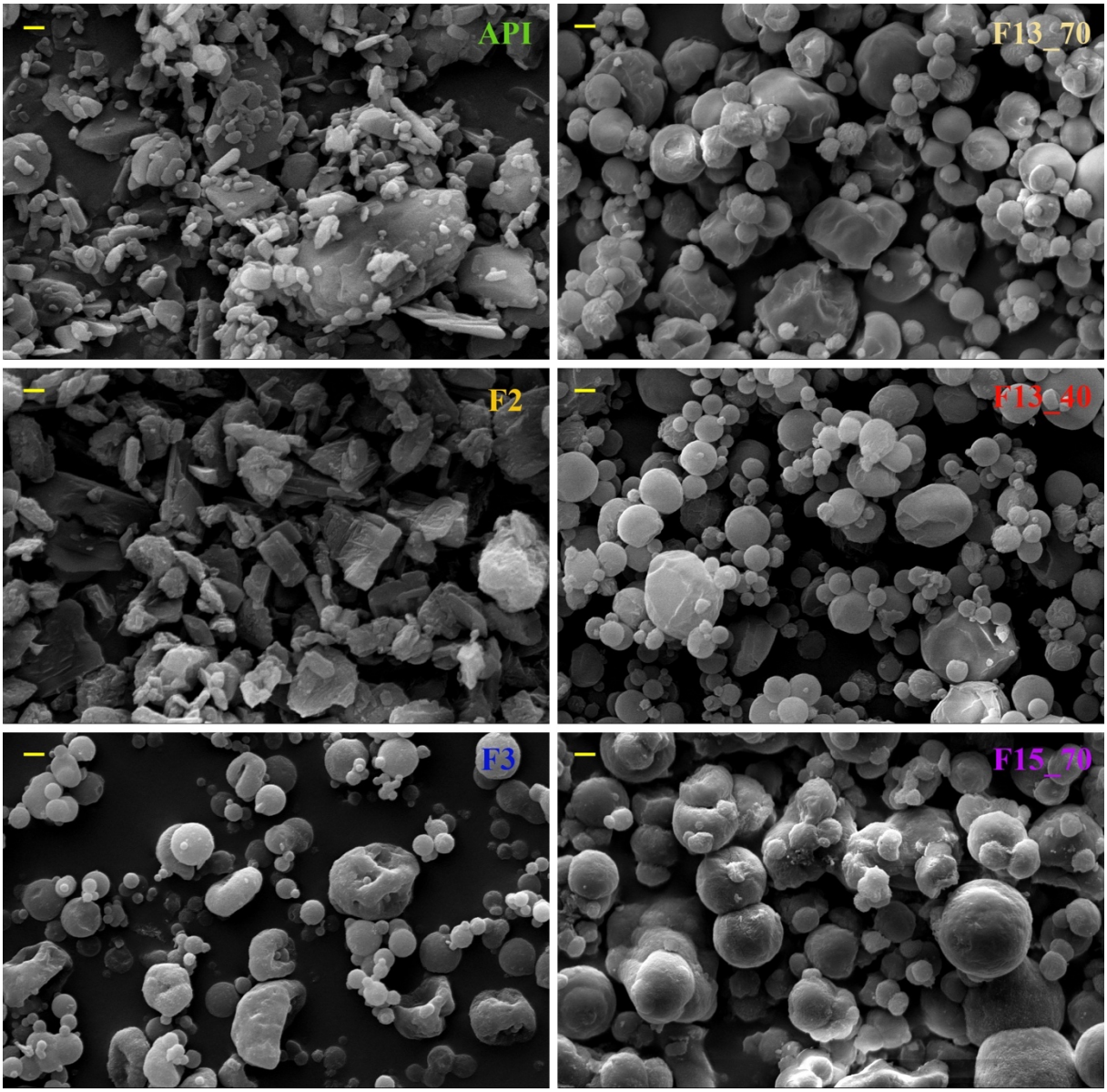

Figure 2.3. *SEM micrographs (5000x, size bar: 2 µm). Left panels, from top to bottom: FB-COOH raw material (API); Mini B-191 FB-COOH (F2); Mini B-191 FB-COONa (F3).*

Right panels, from top to bottom: Nano B-90 FBCOONa dried at 70 °C (F13_70); Nano B-90 FB-COONa dried at 40 °C (F13_40); Nano B-90 FB-COONa with lecithin dried at 70 °C (F15_70).

In contrast, FB-COONa (F3, F13_40 and F13_70) was spray-dried from a solution, thus particle formation occurred following solvent evaporation and spherical particles were formed, with the larger among them collapsed (Fig. 2.3C and 2.3D). Compared to F2, Mini spray-dried FB-COONa particles (F3) had a significantly lower median diameter ($P < 0.05$), but a non significantly broader size distribution (SPAN).

F3 particle shape and morphology derived from the complete dissolution of FB-COONa in the liquid feed prior to spray drying and were a sign of hollow particles. In spray drying, the microparticle structure is governed by the ratio between solvent evaporation rate and solute diffusion rate, as described by the Peclet number. In dependence of the respective prevalence of these two rates, a number higher or lower than 1.0 explains the formation of hollow or solid particles, respectively (Tsapis et al., 2002; Huang et al., 2011; Belotti et al., 2015). During drying of the FB-COONa solution droplets with the Mini B-191 equipment, the drug diffusion rate was slower than the solvent evaporation rate due to the high air temperature. This provided a sufficient drug enrichment of the droplet surface for the formation of hollow particles, as evidenced by the presence of collapsed structures (Vehring, 2008).

Similarly, the Nano spray-dried FB-COONa microparticles were significantly smaller than the other spray-dried microparticles, but showed the broadest size distribution when dried at 70 °C (Fig. 2.3D; Tab. 2.II). They were smaller than the counterpart sprayed with the Mini spray dryer, even though the size difference between F3 and F13_70 was significant only for the $d_{v,50}$ value at $P < 0.05$. The SPAN values measuring the width of the distributions, were not significantly different ($P > 0.05$). In the comparison between F3 and F13_40, both $d_{v,50}$ and $d_{v,90}$ were significantly different ($P < 0.05$). The lower particle size obtained with the Nano spray dryer *versus* the Mini spray dryer may be due to several process factors, including the lower inlet temperature and different drying airflow, liquid feed flow, spray nozzle and particle collection mechanism. Temperature and airflow factors as well as liquid feed flow and their interactions determine the rate at which the solvent evaporates from the drying droplets and can affect the size and morphology of the resulting particles (Santhalakshmy et al., 2015).

Here, in the comparison between the two spray dryers processing the FB-COONa aqueous solution, the feed composition was the same (i.e., same drug diffusion rate), but the drying rate of the Nano spray dryer was different. The result was smaller FB-COONa spray-dried microparticles with the Nano spray dryer. However, when the inlet temperature of the Nano spray dryer was reduced from 70 to 40 °C, the average diameter ($d_{v,50}$) of the resulting spray-dried microparticles further decreased from 5.69 ± 0.36 µm to 4.31 ± 0.44 ($P < 0.05$). The size difference between F13_70 and F13_40 pairs with a different morphology of the particles at SEM (Fig. 2.3D and E). The F13_40 smaller spray-dried microparticles were spherical, smoother and very few appeared corrugated or collapsed compared to F13_70. Such morphology was interpreted by examining the process in the light of the Peclet number (Tsapis et al., 2002): if the droplet evaporation rate is lower than the solute diffusion rate, the Peclet number is less than 1.0 and smaller solid particles are predicted due to the slower surface drug enrichment during drying. In other words, drug precipitation at the surface of the droplet is delayed and the resulting particles are smaller and denser.

In addition, another operating parameter influencing the particle size is the rate at which the feed is sprayed. Together with the spray nozzle, it affects the droplet size. This was lower for the Nano SD and may have contributed to the size reduction of the particles, as observed by Belotti et al., 2014.

Finally, the mechanism of particle collection of Nano SD may influence the microparticle size distribution as the equipment retains the particles regardless of their size up to 80% of the dried product.

The Nano SD microparticles of FB-COONa with lecithin (F15_70) were less spherical with a slightly rough surface (Fig. 2.3F) compared to those without the phospholipid. They seem coated by lecithin and partially agglomerated as if lecithin made them cohesive. The presence of lecithin on the particle surface is due to the surface-active property of this substance that determines its accumulation at the droplet surface during the drying process (Parlati et al., 2009). Laser light scattering analysis confirmed that these particles were 4-fold as larger as without lecithin (Tab. 2.II).

FB-COOH content in the spray-dried microparticles is reported in Tab. 2.II, expressed as weight percent. Drug content was between 77%-99%, depending on the equipment used and the chemical form of the drug (FB-COONa or FB-COOH). Only F2 spray-dried microparticles contained 99% drug because it was present in the acidic form. The drug content in FB-COONa spray-dried microparticles has to take account of the

presence of sodium ion. In addition to considering the sodium ion, the calculations of flurbiprofen content also has to consider the presence of two water molecules. They are included in the crystal habit to form a dihydrate salt. Dihydrate formation occurs often with sodium salts of various drugs (Rubino, 1989). In addition, the USP monograph of FB-COONa reports that FB-COONa is a dihydrate. The presence of water content in the FB-COONa microparticles was also evidenced during DSC analysis. In FB-COONa spray-dried microparticles the drug content slightly decreased passing from the Mini B-191 to the Nano B-90 apparatus. This was attributed to the lower evaporation temperatures used with the Nano B-90, which may leave residual moisture (not quantified). Finally, in the spray-dried drug microparticles containing lecithin, the drug content agreed with the presence of lecithin, but was slightly higher than expected. The content data confirmed that the drug was stable during spray drying, even at the high temperatures of the Mini SD.

2.3.1.2 Microparticle physical state characteristics

Thermal analysis by DSC compared FB-COOH raw material with the spray-dried microparticles to assess the effect of the process on the drug physical state.

The FB-COOH raw material (Fig. 2.4, trace D) showed an endothermal event at 122 °C, which was attributed to FB-COOH melting. The Ph. Eur. FB-COOH monograph reports a melting point of 114-116 °C. The same endothermic peak was seen for the Mini SD FB-COOH microparticles (F2; Fig. 2.4, trace E). This confirmed that spray drying of FB-COOH did not modify the physical state of the compound.

The DSC traces of the FB-COONa spray-dried microparticles show no thermal event around 100 °C because of the de-hydration treatment prior to DSC scan. De-hydration removed the bound water as well as any residual water from the spray drying. Then, the use of sodium hydroxide as the base for salt formation significantly increased the melting point of FB-COONa as witnessed by the endothermic peak at about 240 °C of the Nano spray-dried FB-COONa microparticles (F13_70; Fig. 2.4, trace A). A study by David et al. (2012) evaluated the effect of the counterion on the physical state properties of a series flurbiprofen salts with different amines. They observed that the relationship between salt formation and melting point is not unidirectional, i.e., the salt can melt at lower or higher temperature than the parent drug depending on the counterion, which determines the ionic and intermolecular forces within the solid particle. In addition, the hydration water molecules could be involved as they bring

additional H-bonding capacity into the solid structure.

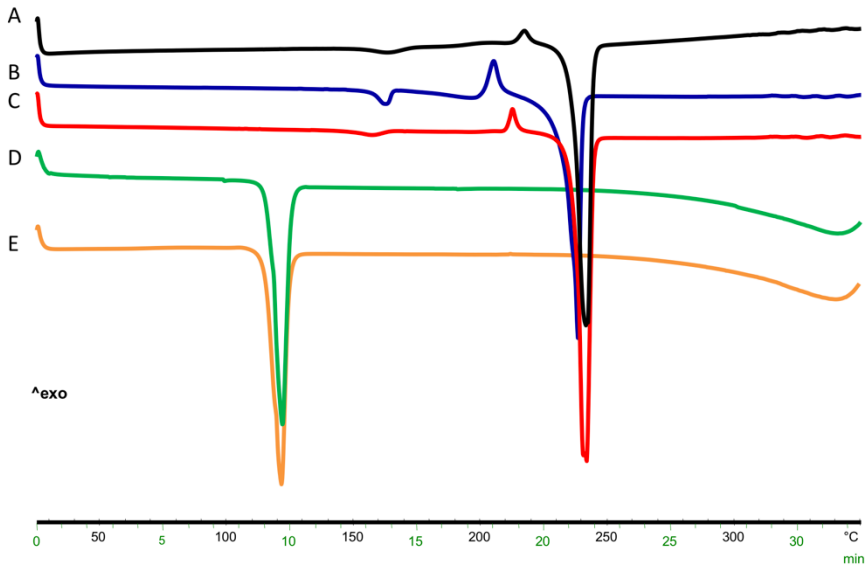

Figure 2.4. *Thermograms of A) Nano SD FB-COONa (F13_70); B) Mini SD FB-COONa (F3); C) Nano SD FB-COONa (F13_40); D) raw material and E) Mini SD FB-COOH microparticles (F2).*

The thermogram of Mini SD FB-COONa microparticles (F3; Fig. 2.4, trace B) showed two melting events that could be related to the existence of two polymorphs: the first event characterized by the endothermic peak around 160 °C, could correspond to the melting of a metastable polymorphic form of FB-COONa. The subsequent exothermic event around 200 °C precedes the fusion of the more stable polymorph around 240 °C (Bottom, 1999). As drying and solid particle formation are faster with the Mini B-191 due to the higher inlet temperature, the formation of a metastable polymorph is possible (Davis et al., 2004). The Nano B-90 spray-dried microparticles containing lecithin displayed the same two endothermic peaks, with no effect on the thermal behavior due to the presence of lecithin (data not shown).

Although spray drying often leads to amorphous powders (Broadhead et al., 2007), in this study, independently of the apparatus employed, FB-COOH and FB-COONa spray-dried microparticles were always crystalline, as shown by the sharp peaks in the X-ray diffraction spectra. In particular, the FB-COOH spray-dried microparticles (F2) retained the crystalline structure of the raw material (Fig. 2.5A). However, the intensity of the signal was lower for the spray-dried microparticles. This indicates that the F2 crystals were smaller than the raw material ones. In X-ray diffraction, the bigger the crystal's size, the higher the number of diffracted electrons, i.e., the signal's intensity.

The crystal's size is determined by the crystallization process: if the process is fast, the crystals have little time to grow. Indeed, spray drying had reduced the size of F2 compared to the raw material (Tab. 2.II). The X-ray diffraction agreed with the DSC results indicating the same thermal behavior for FB-COOH raw material and FB-COOH spray-dried microparticles.

The X-ray diffraction pattern of the salt form showed a quite different crystal phase compared to the acid (Fig. 2.5B-C). The Mini B-191 (F3) and the Nano B-90 FB-COONa microparticles dried at 70 °C (F13_70) showed superimposable diffractograms, with the exception of the sharp peak at 7°-8° 2θ for F3 that corresponded to a minimal residue of FB-COOH (Fig. 2.5B). The crystal phase of the salt remained the same independently of the spray dryer, whereas the peak intensities did not. The less intense F3 peaks again depended on the crystals' size. However, in this case the respective intensities did not match with the measured particle size because F3 was bigger than F13_70 (Tab. 2.II). It was considered that with the two spray dryers the size distribution of the spray-dried microparticles depends not only on solvent evaporation, but also on the mechanism of particle collection. Thus, a relationship between size and X-ray diffraction intensity is not straightforward.

F13_40 spray-dried microparticles showed differences compared to F13_70 (Fig. 2.5C). The new peak at 5° 2θ, the shift of the two peaks between 31°-34° 2θ and the shift of the peak at 46° 2θ, indicated the presence of a second polymorph. The height ratio of the peak at 5° 2θ and hat at 3° 2θ indicated that this polymorph accounted for about 20% of the powder. In addition, the diffraction between 5° and 16° 2θ was attributed to the presence of some amorphous drug. Overall, F13_40 was less crystalline than F13_70 and this was related to the evaporation temperature.

The presence of lecithin in the composition of the Nano B-90 FB-COONa spray-dried microparticles did not modify the X-ray diffraction pattern, except for the intensity, which was higher for the lecithin-containing spray-dried microparticles (Fig. 2.5C).

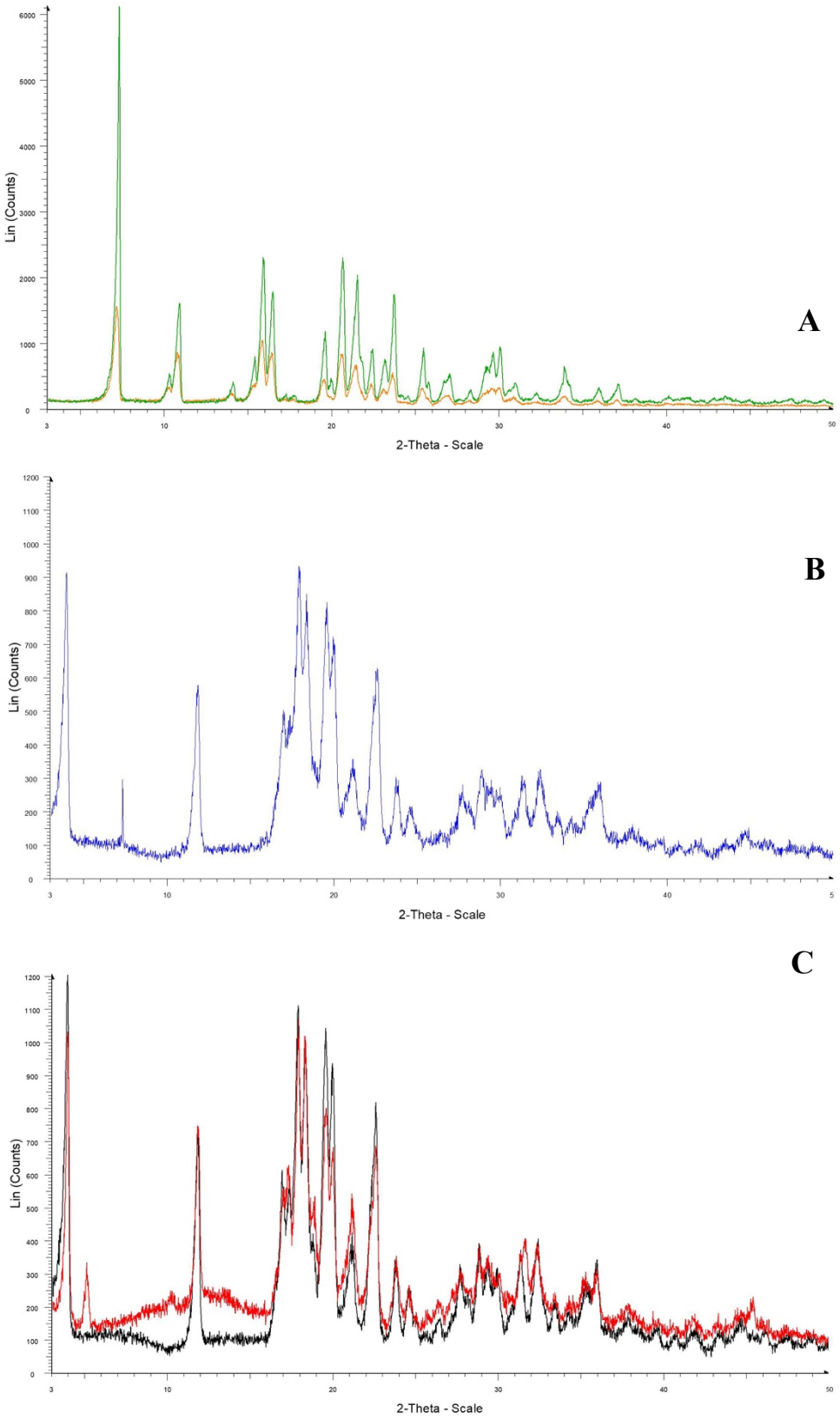

Figure 2.5. *X-ray diffraction spectra. Top: flurbiprofen API (green) and Mini B-191 FB-COOH microparticles (F2, yellow); center: Mini B-191 FB-COONa (F3); bottom: Nano B-90 FB-COONa dried at 70 °C (F13_70, black) and dried at 40 °C (F13_40, red).*

2.3.1.3 Biopharmaceutical characterization of flurbiprofen microparticles

In vitro flurbiprofen dissolution

The test apparatus was a Franz cell with a non-partitioning membrane of regenerated cellulose separating the donor from the receptor. In these conditions the drug transport across the membrane from the microparticles was governed by the dissolution of the solid formulation deposited on the membrane. In other words, given that the membrane had the same permeability for all the powders, the transport profiles across were determined by the drug concentration in the donor, resulting from the dissolution rate of the microparticles on the membrane (Floroiu et al, 2018).

The limiting factor for the dissolution of FB-COOH is its low solubility in aqueous media. Despite the spray drying process reduced the particle size compared to the raw material, this was not enough to modify FB-COOH dissolution rate in PBS pH 7.4 (Fig. 2.6). The equilibrium solubility of FB-COOH spray-dried microparticles in this buffer, in fact, was unchanged compared to the FB-COOH raw material (1.5 mg/ml at 37 °C).

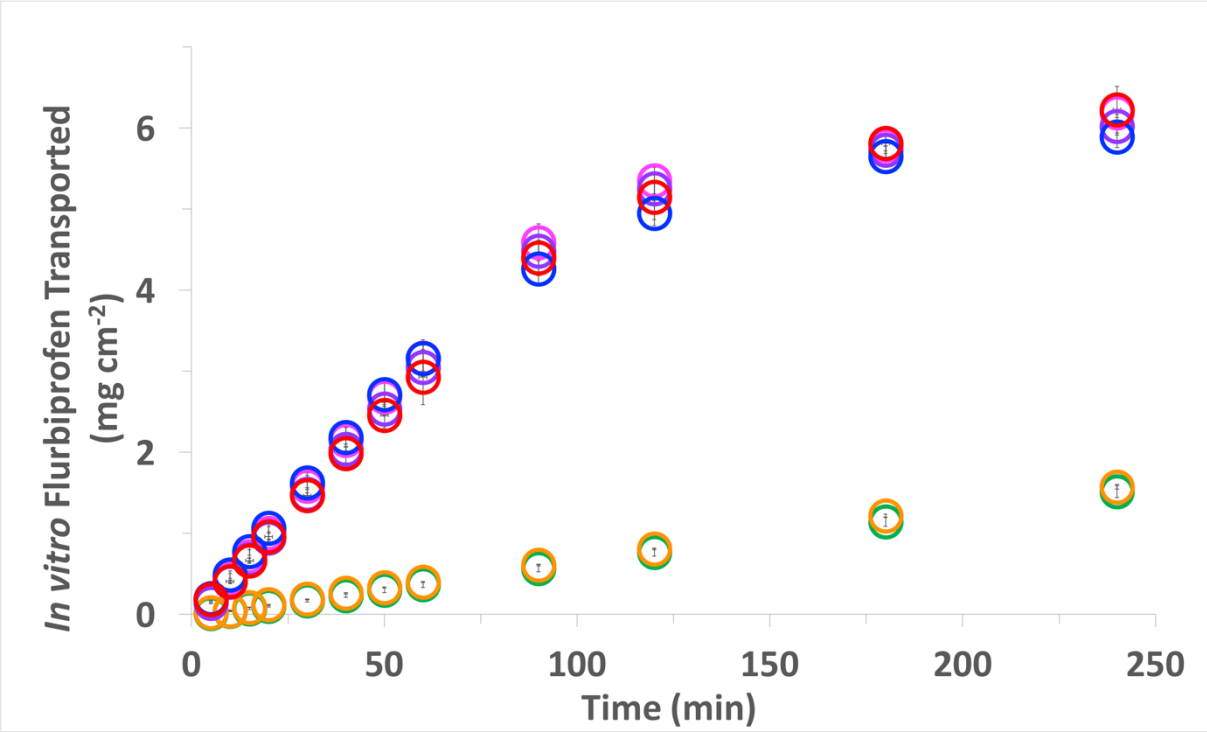

Figure 2.6. *Flurbiprofen dissolution/transport across a regenerated cellulose membrane in PBS pH 7.4 at 37 °C from: raw material (green), Mini B-191 FB-COOH (F2; orange), Mini B-191 FB-COONa (F3; pink), Nano B-90 FB-COONa dried at 70 °C (F13_70; violet), Nano B-90 FB-COONa dried at 40 °C (F13_40; red), Nano B-90 FB-COONa with lecithin (F15_70; blue) microparticles. Data are expressed as mean ± SEM, n=3.*

In contrast, regardless of the equipment used for their manufacturing, the dissolution of the drug from all the FB-COONa spray-dried microparticles measured with Franz cells, started almost immediately and continued rapidly. After 4 h, the amount of drug released per unit area across the artificial membrane was 6.19 ± 0.02 mg cm^{-2}, 6.02 ± 0.11 mg cm^{-2} and 6.23 ± 0.3 mg cm^{-2} (amounts expressed as FB-COOH), respectively for Mini spray-dried (F3) and Nano spray-dried FB-COONa microparticles spray-dried at 70 °C and 40 °C (F13_70 and F13_40) (P >0.05). The linearity of the dissolution profiles during the first h allowed to calculate the drug dissolution rate from the slope of the straight line (Tab. 2.III).

Table 2.III. *In vitro flurbiprofen dissolution rates during the first hour with Franz cells and the regenerated cellulose membrane (mean ± SEM, n=3); flurbiprofen steady-state flux (J_{SS}) and apparent permeability coefficient (P_e) from the ex vivo transport experiments with Franz cells and the nasal mucosa (mean ± SEM, n ≥5).*

FORMULATION	***In Vitro* Dissolution Rate 0-60 min (µg min^{-1})**	***Ex vivo* J_{SS} *10^{-4} (mg cm^{-2} s^{-1})**	***Ex vivo* P_e *10^{-5} (cm s^{-1})**
Saturated solution	-	0.43 ± 0.02	2.9 ± 0.1
Raw material	3.7 ± 0.3	0.75 ± 0.08	5.0 ± 0.5
F2	4.0 ± 0.0	1.44 ± 0.04	9.6 ± 0.3
F3	31.9 ± 2.3	2.99 ± 0.08	2.0 ± 0.1
F13_70	30.8 ± 0.5	3.04 ± 0.22	2.0 ± 0.1
F13_40	29.3 ± 3.1	4.23 ± 0.19	2.8 ± 0.1
F15_70	31.6 ± 1.5	2.62 ± 0.26	1.7 ± 0.2

Compared to FB-COOH, the significantly faster dissolution (P <0.05) was the result of the higher solubility of the FB-COONa spray-dried microparticles in the release medium, which was 10-fold as higher as that of the parent acid drug (15.6 mg/ml at 37 °C). The comparison of the salt spray-dried microparticles among them showed that they dissolved at the same rate, despite the differences observed in their particle size distributions. In the experimental set-up with Franz cells, powder dissolution on the

membrane is followed by drug permeation and dilution in the receptor medium. It has been observed with nanoparticles that the combination of dissolution and permeation across a permeable membrane can modify the particle dissolution behavior *in vitro* compared to a dissolution set-up where permeation is impeded (Sironi et al., 2017). Thus, the experimental set-up here adopted may have hidden the effect of particle size on the dissolution rate of the different types of FB-COONa spray-dried microparticles. The addition of 8% (w/w) lecithin to the FB-COONa spray-dried microparticles composition (F15_70) did not affect drug dissolution (5.89 $\pm$ 0.13 mg cm^{-2} as acid).
None of the salt spray-dried microparticles reached 100% of drug dissolved at the end of the 4 h and dissolution significantly slowed down beyond 90 minutes due to the substantial reduction of the concentration gradient across the diffusional barrier. Drug dissolution was measured *in vitro* over 4 h, being aware that this time frame greatly exceeds the residence time of any formulation in the nasal cavity (Illum et al., 2003). Indeed, the amounts dissolved in 1 h (>40% of the initial loading in the cell) and the corresponding dissolution rates (Tab. 2.III) are relevant for the purpose of nose-to-brain delivery for all spray-dried microparticles containing the drug salt form, with and without lecithin.

Ex vivo flurbiprofen transport across rabbit nasal mucosa

FB-COOH belongs to the Class II of the Biopharmaceutical Classification System of drugs, i.e., it has low aqueous solubility and high permeability. Aiming to its administration in powder form via the nasal route, the penetration into the mucosal barrier relies on its capability to dissolve on the tissue surface and diffuse across it. Thus, the transport of flurbiprofen across excised rabbit nasal mucosa from the spray-dried microparticles was studied. The FB-COOH raw material and a saturated solution in PBS pH 7.4 thereof were the references.
The FB-COOH transported across the tissue in 4 h from the saturated solution was 0.60 ± 0.03 mg cm^{-2} (profile not shown in Fig. 2.7). The absolute amount transported corresponded to about 47% of the drug initially loaded in the donor. The amount loaded was small, limited by the solubility of the drug in the aqueous solvent and the volume of the donor compartment. The same limitation exists *in vivo* and drives the interest toward solid nasal dosage forms like powders. Indeed, the drug transport was improved using the FB-COOH raw material (1.02 ± 0.11 mg cm^{-2}, as FB-COOH; profile shown in Fig. 2.7), even though the difference with the saturated solution became

statistically significant only from the 2 h on ($P < 0.05$). 14% of the FB-COOH loaded at time zero was found in the receptor after 4h. The linearity of the profiles up to 3 h proved that steady state flux was attained, being with the solid form almost twice that measured with the saturated solution (Tab. 2.III). The apparent permeability coefficient was calculated in both cases assuming that the concentration of flurbiprofen in the donor was equal to its equilibrium solubility in PBS pH 7.4 at 37 °C and did not change during the experiment. In this regard, the progressive dissolution of the raw material at saturation in the small fluid volume layering on the mucosa kept the concentration gradient constant across the barrier for the whole duration of the experiment. Consequently, the permeability was significantly higher for the solid. Conversely, the initial concentration of FB-COOH in the solution substantially decreased in consequence of the permeation, not sustaining the drug diffusion process and the flux. This result confirmed the interest toward a solid dosage form of the drug for nasal administration. Thus, FB-COOH was processed by spray drying to obtain the first spray-dried microparticles (F2). Compared to the raw material, the FB-COOH Mini B-191 spray-dried microparticles (Fig. 2.7) enhanced the permeation of flurbiprofen across the mucosal membrane (1.95 ± 0.09 mg cm^{-2} permeated in 4 h, corresponding to 23 ± 3% of the flurbiprofen loaded; $P < 0.05$). This result did not pair with what seen in the *in vitro* dissolution experiments with the artificial membrane, where the dissolution rate of the F2 spray-dried microparticles was not significantly different from the raw material (Fig. 2.6, Tab. 2.III). This apparent mismatching could be explained recalling the effect of permeation on dissolution rate. As the powder dissolves on the barrier surface, the molecules will leave the dissolution environment. The regenerated cellulose membrane and the excised nasal mucosa are different barriers, the latter being thicker, less permeable and depending on the partition coefficient. Thus, permeation should occur more slowly across the mucosa than the artificial membrane. This barrier-dependent slower permeation may affect the dissolution rate of powder on the membrane compared to what happens with the artificial membrane. In these conditions the effect of particle size on powder dissolution can be determinant. Since the size difference between the spray-dried F2 microparticles ($d_{v,50}$ 14.16) compared to the raw material ($d_{v,50}$ 16.27) was not significant, one would expect that, from the same formulation, flurbiprofen transport occurred more slowly across the mucosa than the artificial membrane. This was not the case for F2. One could also expect that the actual powder distribution on the mucosa of F2 spray-dried microparticles, compared

to the cellulose membrane, may have impacted the effective surface for microparticle dissolution (Table 2.III). The biological barrier combined positively with the better F2 microparticle characteristics relevant to transport, like wettability and dissolution, not disregarding the deposition and contact between powder and surface. (Tab. 2.III).
In addition, a significant difference was found in the small amounts of flurbiprofen accumulated in the nasal mucosa (0.13 ± 0.01 mg vs 0.09 ± 0.01 mg as FB-COOH, respectively for the raw material and F2 spray-dried microparticles; $P < 0.05$). It cannot be excluded that these amounts of drug accumulated in the tissue, although small, were due to a structural difference in the nasal mucosa specimens.

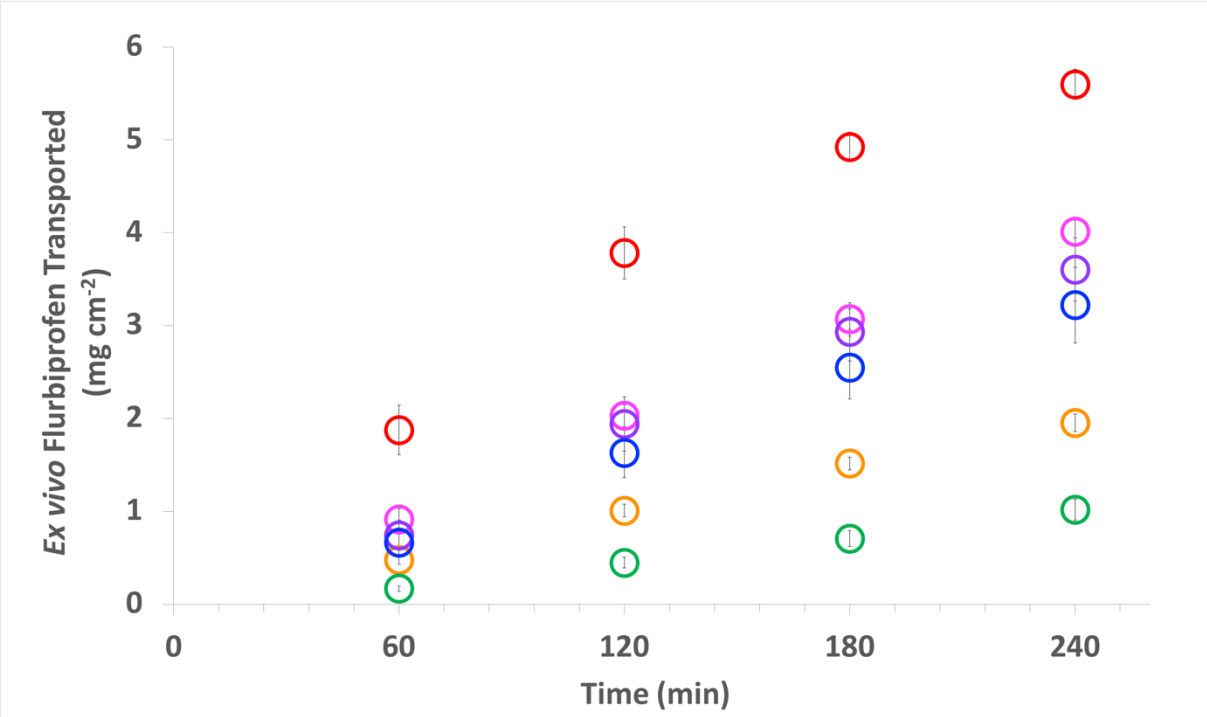

Figure 2.7. *Flurbiprofen transport across rabbit nasal mucosa from: FB-COOH raw material (green); Mini B-191 FB-COOH microparticles (F2; orange), Mini B-191 FB-COONa microparticles (F3; pink), Nano B-90 FB-COONa microparticles spray-dried at 70 °C (F13_70; violet), Nano B-90 FB-COONa microparticles spray-dried at 40 °C (F13_40; red), Nano B-90 FB-COONa with lecithin microparticles spray-dried at 70 °C (F15_70; blue). Data are expressed as mean ± SEM (n≥5).*

In contrast, a significantly higher drug transport was measured in 4 h from the Mini B-191 FB-COONa microparticles F3 (4.0 ± 0.2 mg cm^{-2}, 56 ± 6% of the initial loading; $P < 0.05$) (Fig. 2.7). This result was the consequence of the higher water solubility and dissolution rate of the sodium salt of the drug. The steady state flux was doubled compared to the FB-COOH particles F2, whereas the permeability coefficient was

reduced to one fifth. P_e is the ratio between steady state flux and drug equilibrium solubility in the donor, which is higher for the sodium salt. The amount of flurbiprofen extracted from the mucosa was 0.36 ± 0.02 mg for F3 (*vs* 0.09 ± 0.01 mg for F2).

The spray dryer equipment did not produce an effect on the drug transport across the mucosa when comparing the Nano B-90 FB-COONa microparticles dried at 70 °C (F13_70) with the Mini B-191 ones (F3). In fact, their 4 h transport profiles, steady state flux across the mucosa and permeability coefficient were not significantly different (Fig. 2.7, Tab. 2.III). The mucosa contained the same amount of flurbiprofen (0.36 ± 0.03 mg). This result paired with the observed no difference in the respective *in vitro* dissolution rates (Fig. 2.6).

In contrast, the inlet temperature at which the Nano B-90 was operated, affected the drug transport, being the amount permeated per unit area significantly higher for the FB-COONa microparticles spray-dried at 40 °C (5.60 ± 0.16 mg cm^{-2} *vs* 3.61 ± 0.34 mg cm^{-2}, for F13_40 and F13_70, respectively; Fig. 2.6). The permeation parameters were increased (Tab. 2.III) and the higher permeation was also associated with a significantly lower amount of flurbiprofen accumulated in the mucosa (0.23 ± 0.01 mg; $P < 0.05$). The size analysis of the two Nano B-90 microparticle formulations had evidenced that F13_40 size was significantly smaller than F13_70. It is reasonable that the higher drug permeation across the mucosa derives from the smaller size, despite no differences were measured in the respective dissolution rates with the artificial membrane. As previously discussed, the conditions of powder dissolution on the artificial membrane may have been non-discriminating with respect to particle size. The higher flux of F13_40 microparticles could derive in part from their significantly smaller size distribution compared to F13_70. In addition, as seen by PXRD analysis, F13_40 had a different crystallinity, characterized by the presence of a second polymorph and certain amorphous content. In light of this, there is the possibility that this powder dissolved on the mucosa giving rise to the formation of a supersaturated solution. However, the respective dissolution rates on the artificial membrane were very similar for all the salt formulations. Aiming to understand the divergence between *in vitro* and *ex vivo* data, we considered again the existence of a positive combination with the mucosa, as observed with the spray-dried flurbiprofen particles F2.

The lecithin presence in the composition of the Nano spray-dried FB-COONa microparticles (F15_70) did not significantly modify flurbiprofen permeation compared

to the composition without lecithin sprayed at the same conditions (F13_70) (3.22 ± 0.41 mg cm^{-2}. P >0.05). Thus, lecithin effect on *ex vivo* drug permeation across rabbit nasal mucosa was substantially neutral, likely because flurbiprofen from the sodium salt compositions permeated extensively by itself. As a final remark, all transport profiles in Fig. 2.7 are linear up to 3 h of permeation, then a slight decrease in their slope is perceivable. As the extensive permeation progressed, the drug concentration in the donor decreased and the steady state conditions were lost. The sink conditions were guaranteed in all cases, with the drug concentration in the receptor solution always below 10% of the solubility in PBS pH 7.4 of the salt form.

2.3.2 Agglomerates of spray-dried microparticle powders

2.3.2.1 Manufacturing: yield and drug content

The previously characterized FB-COOH and FB-COONa spray-dried microparticles were used as building blocks to construct the soft pellets or agglomerates, which constitute the final dosage form for nasal drug delivery. Mainly due to their coarse size, these agglomerates already proved suitable as solid dosage form for i.n. administration, by facilitating dosing and delivery compared to the smaller microparticles (Giuliani et al., 2018). The delivery by a nasal device breaks them into smaller fragments (Russo et al., 2004). After i.n. deposition and wetting by the mucosal fluid, the fragments de-agglomerate restoring the advantages of the original microparticles in terms of dissolution rate and transmucosal permeation (Balducci et al., 2013). Microparticle agglomerates can be of two types depending on whether they are composed of one or multiple microparticle populations (Russo et al., 2004 and 2006; Raffin et al., 2007). An example of the first type could be the agglomerates of pure drug microparticles (here the FB-COONa spray-dried microparticles) or microparticles of drug formulated with excipient (here the FB-COONa spray-dried microparticles with lecithin). The second type of agglomerate system comprises pure drug microparticles (population 1) blended with a second microparticle population at a given ratio. Population 2 can be represented by microparticles of a second drug or by drug-free microparticles. In the first case, this opens to the possibility of combining two drugs in the same dosage form.

In the phase-III clinical trial, the R-enantiomer of flurbiprofen was administered orally to AD patients at doses of 400 mg or 800 mg twice a day (Green et al., 2009). Flurbiprofen topical oromucosal products already on the market, provide the patient

with a dose of about 8 mg flurbiprofen per spray, which could be easily deposited and cover the nasal mucosa. In addition, a commercial nasal powder of sumatriptan deliver 20 mg of powder (Tepper, 2016). Thus, agglomerates of pure drug microparticles appeared more suitable for delivering a high drug dose *per* puff of nasal powder of flurbiprofen. For envisaged AD prevention therapy, it may require doses in the order of tenths of milligrams, i.e., the same order of magnitude of the amount of powder that can be insufflated daily by a man (Tiozzo Fasiolo et al., 2018). For this reason, it was decided to produce agglomerates with the FB-COONa spray-dried microparticles. These were preferred as they were superior to FB-COOH ones for dissolution rate and *ex vivo* permeation. The agglomeration process was carried out only by the sieve vibration method with the Mini SD (F3) and Nano SD FB-COONa (F13_70 and F13_40) microparticles. Agglomerates did not form in all cases, as the particles did not aggregate spontaneously. Concerning F3, their behavior was different from what previously described in literature using primary spray-dried microparticles mainly composed of mannitol plus 8% (w/w) lecithin (Balducci et al., 2013) and obtained using the Mini SD B-191 with a water/ethanol feed. It was hypothesized that the particle composition and/or the organic solvent in the feed influenced the agglomeration properties of the primary spray-dried microparticles. Thus, mannitol/lecithin (ML), weight ratio 92:8, spray-dried microparticles named “excipient microparticles”, were manufactured with the Mini spray dryer according to Balducci et al., 2013. The feed was a solution in a 92:8 (v/v) mixture of water and ethanol (Mini ML_Et) or isopropanol (Mini ML_iPr) (Tab. 2.I). It was found that, with both organic solvents, microparticles were smaller and more narrowly distributed than the Mini SD FB-COONa microparticles (F3) (Tab. 2.II). This could depend on the use of the organic solvent to spray dry the mannitol/lecithin microparticles that accelerated the feed’s evaporation (FB-COONa was spray-dried from an 100% aqueous feed). In addition, ethanol led to slightly smaller particles than isopropanol, likely due to its lower vapor tension. Similarly to Balducci, excipient spray-dried microparticles were agglomerated successfully by sieve vibration, yielding more than 80% in mass of agglomerates bigger than 106 µm in diameter (93% and 79%, respectively for Mini ML_Et and Mini ML_iPr, as reported in tab. 2.IV). In general, the size of the microparticles correlates with their specific surface area: compared to the bigger Mini SD FB-COONa F3 microparticles, the smaller spray-dried excipient microparticles should have greater specific surface area per unit mass. The particle surface is where the cohesive forces

develop, favoring the agglomeration. In addition, the spray-dried excipient microparticles contained lecithin as binder. Unfortunately, FB-COONa could not be spray-dried together with lecithin with the Mini SD apparatus, but only with the Nano spray dryer.

We hypothesized that the non-agglomeration of the drug spray-dried microparticles alone was caused by the absence of lecithin. Thus, Nano SD FB-COONa microparticles (F15_70) containing of 8% (w/w) of lecithin in their composition were manufactured. However, the microparticles did not form agglomerates either. As the two spray dryers operate at different inlet temperatures, spray generation and particle collection mechanisms, they could have an influence on the spray-dried microparticle properties relevant to agglomeration like size, surface composition, cohesiveness. Hence, mannitol/lecithin excipient spray-dried microparticles (Nano ML_Et and Nano ML_iPr) were also manufactured with the Nano spray dryer from the same liquid feeds used with the Mini spray dryer, but at lower inlet temperature (40 °C instead of 90 °C). In comparison with the Mini B-191 excipient microparticles, the Nano B-90 excipient microparticles were larger, in particular when using the more volatile isopropanol, and agglomerated with lower yield. Moreover, with no substantial difference in the agglomeration yield depending on the organic solvent (Tab. 2.IV) was obtained with the Nano B-90. This could be related to the lower specific surface area per unit mass of particles deriving from the increased size. Yet these Nano spray-dried excipient microparticles were half the size of the Nano spray-dried FB-COONa microparticles, which did not agglomerate at all.

Thus, it was confirmed that the excipient spray-dried microparticles containing lecithin and manufactured with both apparatuses, were self-agglomerating, although at different extent (Mini B-191 >> Nano B-90). The presence of FB-COONa instead of mannitol, caused the agglomeration properties of the spray-dried microparticles to be lost, irrespective of the spray dryer and the use of lecithin. Maybe, with FB-COONa, lecithin was embedded inside the spray-dried microparticle structure and not available at the surface to promote microparticle cohesion. Parlati et al. (2009) observed that, by spray drying a solution of the surface active sodium stearate (the “additive”) and tobramycin, microparticles for inhalation at high concentrations of the additive on the surface was obtained when the additive amount in solution was lower than its critical micelle concentration (CMC). Additive accumulation on the particle surface was reduced, when the additive concentration in solution was higher than CMC, due to the

formation of micelles in the liquid to spray dry. In this research, the concentration of lecithin was the same in the liquid feed with FB-COONa or mannitol, but the feed of the FB-COONa spray-dried microparticles contained less isopropanol (5% instead of 8% v/v). As lecithin is soluble in the organic part of the hydroalcoholic mixture, at the 5% (v/v) organic solvent concentration supramolecular assemblies, liposome-like, may have formed. Therefore, less lecithin was present at the air/droplet interface and consequently, accumulated on the microparticle surface. To verify this hypothesis, the liquid feeds of F15_70 and Nano ML_iPr microparticles were analyzed by Photon Correlation Spectroscopy. A population of “nanoparticles” was detected, whose diameter was around 30 nm, only in case of F15_70 feed.

Based on these results, the option of agglomerating the drug spray-dried microparticle population alone was abandoned. The FB-COONa spray-dried microparticles obtained with both spray dryers, needed to be blended with a second population of self-agglomerating particles i.e., mannitol/lecithin spray dried microparticles. This explains why they have been called “excipient microparticles”. The agglomeration was carried out by the two methods i.e., by sieving or by tumbling, focusing on agglomeration yield and drug content in the agglomerates.

Sieve vibration was the first method considered and the agglomerates were initially designed to contain 10% in weight of the non-agglomerating FB-COONa spray-dried microparticles. Thus, 90% of the composition was represented by the excipient spray-dried microparticles. The Mini spray-dried excipient microparticles (Mini ML_Et, ethanol in the feed) were the first choice as they had alone the best agglomeration properties (yield 93%). However, compared to this agglomerate yield, the agglomeration decreased due to the presence of the drug spray-dried microparticles (F3) to about 50% yield (Tab. 2.IV). In addition, the drug content in the agglomerates was lower than the expected value.

Hence, the mass ratio between drug and excipient powders in the agglomerate composition was increased to 50:50 to have higher drug content (equivalent to about 40% w/w as FB-COOH). All the FB-COONa spray-dried microparticles were agglomerated with the Mini ML_Et spray-dried excipient microparticles by sieve vibration, after blending the two particle populations by manual mixing at the intended mass ratio. Having increased the proportion of non-agglomerating drug spray-dried microparticles in the blend, the agglomerate yield was not as high (34%, 26% and 66% of agglomerates >106 µm in diameter, respectively with F3, F13_70 and F13_40, Tab.

2.IV). The drug spray-dried microparticles confirmed their poor agglomeration properties, with the exception of F13_40. Recalling that these particular drug spray-dried microparticles were the smallest ones, the effect of particle size on the agglomeration should be considered, also considering the similarity between to drug spray-dried microparticle and excipient spray-dried microparticle sizes. Moreover, looking at their drug content (Tab. 2.II), F13_40 likely contained some residual moisture from the spray drying, which could have increased cohesiveness.

The drug content in these agglomerates was lower than the theoretical value in all cases, following the same trend as the yield (F13_70 < F3 < F13_40; Tab. 2.IV). It meant that the agglomeration process altered the initial proportion of the two particle populations in the blend pre-agglomeration. The worse the yield, the lower the drug content in the agglomerates. FB-COONa was found concentrated in the non-agglomerated powder, recovered from the collector at the bottom of the sieve pile.

The Nano spray-dried FB-COONa microparticles (F13_70 and F13_40) were sieve-agglomerated also with the excipient microparticles produced with the Nano spray dryer and isopropanol as organic solvent (Nano ML_iPr). The agglomeration yield was quite improved for F13_70 (60% and 54% of agglomerates >106 μm in diameter, respectively for F13_70 and F13_40, Tab. 2.IV), as well as the homogeneity of the agglomerate composition (about 30% and 35% as FB-COOH, respectively). The FB-COOH content still did not comply with the theoretical value. These agglomerates reinforced the observation that agglomeration was favored if the primary spray-dried microparticles had similar size. The first part of this study showed that the spray dryer determined the microparticle particle size, mainly because of the different inlet temperatures and not disregarding the role of the organic solvent, when present. Looking at the respective size distributions of the primary spray-dried microparticles (Tab. 2.II), the agglomeration of drug and excipient spray-dried microparticles both made with the Nano spray dryer likely was favored by the very similar particle size of the two populations. Conversely and with the exception of the agglomerates between F13_40 and Mini ML_Et, the Mini spray-dried excipient microparticles were the smallest ones and, when mixed with drug spray-dried microparticles that were about 3-4 folds bigger, tended to self-agglomerate and exclude the drug ones. In fact, those agglomerates had a quite low FB-COOH content.

The yields obtained with the sieve vibration method were not completely satisfactory as a significant amount of the processed powders was lost because of adhesion to the

sieve mesh. Moreover, the sieves allowed for the segregation of the two spray-dried microparticle populations, negatively affecting the agglomerate FB-COOH content.
Hence, the agglomeration method was changed to powder tumbling, to increase the yield and drug content, while also reducing the effect of environmental humidity. Preliminary trials of agglomeration of Nano spray-dried excipient microparticles alone had led to significantly higher yields than those obtained with the same spray-dried microparticles with the sieves (data not shown). No agglomeration attempt by tumbling was carried out with the drug spray-dried microparticles alone.
Tumbling resulted more efficient for the manufacturing of agglomerates composed of drug and excipient spray-dried microparticles. One reason could be that all the powder remained in the same container during the process, which was not the case with the sieves. As observed with the sieve method, agglomerate formation was favored by excipient particles dried with the same equipment as the drug ones. In fact, tumbling of F13_70 drug spray-dried microparticles with Nano ML_iPr spray-dried excipient microparticles led to higher agglomeration yield than with Mini spray-dried excipient microparticles (87% *vs* 64%, respectively as reported in Tab. 2.IV). Favorably, the drug content was closer to the theoretical proportions in the “all Nano SD” agglomerates (35-44% and 24% as FB-COOH, respectively for F13_70 agglomerated with Nano ML_iPr or Mini ML_Et as reported in Tab. 2.IV). The same behavior was seen with the Nano spray-dried FB-COONa microparticles dried at 40 °C (Tab. 2.IV).
Finally, Mini spray-dried FB-COOH microparticles (F2) were also agglomerated with Mini spray-dried excipient microparticles (Mini ML_Et), by both methods, at (50:50) weight ratio. Tumbling was better than sieve vibration method in terms of yield, as previously seen with FB-COONa spray-dried microparticles. The drug content was around 45% regardless of the method (Tab. 2.IV), with no problems of de-mixing of the initial blend.
In conclusion, for microparticle agglomeration, the sieve vibration method was efficient in case of single microparticle population, but deficient when a blend of two different populations was processed. In this case, the microparticle characteristics must be the same, in order to obtain an agglomerates’ population having uniform composition and the drug content expected.
The tumbling method resulted more useful in these mixtures, since the microparticles of the two mixed populations were not separated, as it happens with sieve vibration. However, in the tumbling method, the agglomerated microparticles need to be

collected in the appropriate size range by sieving at the end of the process, whereas this is done automatically during “agglomeration by sieving”, directly recovering the agglomerates having the requested size.

Table 2.IV. *Agglomerates of flurbiprofen and excipient spray-dried microparticles. The table lists the pairs of drug and excipient microparticles and their theoretical mass ratio in the blend before agglomeration, yield of agglomerates with a diameter >106 μm (as % of total processed powder) and drug content as FB-COOH (% w/w). For drug content, data are reported as mean ± standard deviation (n=3 samples). (FB-COOH: flurbiprofen acid; FB-COONa: sodium flurbiprofen; ML: Mannitol/Lecithin; iPr: isopropanol; Et: ethanol).*

Agglomeration method	**Drug spray-dried microparticles ***	**Excipient spray-dried microparticles**	**Drug:excipient microparticles (w/w)**	**Yield (%)**	**FB-COOH content (% w/w)**
Sieve vibration	-	Mini ML_Et	-	93	-
	-	Mini ML_iPr	-	79	-
	-	Nano ML_Et	-	36	-
	-	Nano ML_iPr	-	39	-
	F3	Mini ML_Et	10:90	56	6.1 ± 0.2
	F3	Mini ML_Et	50:50	34	16.8 ± 0.8
	F13_70	Mini ML_Et	50:50	26	12.1 ± 0.4 (size fraction 106 < d < 850 μm) 14.3 ± 3.3 (size fraction >850 μm)
	F13_40	Mini ML_Et	50:50	66	30.6 ± 3.0
	F13_70	Nano ML_iPr	50:50	60	30.3 ± 0.7

	F13_40	Nano ML_iPr	50:50	54	35.0 ± 0.5
	F2	Mini ML_Et	50:50	79	44.0 ± 1.4
Tumbling	F13_70	Mini ML_Et	50:50	64	24.2 ± 1.3
	F13_70	Nano ML_iPr	50:50	87	34.6 ± 2.3 (size fraction 106 < d < 500 μm) 44.2 ± 2.4 (size fraction >500 μm)
	F13_40	Mini ML_Et	50:50	59	23.8 ± 0.6
	F13_40	Nano ML_iPr	50:50	84	35.0 ± 0.7 (size range 106-500 μm) 37.9 ± 1.8 (size fraction >500 μm)
	F2	Mini ML_Et	50:50	88	47.8± 3.8

**The drug content of flurbiprofen spray-dried microparticles is reported in Table 2.II.*

2.3.2.2 *In vitro* flurbiprofen dissolution and *ex vivo* transport across nasal mucosa from agglomerates

The biopharmaceutical characterization focused on the agglomerates produced with the best yields. The *in vitro* flurbiprofen dissolution was studied only for the agglomerates manufactured by sieve vibration with the Nano spray-dried FB-COONa microparticles dried at 40 °C (F13_40) and the Nano ML_iPr spray-dried excipient microparticles (50:50). The agglomerate dissolution profile was not statistically different from that of the corresponding primary drug spray-dried microparticles ($P < 0.05$), despite the mass of powder loaded in the donor at time zero was twice as higher with the agglomerates to guarantee the same flurbiprofen loading. The agglomerates released 6.5 ± 0.1 mg cm^{-2} FB-COOH per unit area across the artificial membrane in 4 h, corresponding to approximately 90% of the drug loading at time zero. Interestingly for the intended nasal administration, where intranasal residence time is short, about 50% of flurbiprofen dissolved from the agglomerates within the first hour. The presence of the excipients in the agglomerate composition did not impact on FB-COONa dissolution in this experimental set-up. Although mannitol is very soluble in water, apparently there was no competition with FB-COONa for the solvent. The solvent volume introduced in the donor for powder dissolution was the same in the two cases.

The *ex vivo* transport across rabbit nasal mucosa was measured for the agglomerates [F13_70:Nano ML_iPr] (size fraction $106 < d < 500$ µm) and [F13_40:Nano ML_ iPr] (size fraction $d > 500$ µm), manufactured by tumbling. The size fractions considered were not the same but had a very similar drug content (Tab. 2.IV). FB-COONa was loaded in the Franz cell's donor in the same amount, which meant that the total powder mass was different for spray-dried microparticles and agglomerates. After 4 h, 4.5 ± 0.2 mg cm^{-2} and 4.9 ± 0.3 mg cm^{-2} FB-COOH permeated per unit area across the nasal mucosa (Fig. 2.8), corresponding to $68 \pm 3\%$ and $65 \pm 4\%$ of the amount loaded, respectively for F13_70 and F13_40 agglomerates. The amount of FB-COOH accumulated in the mucosa was 0.38 ± 0.07 mg and 0.29 ± 0.04 mg, respectively for [F13_70:Nano ML_iPr] and [F13_40:Nano ML_iPr]. The agglomerates' transport profiles differed from those of the corresponding spray-dried microparticles, in particular for F13_70. These agglomerates gave a significantly higher transport than the corresponding spray-dried microparticles at the same "flurbiprofen dose" in the

donor (P <0.05). This may suggest a positive effect of the excipients on drug transport, which was seen here for the first time. In fact, mannitol/lecithin spray-dried microparticles agglomerated with ribavirin had negatively affected *ex vivo* drug transport (Giuliani et al., 2018).

The *ex vivo* drug transport was slightly different for F13_40 and its agglomerates, although statistical significance was not found. The amount permeated was lower from F13_40 agglomerates compared to the spray-dried microparticles. The possibility of a negative effect of the excipients could not be excluded, but it would be hard to pair with the results obtained for F13_70. In addition, another variable to consider is the different deposition density of the powder on the permeation area. Agglomerates are bigger and may not fully cover the available surface. Indeed, F13_40 agglomerates with a diameter >500 µm were tested.

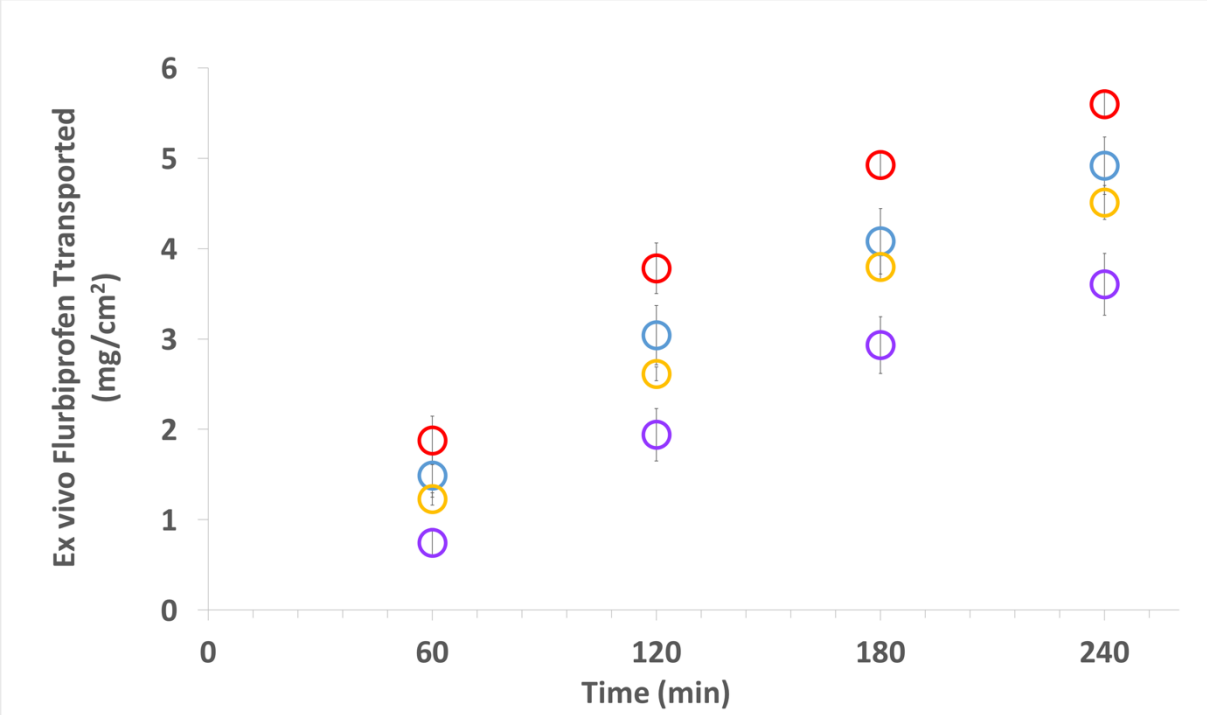

Figure 2.8. *Ex vivo flurbiprofen transport across rabbit nasal mucosa from agglomerates of F13_40 (blue) or F13_70 (yellow) with Nano spray-dried ML_iPr microparticles versus F13_40 (red) and F13_70 (violet). Data are expressed as mean ± SEM (n≥5).*

2.4 CONCLUSIONS

The flurbiprofen spray-dried powders, in particular the ones comprising FB-COONa, exhibited physico-chemical and biopharmaceutical characteristics fitting the product

target profile for nasal administration in view of nose-to-brain targeting. By spray drying FB-COONa, the resulting microparticulate powders dissolved at high rate and sustained the *ex vivo* drug transport across rabbit nasal mucosa for a convenient time. The manufacturing of these drug spray-dried microparticles was more efficient using the Nano B-90 spray dryer not only for the yield of production. In fact, compared to the conventional Mini B-191 spray dryer, the Nano B-90 provided particle size and crystallinity properties leading to a more suitable biopharmaceutical profile with respect to the intended nasal application. Finally, the particle resulted stable in terms of drug content and dissolution rate for the nasal product preparation.

The biopharmaceutical behavior of agglomerates showed some differences compared the respective primary spray-dried microparticles. In particular, it was found that agglomerates containing F13_70 spray-dried microparticles gave a significantly higher transport than the corresponding spray-dried microparticles, while agglomerates containing F13_40 spray-dried microparticles led to a lower transport profile *versus* the respective spray-dried microparticles.

Based on these findings, the agglomerates of Nano B-90 FB-COONa spray-dried microparticles and Nano B-90 spray-dried mannitol/lecithin microparticles were selected for the subsequent evaluation *in vivo*.

CHAPTER 3
IN VIVO ADMINISTRATION OF FLURBIPROFEN

In **this phase**, the *in vivo* serum levels and brain uptake of flurbiprofen after i.n. administration in powder form were investigated. Two powders, in the form of spray-dried microparticles and agglomerates, were administered i.n. to rats by means of a commercially available delivery device. For comparison purposes, flurbiprofen sodium salt solution administered intranasally (i.n.) and intravenously (i.v.) were investigated by measuring serum level and brain uptake of drug.

The *in vivo* experiments were carried out during the mobility period at the National and Kapodistrian University of Athens, under the supervision of prof. Georgia Valsami and prof. Dimitrios Rekkas.

3.1 MATERIALS AND EQUIPMENT

Materials

Flurbiprofen raw material (batch n° T17121044) was kindly donated by Recordati S.p.A. (I-Milano). It was used for manufacturing of nasal powders to be administered *in vivo*,; the same substance was elected reference standard for HPLC analysis.

Ibuprofen raw material (batch n° 1301320) was obtained from Dipharma S.R.L. (I-Tomba, UD) and used as internal standard (IS) for the HPLC analysis of the samples from the *in vivo* experiments.

Mannitol (Ph. Eur.) was supplied by Lisapharma S.p.A. (I-Erba) and lecithin (Lipoid® S45) by Lipoid AG (CH-Steinhausen). Acetonitrile, ethanol, isopropanol and methanol were supplied by Sigma-Aldrich® (St. Louis, MO, USA). All other reagents and solvents were HPLC grade.

Equipment

- KERN-AEJ analytical balance (Kern & Sohn GmbH, Balingen, Germany) (0.01-220 g ± 0.1 mg)
- HERMLE Z32HK centrifuge (HERMLE Labortechnik GmbH, Wehingen).

3.2 METHODS

3.2.1 Preparation of flurbiprofen formulations for nasal administration

3.2.1.1 Flurbiprofen aqueous solution

A flurbiprofen solution for intravenous (i.v.) and intranasal (i.n.) administration was prepared by adding an excess amount of a FB-COONa lyophilized powder into water for injection and leaving it under magnetic stirring for 24 hours at room temperature. The saturated solution obtained was then filtered through a regenerated cellulose membrane filter (0.45 µm). Flurbiprofen concentration in the filtrate was measured by HPLC method immediately and was equal to 15.61 ± 0.01 mg/ml. The solution was divided in 2 ml aliquots using Eppendorf tubes and stored at -20 °C until use *in vivo*. These storage conditions guaranteed solution stability, as confirmed by HPLC determination prior to use.

3.2.1.2 Flurbiprofen nasal powders

Flurbiprofen powders for nasal administration were the spray-dried microparticles of FB-COONa and their agglomerates with the spray-dried excipient microparticles. In

particular, the spray-dried microparticles were those coded F13_70, i.e., FB-COONa spray-dried microparticles obtained with the Nano B-90 at 70 °C inlet temperature. As seen, this powder contained 80% FB-COOH (Tab. 2.II). Drug content was confirmed by HPLC determination before use *in vivo*. Hence, the choice to employ F13_70 spray-dried microparticles was mainly based on the drug content, that was the highest of the microparticles manufactured with the Nano B-90.

The agglomerates studied in vivo were those prepared from a 50:50 blend of FB-COONa spray-dried microparticles (F13_40) with Nano ML_iPr spray-dried excipient microparticles, since these agglomerates showed no difference in *ex vivo* study compared to F13_70:Nano ML_iPr agglomerates. Both drug and excipient spray-dried microparticles had been manufactured by Nano SD and agglomerated by the tumbling method. The agglomerated fraction administered *in vivo* was in the range 106-500 μm, which was assayed by HPLC before use. These agglomerates confirmed the drug content.

FB-COOH spray-dried microparticles (F2) (Tab. 2.II) were also administered i.n.

3.2.2 *In vivo* experiments

Animals and housing conditions

All animal experiments were performed in the animal facility of the Centre of Clinical, Experimental Surgery and Translational Research of the Biomedical Research Foundation of the Academy of Athens. The facility is registered as “breeding” and “experimental” facility according to the Greek Presidential Decree 56/2013, which harmonizes the national legislation with the European Community Directive 2010/63 on the Protection of Animals used for Experimental and Other Scientific Purposes.

Wistar-type rats were housed in individually ventilated cages (Techniplast, I-Varese) under specific pathogen-free (SPF) conditions and constant environmental conditions (12:12 hours light:dark cycle, temperature 22 ± 2 °C, relative humidity 45 ± 10%). The rats were fed irradiated pellets (2918 Teklad Global 18% Protein Rodent Diet, Harlan Laboratories, Indianapolis, USA) and had access to tap water *ad libitum*. The cage bedding, comprising corncob granules (REHOFIX®, J. Rettenmaier & Söhne Co., Rosenberg Germany), was changed once a week as well as the cage. All rats were screened regularly by using a health-monitoring program, in accordance to the Federation of European Laboratory Animal Science Associations’ recommendations.

The experimental protocol of the study was approved by the Veterinary Authorities of Region of Athens Greece (Ref. Num. 5043/21-09-2017, EL25BIO03).

Pharmacokinetic study protocol

8-week old Wistar-type rats were included in the pharmacokinetic study. The animals were randomly divided in four groups. In each group the same drug dose was administered to the animals independently on their actual weight (body weight 350 ± 50 g, mean ± standard deviation):

a) 4.5 mg of FB-COOH intravenously (0.3 ml of the 15 mg/ml aqueous solution through the left tail vein, i.v. group)
b) 0.3 mg of FB-COOH intranasally (0.02 ml of the 15 mg/ml aqueous solution, i.n. solution group)
c) (6.7 ± 1.0 mg)** of FB-COOH intranasally with the FB-COONa spray-dried microparticles F13_70 batch (i.n. salt microparticle group)
d) (4.2 ± 0.4 mg)** of FB-COOH intranasally with the agglomerates of FB-COONa spray-dried microparticles F13_40 batch with Nano ML_iPr excipient microparticles (i.n. agglomerate group).

The two asterisks (**) indicate that the dose corresponds to the powder amount insufflated in the rat nose.

The rats in each group were divided in cohorts of five and each cohort represented a different sampling time point. Additionally, three animals received (8.2 ± 1.5 mg)** of FB-COOH intranasally with the F2 spray-dried microparticles (i.n. acid microparticle group). The administration data of the powder are summarized in Table 3.I.

The animals were anaesthetized with an intraperitoneal injection of ketamine (100mg/kg) and xylazine (0.1 mg/kg). Nasal administration of flurbiprofen formulations was performed following different procedures for solution and powders. For the solution administration, both the nostrils were used with the rat lying and hold in supine position. 20 μl of flurbiprofen solution (equivalent to 0.3 mg dose of FB-COOH) were introduced in the rat's nostrils using a semiautomatic pipette: 5 μl fractions were pipetted alternatively into the right and left nostril. The administration lasted less than 1 min. For the powders, the rat lay down on the right side, making the left nostril accessible for the administration (Fig. 3.1).

Figure 3.1. *Position of the rat during the administration of the nasal powders: the rat lay down on the right side to administer the powder into the left nostril.*

A single-dose pre-metered powder sprayer device was employed, namely the UDS nasal spray device for powders (Aptar, F-Louveciennes). The device comprises a mechanical pump connected to a nasal adapter (designed for small animals) and a reservoir of the solid formulation (see Fig. 1.6). Prior to powder administration to the rat, either the spray-dried microparticles or the agglomerate powder were accurately loaded into the devices. The sprayer's cartridge was filled with 12-15 mg of each powder; then, the assembled device was weighed to 0.1 mg. The insufflator tip was introduced in the rat nostril for a depth of 1-2 mm.

After actuation into the animal left nasal cavity, the device was re-weighed to determine the quantity of powder emitted and calculate the actual dose administered. Then, blood samples were collected in non-heparinized Eppendorf tubes at 5, 10, 20 and 30 min after administration via puncture of the right tail vein. Brain sampling was also performed at the same time points after the rat's sacrifice, performed by sampling 5 ml blood from the caudal vena cava, followed by total body perfusion with cold PBS pH 7.4 (5 min, 120 ml) to remove the blood from the intracerebral vessels (see section 3.2.3). Blood samples were directly centrifuged to separate the serum. Serum and brain samples were frozen and stored at -70 °C until HPLC analysis.

3.2.3 Extraction of flurbiprofen from serum and brain samples

The flurbiprofen extraction procedure from rat's biological samples was adapted from the method reported by Christodoulou et al., 2015 using ibuprofen as internal standard (IS).

Flurbiprofen extraction from rat's serum

0.5 ml of IS solution in acetonitrile (ibuprofen 0.7 mg/ml) and 0.05 ml of methanol were added to 0.25 ml of serum and vortexed for 15 sec. After centrifugation (10 min, 7.500 x g, 20 °C) for the separation of the precipitated proteins, the clear supernatant was directly used for flurbiprofen quantification in the sample by HPLC. When flurbiprofen concentration in serum exceeded the linearity range for drug quantification, each serum sample was properly diluted with blank serum before extraction procedure. The efficiency of the drug extraction method from the serum samples was studied in samples containing from 5 to 1260 ng/ml flurbiprofen. Drug recovery was determined to be exactly 100% in the range 90-1260 ng/ml flurbiprofen concentration in serum samples.

Flurbiprofen extraction from rat's brain

After the animal's death, the rat's body was perfused with cold PBS pH 7.4 1M (120 ml) to remove the blood. To this purpose, the rat's abdominal area was disinfected with a hydro-alcoholic solution (ethanol 70% v/v) before being opened with bistoury. The caudal vena cava was catheterized and 5 ml blood were immediately collected with a 10 ml syringe. Then, the xiphoid cartilage was lifted up, the chest opened and the pleura removed to release the heart. PBS was perfused at 24 ml/min rate by mean of a Watson Marlow 323 peristaltic pump (I-Mazzano, BS) connected with a 23G butterfly needle into the left ventricle of the rat's heart. After the perfusion, the brain was dissected from the head, washed superficially with water for injection, weighed and stored in the freezer (-70 °C) into a plastic box.

For the i.v. group, the total brain was considered, including the olfactory bulb. For the i.n. groups, the olfactory bulb was separated and studied independently of the brain, considering that the i.n. administration may determine high drug concentration in this compartment very close to the nasal cavity.

On the day of analysis, the brain was defrosted at room temperature and homogenized with IKA® ULTRA TURRAX® (IKA-Werke GmbH & Co. KG, Staufen im Breisgau, Germany) after adding a suitable volume of PBS 1M pH 7.4. For the bulb, the homogenization in PBS took place in a 2-ml Eppendorf by crushing the tissue with a polypropylene micro-pestle (Sigma-Aldrich, St. Louis, MO, USA). The tissue suspension resulting after homogenization was centrifuged to remove the coarse material (3 min, 3.000 x g, 20°C). Then, the supernatant of the suspension was used

for the extraction procedure (as described for the serum) and subsequent HPLC analyzed.

3.2.4 HPLC-FLD method for flurbiprofen determination

Quantification of flurbiprofen in the drug formulations and biological samples was performed by reverse phase high performance liquid chromatography with fluorescence detector (HPLC-FLD). The method was different from the one described in chapter 2. The apparatus was a Shimadzu chromatographer (Kyoto, Japan) equipped with a LC-20AD pump, a fluorescence detector Shimadzu SPD-M20A, a DGU-20A5R degasser, a SIL-HTc autosampler and a CTO-20AC prominence oven. Isocratic elution was carried out with a NaH_2PO_4 20 mM:CH_3CN (40:60) mobile phase (pH 3.0 $\pm$ 0.1) at 30 °C. The detection wavelength was set at 254 nm and 308 nm for excitation and emission, respectively. The column was a Zorbax Eclipse XDB C18, 5 µm (4.6 x 15 mm; Agilent, Santa Clara, CA, USA). The flow rate was 1 ml/min and the injection volume 20 µl.

In these conditions, the retention time of flurbiprofen was 3.9 min, while the IS (ibuprofen) was eluted at 5.1 min. The method was developed in-house and validated with respect to linearity, repeatability, matrix effect, limit of quantification (LOQ) and limit of detection (LOD).

The stock solution of flurbiprofen (0.5 mg/ml) and the one of IS (ibuprofen, 0.7 mg/ml) were prepared in acetonitrile and stored at 2-8 °C for up to 2 weeks before use. By dilution of aliquots of both stock solutions with acetonitrile, standard solutions of flurbiprofen 3-1300 ng/ml with the IS concentration fixed at 24 µg/ml were obtained and used for the construction of the calibration curves in the biological matrices, which were rat serum and brain homogenate in PBS 1M pH 7.4. Each point of the calibration curve corresponded to a sample obtained adding 0.5 ml of standard solution and 0.05 ml of HPLC grade methanol to 0.25 ml of rat serum or brain previously homogenized in the buffer solution.

Linearity range was described by the equation y= 0.0349x + 0.1764, R^2= 0.9999 (mean of 3 calibration curves in rat serum, 3-1300 ng/ml FB-COOH). The **matrix effect** on the slope and intercept of the straight line was found not influential comparing the straight lines from samples rat serum with those from brain homogenate (data not reported). **Repeatability** of HPLC method was assessed by 6 consecutive injections of samples at 3 ng/ml, 95 ng/ml, 1260 ng/ml flurbiprofen and 24 µg/ml ibuprofen in

serum. Relative standard deviation resulted equal to 3.2, 0.4 and 0.31 for the lowest, medium and highest flurbiprofen concentration, respectively. Repeatability of calibration curves was also evaluated, both intra-day and inter-day. The calibration curves were always superimposable. **LOQ** (Eq. 3.1) and **LOD** (Eq. 3.2) were calculated based on the Standard Deviation of the Response and the Slope, according to the EMA Guideline (https://www.ema.europa.eu/documents/scientific-guideline/ich-q-2-r1-validation-analytical-procedures-text-methodology-step-5_en.pdf).

$$LOQ = \frac{10\sigma}{S} \qquad \text{Eq. 3.1}$$

$$LOD = \frac{3.3\sigma}{S} \qquad \text{Eq. 3.2}$$

where σ is the standard deviation of the response and S is the slope of the calibration straight line.

LOQ was 5.80 ng/ml and 3.87 ng/ml for flurbiprofen in rat's serum and in brain homogenate in PBS, respectively. LOD was 1.91 ng/ml and 1.28 ng/ml for flurbiprofen in rat's serum and brain homogenate in PBS, respectively.

3.2.5 Non-compartmental PK analysis

Sparse sampling non-compartmental PK analysis (NCA) was performed for both i.v. and i.n data using Phoenix® 7.0 (Certara, Princeton NJ, USA) to determine basic serum and tissue PK parameters, namely $AUC_{0\text{-}t}$, C_{max} and t_{max}, and calculate the absolute bioavailability of flurbiprofen after i.n administration of powders and solution. According to this method for the calculation of the PK parameters and their standard errors (SE), the mean concentration curve was calculated and used in conjunction to the available subject information. The log-linear trapezoidal method was used to calculate $AUC_{0\text{-}t}$. The terminal slope was estimated by linear regression analysis on the last three points of the log transformed concentration *versus* time plot. Furthermore, the elimination half-life, $t_{1/2}$, was calculated as $t_{1/2}=0.693/\lambda$ (λ = elimination constant calculated from the terminal slope of serum curve). The absolute bioavailability (F) of flurbiprofen after i.n. administration was measured by comparing AUCs after i.n and i.v. administration according to Equation 3.3:

$$\frac{AUC_{0-t(i.n.)} \times Dose_{(i.v.)}}{AUC_{0-t(i.v.)} \times Dose_{(i.n.)}}$$ Eq.3.3

where $AUC_{0\text{-}t(i.n.)}$ and $AUC_{0\text{-}t(i.v.)}$ are the area under the concentration - time curve from time 0 to the last sampling time (calculated according to the log-linear trapezoidal rule) after intranasal and intravenous flurbiprofen administration, respectively. $Dose_{(i.n.)}$ and $Dose_{(i.v.)}$ are the respective administered doses.

3.2.6 Data analysis

Nose-to brain delivery indexes

Two indexes were used to quantify the efficiency of nose-to-brain delivery following nasal administration of powders and solution, namely Drug Targeting Efficiency and Direct Transport Percentage (Kozlovskaya et al., 2014; Sonvico et al., 2018). DTE was calculated according to Equation 3.4:

$$DTE = \frac{\left(\frac{AUC_{0-t(brain)}}{AUC_{0-t(blood)}}\right)i.n.}{\left(\frac{AUC_{0-t(brain)}}{AUC_{0-t(blood)}}\right)i.v.} * 100$$ Eq. 3.4

where $AUC_{0\text{-}t(brain)}$ and $AUC_{0\text{-}t(blood)}$ are the areas under the concentration *versus* time curve of the drug in the brain and in the circulation (serum), respectively, after intranasal (i.n.) and intravenous (i.v.) administration.

DTP was calculated according to Equation 3.5:

$$DTP = \frac{B_{in} - B_x}{B_{in}} * 100$$ Eq. 3.5

where B_{in} is the brain AUC following i.n. administration and B_x is a fraction of the same AUC accounting for the drug fraction that reached the brain *via* the systemic circulation (across BBB). B_x can be calculated according to Equation 3.6:

$$B_x = \frac{B_{iv}}{P_{iv}} * P_{in}$$ Eq. 3.6

where P_{iv} is the blood AUC following i.v. administration, and P_{in} is the blood AUC following i.n. administration.

3.3 RESULTS AND DISCUSSION

3.3.1 Nasal drug powders manufacturing and combination with the insufflator devices for in vivo experiments

Rat serum level and brain uptake of flurbiprofen after i.n. administration in powder form was compared to its administration in solution by nasal and systemic (i.v.) routes. The main aim was to investigate flurbiprofen disposition in the brain and how it was affected by the different nasal dosage forms, i.e., solid *versus* liquid. This comparison also needed a reference, which was flurbiprofen disposition in the brain after systemic administration by i.v. injection.

The solid formulations employed were F13_70 spray-dried microparticles and agglomerates F13_40. After the *in vitro* and *ex vivo* characterization, it was essential to compare *in vivo* the spray-dried drug microparticles and agglomerates, in order to assess the transport to brain via nasal route. In both cases, the nasal powders contained the more soluble flurbiprofen sodium salt, which *in vitro* had proven to speed up the dissolution rate, as well as the *ex vivo* transport across the rabbit nasal mucosa. Comparing the spray-dried microparticles with the agglomerates, the first contained only drug. Conversely, the presence in the agglomerates of mannitol/lecithin reduced the flurbiprofen content. This difference in the powders' drug content affected the dose given to the animals, since the protocol planned to introduce into the nose the same amount of powder. Due to their coarse size, the agglomerates resulted more suitable for the nasal administration, because they facilitated accurate dosing in the device and the almost complete delivery, compared to the smaller spray-dried microparticles (Table 3.I). The F13_70 spray-dried microparticles had a median diameter ($d_{v,50}$) around 5 μm (Tab. 2.II), which could favor the deposition on a larger mucosa surface. Concerning F13_40 agglomerates, the presence of excipients could influence *in vivo* drug dissolution from powder and the drug absorption through mucosa. In particular, both mannitol (Deli et al., 2009; Rapoport, 2000) and lecithin (Tian et al., 2012) were described as drug absorption enhancers by different mechanisms.

In order to perform the *in vivo* administration of the powder, the nasal powder was combined with the insufflator device. The device was Unit Dose System, UDS, a new

version of the previous Monopowder device (Fig. 1.6). First, the selection of the UDS device was determined by the need to produce the insufflation by an active device. Aptar designed UDS for drug deposition in the upper part of the nose (olfactory region), which is exploited for drug nose-to-brain transport.

The device was adapted to rat nose anatomy for the drug deposition into the nasal cavity. Aptar provided a special adapter to fit the device tip to the rat nose.

The device performance was assessed by measuring the emitted amount of powders and dose of drug after the insufflation in rat nose. Considering a powder loading of 13-15 mg of spray-dried drug microparticles or agglomerates, the insufflator emitted fractions of the loaded powders between 65-83 % (Table 3.I). It was determined that the efficiency of powder delivery by the UDS device was superior when the device was loaded with the same mass of agglomerates instead of the spray-dried microparticles. More than 80% of agglomerates were emitted using the agglomerates. When F2 spray-dried microparticles were combined with the UDS, the emitted fraction was the lowest (Tab. 3.I).

Table 3.I. *Insufflation efficiency of UDS powder device. Data are reported as mean ± standard deviation.*

Powder	**Powder loading (mg)**	**Emitted powder (mg)**	**Powder Emitted fraction (%)**	**Flurbiprofen Emitted dose (mg)**
F13_70 Spray-dried microparticles	12.9 ± 0.9	8.4 ± 1.2	65.1 ± 9.3	6.7 ± 1.0
F13_40:ML_iPr Agglomerates	14.6 ± 0.7	11.9 ± 1.1	82.7 ± 6.4	4.2 ± 0.4
F2 Spray-dried microparticles	14.0 ± 1.0	8.3 ± 1.5	59.5± 10.3	8.2 ± 1.5

3.3.2 Flurbiprofen serum pharmacokinetic

Flurbiprofen formulations administered *in vivo* were fully retained inside the rat's nasal cavity. After receiving the dose, the animal continued breathing remaining in the same position as during the administration. After powder administration, the nose produced abundant secretion fluid (Fig. 3.2). These secretions were interpreted as physiological reaction to the powder deposition in the nasal mucosa due to the powder dissolution.

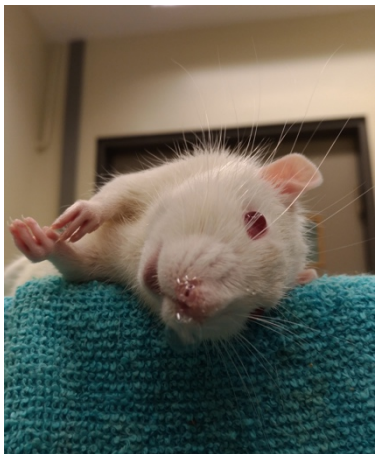

Figure 3.2. *Rat lay down after the nasal powder administration; the white spots around the nostrils are signs of the production of nasal secretion.*

In vivo nasal administration of flurbiprofen microparticles, agglomerates and solution resulted into rapid drug absorption into the blood. When a drug formulation is deposited on the nasal mucosa and the drug is released, its absorption into the blood capillaries occurs across the respiratory region. Flurbiprofen is a lipophilic, low molecular weight molecule and is a weak acid, hence it can cross the nasal epithelium by both the transcellular and a paracellular pathways (Lochhead and Thorne, 2012).

The figure 3.2 reproduces the flurbiprofen levels in serum versus time for all the administrations carried out. Flurbiprofen serum levels for the two nasal powder formulations were higher than for the nasal solution. However, it has to be underlined that the doses administered were not the same and that the dose by i.n. solution was the lowest, i.e., 0.3 mg. The doses administered with the F13_70 microparticles and F13_40 agglomerate powders were 6.7 mg and 4.2 mg, respectively (Tab. 3.I). The C_{max} was achieved within the first 10 min from the administration of both powders (83.3 $\pm$ 3.1 μg/ml serum and 73.4 $\pm$ 6.5 μg/ml, for F13_70 microparticles (n=14) and F13_40 agglomerates (n=10), respectively.). The values reported are mean $\pm$ SEM. F2 spray-

dried microparticles produced flurbiprofen C_{max} at 10 min non-significantly different from the previous powders (data not shown due to the small number of animal tested (n=2).

The flurbiprofen i.n. solution administered led to lower flurbiprofen serum levels compared to the powders (C_{max} 10.0 ± 1.1 µg/ml after 5 min) (Fig. 3.3), due to the much lower drug dose by nasal solution. This was the highest possible dose, being limited by the solubility of FB-COONa in water. Moreover, only 20 µl of solution could be administered into the rat's nose considering the small volume of nasal cavity (0.2 cm^3) (Xi et al., 2016). However, the absorption was faster with the solution than with the nasal solids (t_{max} 5 min vs 10 min), which is reasonable as the drug is already in solution, ready to diffuse across the nasal membranes.

Drug elimination became evident around 30 min, when flurbiprofen serum concentration decreased to 60.6 ± 8.4 µg/ml and 67.4 ± 5.2 µg/ml for the microparticles (n= 5) and agglomerates (n= 3), respectively.

The serum levels following powders administration were not significantly different between microparticles and agglomerates (P> 0.05). Taken together, the results obtained indicate that the microparticles and agglomerated powder were as bioavailable as the i.n. solution. Table 3.II shows the values of fraction absorbed calculated according to Equation 3.1. In particular, the formulation of F13_40 agglomerates provided the highest absorbed fraction, also considering that only one nasal cavity was involved in the administration. This was not case of the i.n. solution that was administered into both the nasal cavities, thus doubling the area available for absorption.

Table 3.II. *Serum absorption and brain disposition of flurbiprofen. Data calculated according to eq. 3.3*

Formulation	Serum absorption	Brain disposition
i.n. microparticles	40.5	127.7
i.n. agglomerates	50.7	110.9
i.n. solution	92.3	73.5
i.v. solution	-	-

Note: compared to the i.n. powders, the i.n. solution was deposited on a double surface area.

Both i.n. F13_70 microparticles and F13_40 agglomerates showed lower drug serum levels in comparison with the i.v. administration of a 4.5 mg dose, value falling between the 4-7 mg dose range administered for the nasal powders (Tab. 3.I): the serum concentration at 5 min after injection was 142.2 ± 6.8 µg/ml (Fig. 3.3).

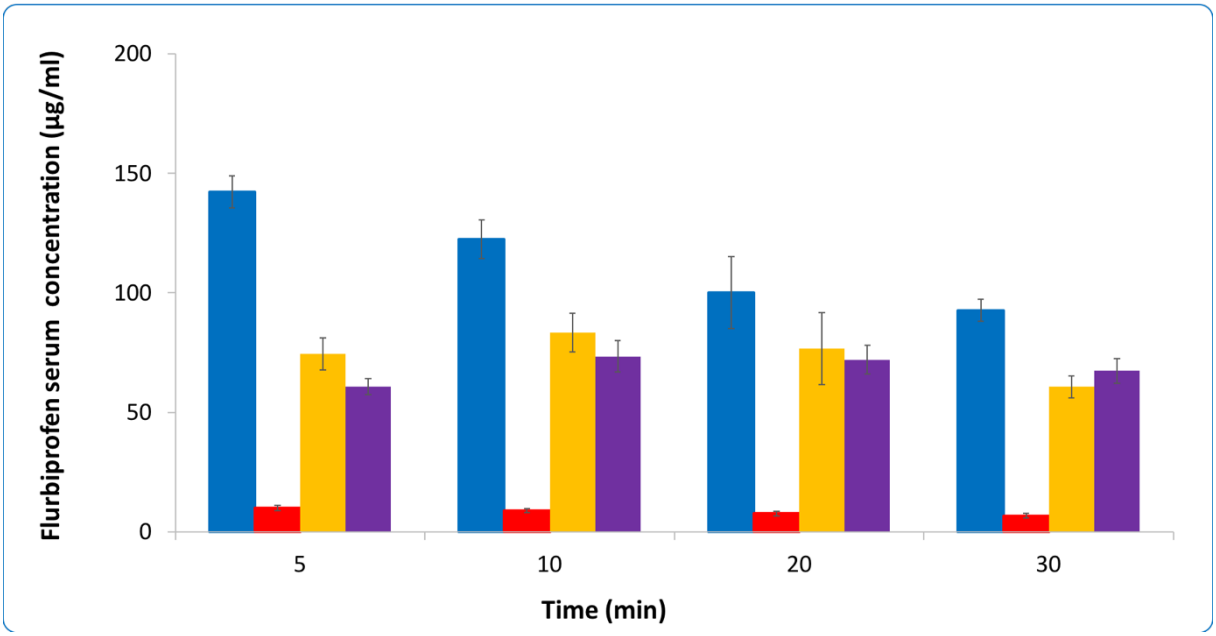

Figure 3.3. *Flurbiprofen concentration in serum after i.v. administration of FB-COONa aqueous solution (blue) and nasal administration of the same FB-COONa solution (red), F13_70 spray-dried microparticles (yellow), FB-COONa-excipient agglomerates (purple). Data expressed as mean ± SEM, n≥5.*

3.3.3 Flurbiprofen brain levels

In Parepally et al. (2006) we read that "There is a widespread interest in NSAIDs regarding the role of COX in CNS disorders. Many traditional acidic NSAIDs show poor delivery to brain based on low brain-to plasma ratios and plasma protein binding. The newer neuroprotective effects recently described to a subset of nonselective NSAIDs, including ibuprofen, indomethacin, and flurbiprofen, and not seen with better penetrating COX-2 or nonselective analogs, suggest that improved brain delivery may be of interest for these poorly distributing NSAIDs to enhance CNS activity and reduce peripheral toxicity. Brain drug delivery in AD is complicated by a number of alterations in the BBB and CSF system leading to decrease in CSF production rate, enhanced CSF volume, and altered expression and function of transporters. Design of NSAIDs with less plasma protein binding, less efflux transport, enhanced cellular uptake, and greater free drug distribution to brain may aid in CNS efficacy."

In the present study, both nasal F13_70 microparticles and F13_40 agglomerate B allowed flurbiprofen to reach the brain (C_{max} 1.2 ± 0.1 µg/g tissue and 0.8 ± 0.1 µg/g, respectively) (Fig. 3.4A).

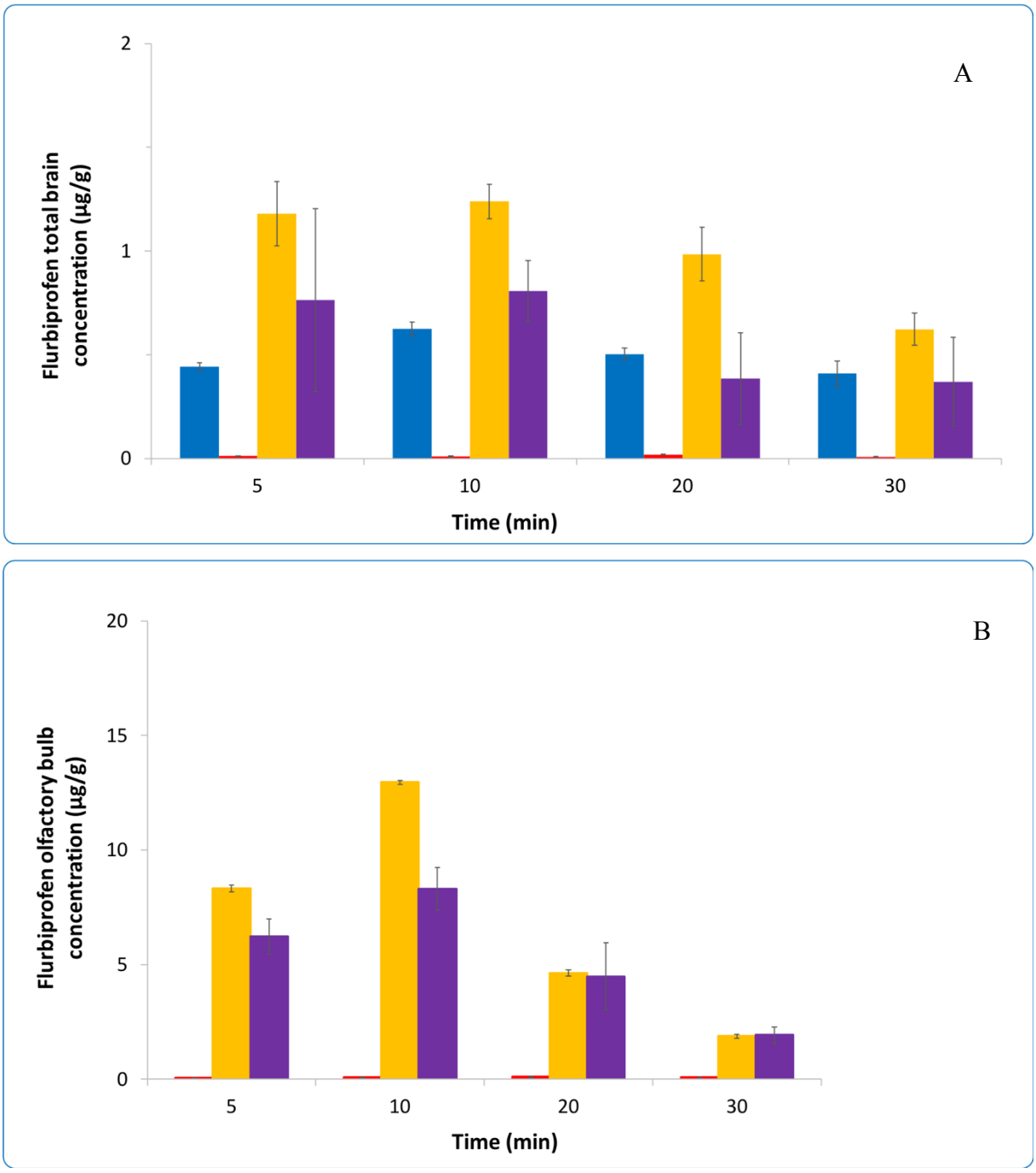

Figure 3.4. *Flurbiprofen concentration in total brain (A) and olfactory bulb (B) after i.v. administration of FB-COONa aqueous solution (blue) and nasal administration of the same FB-COONa solution (red), F13_70 spray-dried microparticles (yellow), FB-COONa-excipient agglomerates (purple). Data are expressed as mean ± SEM, n≥3.*

In particular, flurbiprofen concentrations was high in the olfactory bulb, namely 10 times as higher as in the brain (Fig. 3.4B). The microparticulate powder of flurbiprofen in acid form (F2) given intranasally, produced a certain accumulation of drug in the brain (C_{max} 0.99 ± 0.28 µg / tissue) and in the olfactory bulb (11.8 ± 4.8 µg/g tissue), which was considered preliminary due to the previous reason related to the small number of rat involved in this part of the study.

With the i.n. solution, flurbiprofen concentration reached only 0.012 ± 0.002 µg/g brain and 0.05 ± 0.02 µg/g olfactory bulb (Fig. 3.4A-B). At all time points, the nasal solution led to drug concentrations in the brain that were 50-100 times lower than those produced by the nasal powders. This difference could be explained in light of the dose administered with the three nasal dosage forms, as discussed in paragraph 3.3.2 regarding flurbiprofen serum profiles.

The i.v. injection led to 0.44 ± 0.02 µg/g tissue and 0.63 ± 0.03 µg/g tissue accumulated in the brain at 5 min and 10 min, respectively. At both times, the drug brain concentration was lower compared to the nasal powders. The figure 3.3A shows that flurbiprofen crossed the BBB, but the drug appearance in the brain was slower than with the powder

The brain flurbiprofen disposition was calculated according to the equation 3.3, substituting the serum AUC with the brain AUC. Table 3.II shows the brain disposition values of the intranasal formulations. Remembering that the administration of the solution dose had been done in the two nasal cavities, whereas the powders had been insufflated only in one cavity, the brain disposition of the flurbiprofen in powder forms was remarkably higher than with the i.n. solution. Taken together, these findings suggest that the nasal administration of the drug in powder form enabled a more effective access to the brain than the i.v. and i.n. solution at the same dose.

3.3.4 Nose-to-brain drug delivery

Flurbiprofen presence in the brain after nasal powder administration could result from the contribution of the drug absorbed into the blood and the drug transported by the nose-to-brain pathway. For the nasal powders, compared to i.v. administration, a direct transport from the nose to the brain was suggested by a higher drug accumulation in the brain. Specifically, relevant levels were found in the olfactory bulb. This happened while the serum levels were lower than those measured after i.v. injection. Hence, in

order to understand whether flurbiprofen reached the brain by direct nose-to-brain transport, DTE and DTP were calculated to quantify the actual contribution of nasal delivery to brain targeting and the efficiency of such administration. DTE expresses the exposure of the brain to the drug after nasal administration relative to that obtained by systemic (i.v.) administration. DTE ranges from 0 to +∞: values above 100% indicate a more efficient brain targeting after i.n. than after systemic administration. DTE was found >100% for both the microparticles and the agglomerates (Tab. 3.III). Hence, both nasal powders outperformed the i.v. injection with respect to brain concentrations obtained by the two administration routes.

Table 3.III. *Calculated plasma and brain AUC (Area Under the Curve), Drug Targeting Efficiency (DTE) and Direct Transport Percentage (DTP) of flurbiprofen for intranasal (i.n.) drug powders (F13_70 spray-dried microparticles and F13_40:ML agglomerates thereof) and nasal drug solution compared to i.v. administration.*

Treatment	Tissue	AUC_{last} (hr×µg/mL)	% DTE	% DTP
i.v. flurbiprofen solution	plasma	3687	-	-
	total brain	15.1		
i.n. F13_70 spray-dried microparticles	plasma	2226	-	-
	total brain	28.7	314.8	68.2
i.n. F13_40:ML agglomerates	plasma	1743	-	-
	total brain	15.63	218.9	54.3
i.n. flurbiprofen solution	plasma	226.92	-	-
	total brain	0.74	82.3	-21

DTP estimates the fraction of the i.n. dose reaching the brain via direct nose-to-brain transport *versus* the total amount of drug reaching the brain after i.n. delivery. DTP values can range from −∞ to 100%: values below zero indicate more efficient drug delivery to the brain following systemic administration as compared to i.n. administration. DTP was well above 0% for both nasal powders, indicating the actual contribution of nose-to-brain direct transport to the flurbiprofen levels measured in the brain. Indeed, it must be borne in mind that i.n. administration brings flurbiprofen into the blood, where it can cross the BBB. The DTE and DTP indexes were higher for the nasal microparticles compared to the agglomerates, indicating that the microparticles

enabled a more intense transport of the drug from the nasal cavity to the brain compared to the i.n. drug solution.
The two indexes were not calculated for F2 due to the small number of animals receiving these microparticles.
Based on DTE values, the nasal solution appeared less efficient than the nasal powders in directly delivering flurbiprofen to the brain. The contribution of nose-to-brain direct transport was absent with the solution (DTP negative). First of all, the unsatisfactory performance in brain accumulation of flurbiprofen by the nasal solution has to be attributed to the low drug solution dose administered and the low drug concentration in the nasal solution. These points were already discussed (paragraph 3.3.2 and 3.3.3). Moreover, it is noteworthy that the 20 µl nasal dose of flurbiprofen solution was divided in 5 µl shots administered alternated in both rat's nostril with the aim to avoid nasopharynx deposition. However, the total amount of flurbiprofen solution could have been insufficient to cover completely rat's nasal surface area, while dose fractioning in tiny drops could have result in a deposition primarily in the respiratory epithelium (anterior part of nasal cavity) with poor distribution in the olfactory mucosa (upper nasal region). In fact, other *in vivo* studies reported that rats received a total volume of 40-100 µl given as 6-10 µl nose drops (Dhuria et al., 2010).

Concerning the two nasal powders administered, the nose to brain delivery indexes indicated a superiority in nose to brain direct transport of the micorparticles. Since the brain disposition of flurbiprofen after i.n. administration could come from the double contribution of systemic absorption and BBB crossing (as for i.v. administration) and of the nose-to-brain direct transport, the similar serum levels, obtained with the two powders at different doses, suggest that the systemic contribution should be comparable. Thus, the different flurbiprofen brain levels measured with microparticles and agglomerates should rely on a different powder deposition influencing the nose to brain direct transport. In this regard, although in the rat the olfactory epithelium covers around half of the nasal cavity surface (Xi et al, 2016), the olfactory region is located far from the entrance of the nose, that is in the upper part of the nasal cavity. On the other hand, the respiratory region is located close to the nostrils of rat's nose. Thus, the powder after nasal insufflation, could deposit differently for the two nasal powders in respiratory and olfactory regions (Fig. 3.5).

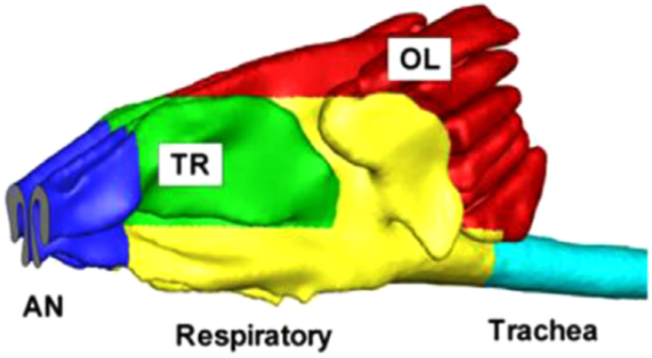

Figure 3.5. *Rat's nasal cavity. OL: Olfactory region. TR: Turbinates. AN: Anterior (reproduced with permission from Xi et al., 2016)*

Considering the different particle size and its effect on powder aerosolization by the device, the microparticles could have determined a more uniform and broad covering of the nasal surface in both the respiratory and the olfactory regions, whereas the agglomerates could be more concentrated in the respiratory region as sparse spots, thus occupying less surface area. The broader the area of deposition, the greater the absorption. It is known that the combination between nasal insufflator and powder influences the shape of the plume emitted and the deposition of the particles within the nasal cavity. The formulation variables are related to the properties of the nasal powder, namely size and density. As they lead to different powder lining of the mucosal surface (either respiratory and olfactory mucosa), this may ultimately affect where drug dissolution and transmucosal transport occur (Buttini et al., 2012; Tiozzo Fasiolo et al., 2018). The agglomerates, due to their size, are aerosolized differently compared to the microparticles, even though they should be de-agglomerated and broken into fragments by the action of the nasal device. However, the fragments likely are bigger than the original microparticles. In a study regarding the technological development and combination with different insufflator devices of spray-dried microparticle agglomerates of caffeine and excipients for nasal delivery, Russo and co-workers (2004) showed that during insufflation the agglomerates broke into fragments, whose size was significantly reduced but still larger than that of original microparticles. (Adi et al., 2011).

3.4 CONCLUSIONS

Both the prepared flurbiprofen nasal powders, namely FB-COONa spray-dried microparticles and agglomerates with excipient spray-dried microparticles, brought the

drug into brain and enhanced its brain disposition compared to systemic administration by i.v. injection and i.n. solution. With the nasal powders, the serum levels were lower compared to the i.v. route, independently of the powder and the drug dose administered. These findings, considered together with the drug levels found in the olfactory bulb after nasal powder insufflation, indicate a direct nose-to-brain drug delivery. The microparticles outperformed the agglomerates in delivering flurbiprofen to the brain, despite their similar flurbiprofen plasma levels. A broader deposition of the microparticles inside the nasal cavity after insufflation by the nasal device could have resulted in a greater lining of olfactory mucosa, hence favoring drug transport through the olfactory nerve into the brain. Deposition studies are required to validate this hypothesis, not disregarding the presence of the excipients in the agglomerates.

A small number of animals received FB-COOH spray-dried microparticles intranasally showed a significant transport of this less soluble form. Thus, despite its different biopharmaceutical performance *ex vivo*, the FB-COOH powder should be kept “handy” as an alternative to the FB-COONa.

Compared to the i.n. solution, the improved cerebral flurbiprofen disposition by the powders (independently of the drug chemical form) was attributed to the higher drug dose given (10 or 20-time more than solution), without forgetting the saturation concentration at deposition site sustaining drug diffusion. Prolonged retention inside the nose should also be considered for the solid dosage form.

Hence, flurbiprofen in powder form for nasal administration was considered worthy for further investigation aiming to AD management. The combination in a unique formulation for nasal delivery of FB-COONa spray-dried microparticles with a second drug in powder form could be the next step to better address the disease by the so-called “multi-target approach”.

CHAPTER 4

IN VITRO AND *EX VIVO* STUDY OF AN INSULIN NASAL POWDER

Insulin has been proposed as a drug candidate for the management of early stage Alzheimer's disease (AD). Nasal delivery by a solution of the hormone has been already performed in mild cognitive impairment and AD patients with promising results with respect to the improvement of memory and general cognition (Claft et al., 2011). Compared to the drug solution, insulin in powder form may be a more interesting for the nasal administration of the peptide.

In this phase, an insulin microparticulate powder for nasal administration was studied. It was produced by spray drying according to Balducci et al., 2014 and characterized with respect to *in vitro* dissolution and *ex vivo* transport of insulin across excised rabbit nasal mucosa in comparison with the insulin raw material with a focus on the chemical stability of the peptide in the *ex vivo* experimental set-up.

4.1 MATERIALS AND EQUIPMENT

Materials

Insulin (human recombinant, batch n° 15G629-B) dry powder was supplied by Sigma-Aldrich. This material was used for the preparation of the HPLC analytical standards and in *in vitro* dissolution and *ex vivo* transport experiments as reference powder. It was also employed for the manufacturing of spray-dried insulin microparticles.

HPLC-grade acetonitrile was supplied by Sigma-Aldrich® (St. Louis, MO, USA). All other reagents and solvents were analytical grade.

Equipment

- Gibertini Crystal 500CAL analytical balance (max weight 510 g, d=1 mg)
- Kern ALS 120-4 (max weight 120 g, d= 0.1 mg, reproducibility =0.2 mg, linearity = +/- 0.2 mg) analytical balance
- Mini Spray Dryer B-191 (Büchi Labortechnik, CH-Flawil)
- Branson 2510 Ultrasonic Bath (Emerson, St. Louis MO, USA).

4.2 METHODS

4.2.1 HPLC-UV method for insulin determination

Insulin quantification was performed by reverse phase high performance liquid chromatography (HPLC) with UV-Vis detection (Agilent 1100 series, Santa Clara, CA, USA). Gradient elution was carried out employing two mobile phases, namely mobile phase A (H_2O:CH_3CN:TFA ratio 80:20:0.04, pH 2.0 $\pm$ 0.1) and mobile phase B (H_2O:CH_3CN:TFA ratio 20:80:0.04, pH 2.0 $\pm$ 0.1) at room temperature, following the method reported in Tab. 4.I. The detection wavelength was set at 220 nm. The stationary phase was an Agilent Poroshell column (SB120, C18, 2.7 µm; Agilent, Santa Clara, CA, USA). The flow rate was 0.5 ml/min and the injection volume 5 µl. Each run lasted 15 min. In these conditions, the retention time of insulin was 6 min.

The HPLC-UV method was developed in-house and validated with respect to linearity range (insulin concentration range 1.25 – 40 µl/ml, y= 8.9037x - 4.3645, R^2= 0.9999), repeatability (0.37% RSD for peak area and 0.69% for retention time; n=7 injections) and limit of quantification (LOQ, 91 ng/ml).

The insulin analytical standard solution was prepared from a 0.4 mg/ml stock solution of insulin dissolved in HCl 0.01 M. This stock solution was stored at 2-8 °C for up to one month after preparation based on the assessed stability. On each day of analysis

an aliquot of stock solution was diluted with the mobile phase A to a final insulin concentration of about 40 µg/ml, which was within the method's linearity range.

Table 4.I. *HPLC-UV gradient method program.*

Time (min)	Mobile Phase A (%)	Mobile Phase B (%)
0	100	0
1	100	0
8	75	25
8.5	75	25
9.5	100	0
13	100	0

4.2.2 Preparation of insulin spray-dried microparticles

Spray-dried insulin microparticles were prepared according to Balducci et al., 2014. Briefly, 1 mg/ml insulin solution was prepared by dissolving human recombinant insulin in acetic acid at 0.4 M concentration. The pH of this insulin solution was 2.9 and was displaced to 3.4 by dropwise addition of ammonium hydroxide 10% (v/v). Spray drying was carried out by means of a Büchi Mini Spray Dryer B-191 apparatus. 300 ml of the above insulin solution was sprayed at inlet temperature 120 °C, drying air flow rate 600 l/h and solution feed rate of 3.5 ml/min. Under these conditions an outlet temperature of 73 °C was measured. Two batches of insulin spray-dried microparticles were prepared. The HPLC-UV analysis allowed to determine an insulin content in the spray-dried microparticles in the range 98-105%.

4.2.3 Physico-chemical characterization of the insulin spray-dried microparticles

Particle size

The particle size of the insulin spray-dried microparticles was determined according to Balducci et al. (2014), using a Mastersizer X (Malvern Instruments Ltd, Worcestershire, UK) laser diffraction system equipped with a 45 mm focal lens, which measures sizes in the range from 0.1 to 80 µm. Briefly, 10 mg of powder were dispersed in cyclohexane containing 0.1% (w/v) of lecithin and sonicated in ultrasonic bath for 5 min. The results

of the analysis were expressed as $d_{v,10}$, $d_{v,50}$, and $d_{v,90}$, corresponding to the cumulative undersize volume diameters of 10%, 50% and 90% of the particle population, respectively.

Morphological analysis

The morphological characteristics of spray-dried powders were assessed by scanning electron microscopy (SEM) (JSM-6400, JEOL Ltd., Japan). Double-sided adhesive tape was placed on an aluminium stub and a minimal amount of particles was deposited on it by lightly tapping on the edge of the stub with a spatula to break up agglomerates. Samples were coated with a carbon layer and analyzed after a 30 min depressurization.

4.2.4 Biopharmaceutical characterization of insulin spray-dried microparticles

In vitro insulin dissolution and release

As described in chapter 2 for flurbiprofen, vertical Franz-type diffusion cells assembled with a cellulose dialysis membrane (MW cut-off 100 kDa, Biotech Cellulose Ester Trial Kit, Spectra/Por® Dialysis Membrane) were used to measure the dissolution rate and release of insulin from the spray-dried powders. The insulin raw material and a commercially available insulin solution (Humulin R® 100 UI/ml, equivalent to 3.84 mg/ml, Eli Lilly Pharma) were used as reference. 5 mg of insulin powder or 0.5 ml of insulin solution (equivalent to 1.9 mg insulin) were loaded in the donor. 500 µl samples of receptor medium were withdrawn every hour up to 4 hours. The residual drug in the donor compartment was quantitatively recovered with HPLC mobile phase A and the membrane was rinsed by sonication in 10 ml of the same solvent for 10 min. All samples were diluted with mobile phase A before injection onto HPLC-UV. For these experiments, the number of replicates was 5-7. Data are reported as mean ± SEM.

Ex vivo insulin transport across rabbit nasal mucosa

The *ex vivo* transport of insulin across excised rabbit nasal mucosa was studied using the same Franz-type diffusion cells of the dissolution experiments. Dissection of rabbit nasal mucosa from the animal's head and the experiment were performed as reported for flurbiprofen (see chapter 2). 5.0 mg of insulin spray-dried microparticles + 100 µl of PBS pH 7.4 were loaded in the donor compartment at the beginning of the experiment. Insulin raw material (5.0 mg + 100 µl PBS) was tested as reference. At the end of the

experiment the residual drug in the donor compartment was quantitatively recovered by rinsing with fresh mobile phase A. Insulin accumulated within the tissue was extracted by comminuting the mucosa with a surgical blade and homogenizing it in 7 ml of PBS pH 7.4 with Ultra-Turrax® IKA homogenizer (T10 basic model, IKA® Werke GmbH & Co. KG, D-Staufen) for 210 s. The homogenates were centrifuged (10 min; 7500 x g) and the obtained supernatant was diluted with mobile phase A. The mass balance was calculated as seen before. The minimum number of replicates was 5. Data are reported as mean ± SEM.

4.2.5 Data analysis

Statistical analysis of data was performed by applying unpaired two-tailed Student's test. Significance was accepted at $P < 0.05$.

4.3 RESULTS AND DISCUSSION

4.3.1 Physico-chemical characteristics of insulin spray-dried microparticles

Size and morphology

Human insulin raw material was composed of crystalline particles with cubic shape and smooth surface (Fig. 4.1A-B). Spray drying completely changed this morphology, leading to new microparticles with wrinkled and shriveled shape, due to the collapse of inflated droplets during spray drying of the protein solution (Fig. 4.1C-D).

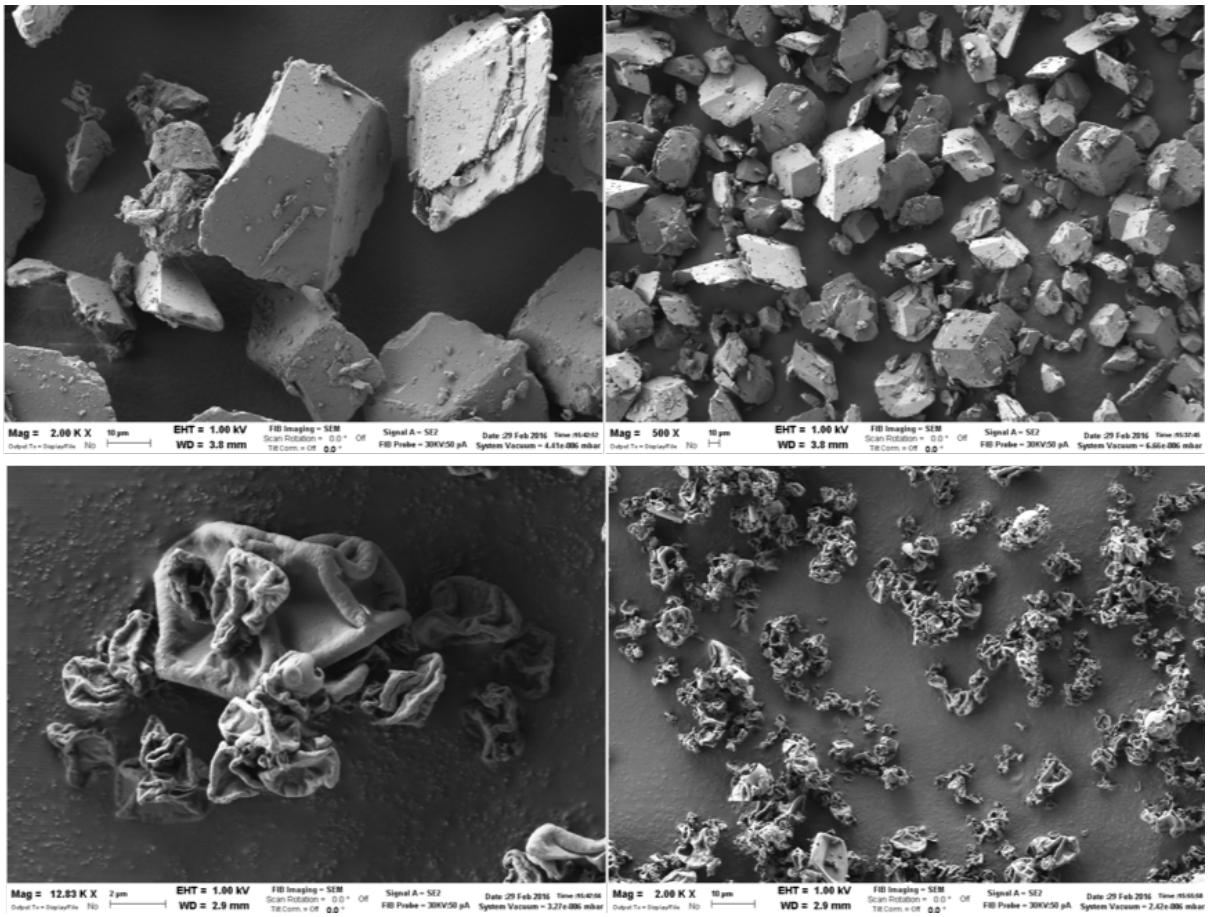

Figure 4.1. *SEM micrographs of human insulin raw material (A-B) and insulin spray-dried microparticles (C-D).*

The spray drying process significantly modified the particle size compared to the raw material, reducing the $d_{v,50}$ more than three folds (Tab. 4.II).

Table 4.II. *Size distribution of insulin microparticulate powders (mean ± standard deviation of a minimum of 3 samples of the same batch).*

Insulin powder	**$d_{v,10}$**	**$d_{v,50}$**	**$d_{v,90}$**	**SPAN**
Raw material	2.78 ± 0.04	8.81 ± 0.13	15.54 ± 0.06	1.44 ± 0.02
Spray-dried microparticles	1.19 ± 0.03	2.74 ± 0.11	8.93 ± 1.83	2.81 ± 0.60

The shape and particle size in the low micrometer range gave the insulin spray-dried microparticles a large surface area, ideal to enhance the drug interaction with biological fluids for drug dissolution. Moreover, since the number of sites where drug particles

can interact is high, these insulin spray-dried microparticles appear suitable for the construction of the final dosage form for the delivery of insulin *in vivo*, such as the agglomerates of spray-dried microparticles for nasal administration. On the other hand, a particle size below 10 μm for microparticles intended to be deposited into the nasal cavity raises a risk of lung inhalation. This justifies the subsequent step of agglomerating the insulin spray-dried microparticles to increase the size of the nasal powder for deposition in the nasal cavity. The point has been discussed in Chapter 1 also based on literature data (Russo et al., 2004).

4.3.2 Biopharmaceutical characteristics of insulin spray-dried microparticles

In vitro insulin dissolution and release

The European Pharmacopoeia (Ph. Eur, 9th Ed.) reports that insulin is *"practically insoluble in water [...]. It dissolves in dilute mineral acids and with decomposition in dilute solutions of alkali hydroxides".* Thus, the limiting factor for the dissolution of insulin in aqueous medium at neutral pH is its low aqueous solubility. Moreover, in aqueous media the peptide is unstable in a pH-dependent manner. The isoelectric point of native insulin is 5.3 (Steiner et al., 1973). In acidic solutions insulin degrades due to deamidation at residue AsnA21. In neutral formulations deamidation takes place at residue AsnB3. Insulin is also sensitive to thermal treatment (Brange et al., 1991).

In the present work, insulin dissolution was studied in PBS pH 7.4 at 37 °C. This medium was selected considering insulin pH-dependent stability. Although in humans the nasal absorption happens mainly within the first 30 min after administration, the time of experiment was extended here to 4 h to obtain a better characterization of the *in vitro* drug dissolution profile. The Franz cell was a convenient approach to this aim, also because it required small amount of drug material. This two-compartment system allowed to study *in vitro* the drug dissolution rate from a solid form, represented by the spray-dried microparticles of insulin and compared to insulin raw material as reference unprocessed powder (Floroiu et al. 2018). The regenerated cellulose membrane separating the compartments, is a non partitioning barrier, thus the transport across it of the compound depends only on the dissolution rate of the solid formulation deposited on the membrane.

Insulin dissolution and transport across the artificial membrane from the spray-dried microparticles were linear in the first three hours. The amount of insulin dissolved in 3 h was 40 ± 2% of the amount loaded in the donor compartment at time zero,

corresponding to an insulin amount transported of 3.25 ± 0.14 mg cm^{-2} (steady state flux 0.32 ± 0.02 µg cm^{-2} s^{-1}, mean ± SEM) (Fig. 4.2).

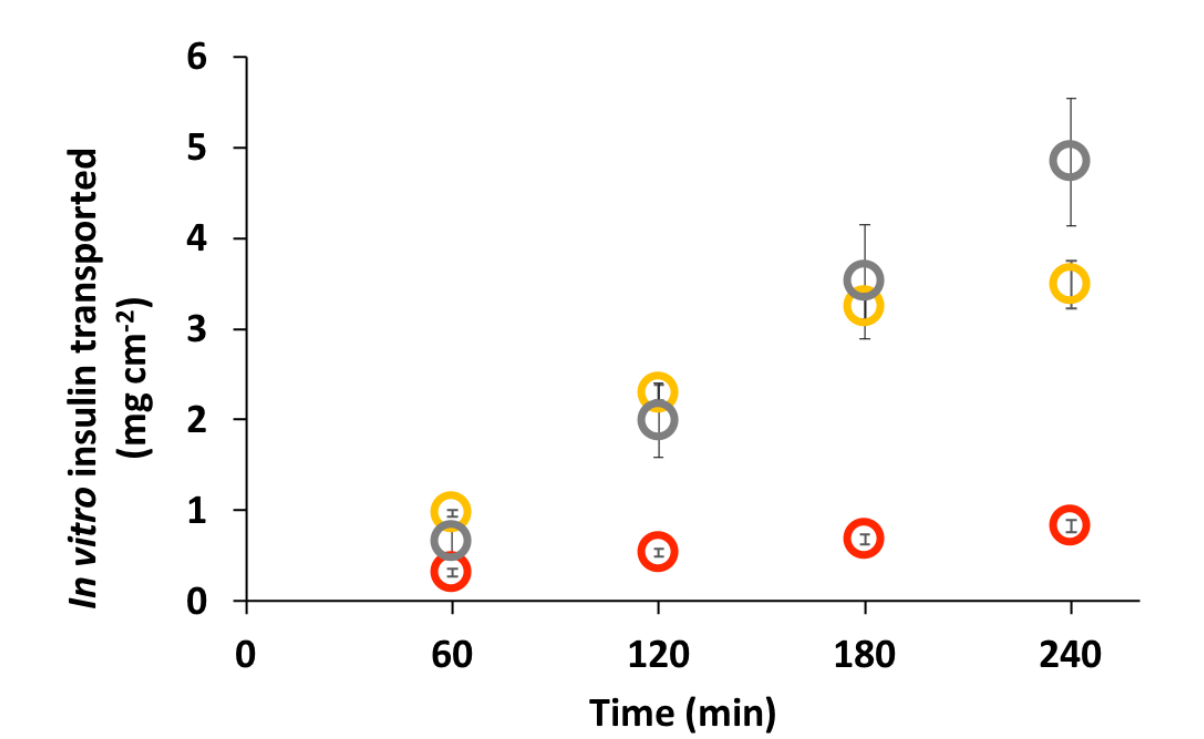

Figure 4.2. *Insulin dissolution/transport across a regenerated cellulose membrane (100 kDa) in PBS pH 7.4 at 37 °C from: insulin solution 3.84 mg/ml (Humulin® R) (red), insulin raw material (grey) and insulin spray-dried microparticles (yellow). Data are expressed as mean* ± SEM (n=*5).*

After the 3rd hour, the transport decreased. As the donor compartment still contained insulin, an interaction between insulin and the membrane was hypothesized that prevented further drug passage to the receptor compartment. Adsorption phenomena depend on the material in contact with the compound and in few cases were observed also for hydrophilic cellulose membranes (Sefton et al., 1984; Brange et al., 1993). In addition, insulin may have formed molecular aggregates. The formation of dimeric or hexameric structures is known for insulin and depends on the peptide concentration in the medium and the pH. Brange et al. (1993) reported that insulin exists as a monomer only at low concentration (<0.1 µM, equivalent to about 0.6 µg/ml), while at higher concentration and neutral pH insulin dimerizes. When insulin concentration is ≥2 mM (equivalent to about 11.6 mg/ml) at neutral pH, three dimers assemble to form an insulin hexamer in the absence of zinc ions. Assuming that the residual insulin in the cell's donor at the end of the 3 hours was completely dissolved, the concentration of the peptide would be above the 2 mM limit, supporting the formation of insulin

hexamers. Although individually smaller than the membrane's pores, they may hinder insulin passage through the barrier due to a steric effect.

Regarding the raw material, the amount of insulin dissolved and transported in 3 h was 40 ± 7% of the amount loaded in the donor compartment at time zero, corresponding to an amount of insulin transported of 3.52 ± 0.63 mg cm^{-2} (steady state flux 0.43 ± 0.05 μg cm^{-2} s^{-1}) (Fig. 4.2). Hence, the dissolution of insulin from the spray-dried microparticles and the raw material were not different up to 3 hours. As observed with flurbiprofen acid (FB-COOH) dissolution *in vitro* in chapter 2, spray drying was not effective in increasing the dissolution rate of insulin in PBS pH 7.4, despite the particle size reduction of insulin spray-dried microparticles *vs* the raw material.

However, differently from the spray-dried microparticles, insulin transport from the raw material continued and remained linear beyond the third hour. The observed differences between the two microparticulate powders were in particle size and morphology. The particle density appears clearly different at SEM (Fig. 4.1). They could have determined a different interaction of each powder with the wetting medium and the membrane, leading to the viscosity increase observed only for spray-dried microparticles, and possibly facilitating the hypothesized formation of hexamers.

The insulin transport across the cellulose membrane was studied also from a commercial insulin solution for injection in diabetic patients. The solution was Humulin® R 100 UI (Eli Lilly, Italia S.p.a), having an insulin concentration of 3.84 mg/ml. It contains human insulin obtained by recombinant DNA technology and metacresol and glycerol as excipients. Metacresol guarantees the chemical stability of insulin. This product does not contain zinc, which in other commercial formulations is used to stabilize the insulin hexamer (Dunn, 2005). Humulin® R was tested as insulin solution as it guaranteed a stable concentration of the peptide. It was found that insulin transported from the solution across the cellulose membrane was 0.68 ± 0.05 mg cm^{-2} in 3 h (flux 0.05 ± 0.06 μg cm^{-2} s^{-1}), corresponding to 21 ± 2% of the insulin loaded in the donor at time zero. In the comparison between this percentage and the corresponding one measured for the two powders, it must be borne in mind that the initial loading was lower for the solution.

Differently from the spray-dried microparticles, but similarly to the raw material, the insulin transport from the solution continued after the third hour. The concentration of insulin in Humulin®, which does not contain zinc, is lower than the limit value causing

the formation of hexamers, possibly interfering with the diffusion across the artificial membrane.

Comparing the liquid and the spray-dried microparticles in the first hour, more relevant to nasal drug delivery, the respective amounts transported were different and more insulin was transported with the powder, likely due to the higher concentration gradient (Fig. 4.2). In terms of percentage permeated in the first hour, the values were not significantly different (9.5 ± 1.2% and 12.0 ± 0.6% for Humulin® and insulin spray-dried microparticles, respectively). This again brings back to the lower insulin loading with the solution. The spray-dried microparticulate powder allowed to load a higher insulin "dose" in the donor compartment of the Franz cell, which positively affected the flux at least for 3 hours compared to the liquid. Insulin dissolution from the powder likely saturated the liquid available in the donor compartment, sustaining the transport across the artificial membrane. In a separate experiment, we were able to dissolve about 6-7 mg of insulin spray-dried microparticles in 1 ml of PBS pH 7.4 without reaching the saturation. In contrast, insulin transport from the solution was driven by a lower concentration gradient, progressively reduced as insulin reached the receptor.

At the end of experiments, the mass balance was 99 ± 2%, 106 ± 1% and 91 ± 3% for insulin spray-dried microparticles, insulin raw material and Humulin®, respectively. Thus, insulin was stable up to 4 h in PBS pH 7.4 at 37 °C, in agreement with Brange et al. (1993) reporting that phosphate buffer counteracts insulin precipitation. Not unexpectedly, insulin was stable with Humulin® R due to its formulation. In fact, it is known that neutral solutions containing phenol show limited insulin degradation by deamidation for the protective effect of phenol on the tertiary structure around the deamidating residue (Brange et al., 1992).

The insulin spray-dried microparticles were further studied in experimental conditions closer to that of the i.n. administration only in comparison with the raw material.

Ex vivo insulin transport across rabbit nasal mucosa

The capability of insulin to diffuse across the nasal mucosa was studied from the spray-dried microparticles only in comparison with the raw material. After 4 h, the amounts of insulin transported from the spray-dried microparticles and the raw material were 0.19 ± 0.07 mg cm^{-2} and 0.19 ± 0.10 mg cm^{-2}, respectively, corresponding to 2.1 ± 0.7% and 2.3 ± 1.3% of the insulin amount loaded in the donor at time zero (Fig. 4.3A).

Both profiles show an initial lower slope, which changes to linearity from the 2nd hour. This indicate the existence of a lag time, likely due to the molecular weight of insulin, affecting the partition and diffusion until a gradient is established across the barrier. The steady-state fluxes were calculated from the linear part of the profiles, i.e., between the 2nd and 4th hour. They were 0.021 ± 0.007 μg cm^{-2} s^{-1} and 0.019 ± 0.010 μg cm^{-2} s^{-1} respectively for the spray-dried microparticles and the raw material. Hence, no significant difference was measured between the spray-dried microparticles and the raw material in terms of transport across a partitioning barrier like the nasal mucosa. Insulin accumulation within the rabbit nasal mucosa (Fig. 4.3B) was very small and not significantly different (0.007 ± 0.004 mg and 0.016 ± 0.005 mg for the spray-dried microparticles and the raw material, respectively).

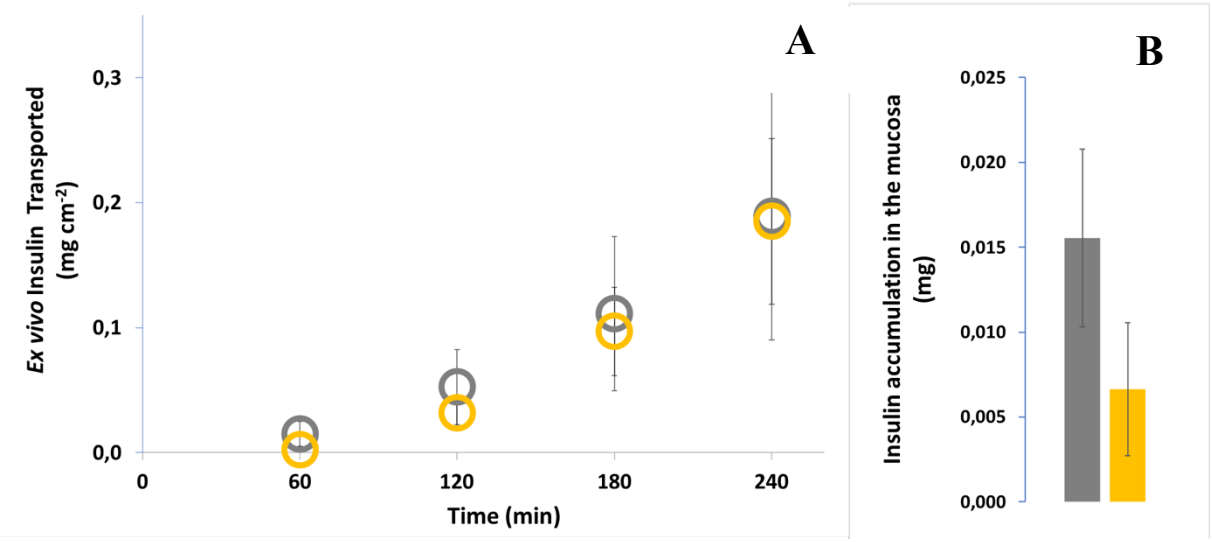

Figure 4.3. *A: Insulin transport across rabbit nasal mucosa from: insulin raw material (grey) and insulin spray-dried microparticles (yellow). B: Insulin accumulated within the nasal tissue in 4 h (mean* ± SEM; n≥*5*).

Considering that the penetration of insulin into the mucosal barrier and its transport across first rely on the powder dissolution in contact with the tissue, the non-different transport profiles confirm a similar dissolution rate of the two microparticulate powders, as obtained with the regenerated cellulose barrier. The spray drying process did not modify the particle characteristics in a way to determine an effect on dissolution and permeation, irrespectively of the type of barrier (artificial or biological). However, the interruption of the transport from the spray-dried microparticles after the 3rd hour was not seen with the biological membrane. Beside the partitioning effect, which exists only

with the mucosal barrier, another difference in the two experiments (*in vitro* and *ex vivo*) is the availability of the solvent for powder dissolution in the donor. *Ex vivo* the only available solvent was the 100 µl of PBS introduced with the formulation, whereas the artificial membrane may have allowed extra solvent to be available from the receptor due to an osmotic effect. This variable may modify the conditions for insulin aggregation.

Insulin mass balance at the end of experiment was close to 100% for both the spray-dried microparticles and the raw material, indicating that insulin was stable in the *ex vivo* conditions.

4.4 CONCLUSIONS

The prepared insulin spray-dried microparticles provided a more pronounced insulin transport *ex vivo* across rabbit nasal mucosa compared to a commercial insulin solution. This was due to the solid microparticulate formulation sustaining the concentration gradient across the barrier, while also enabling to load a greater mass of insulin in the donor. Even though the biopharmaceutical performance of the insulin spray-dried microparticles was equivalent to that of the raw material in terms of peptide dissolution and transport across the barrier, the size and morphology of the spray-dried microparticulate powder should make them preferable for the subsequent combination with the flurbiprofen spray-dried microparticles and nasal agglomerate powder construction. In fact, the smaller particle size and wrinkled morphology resulting from the spray drying process, determine a significantly higher surface area for the establishment of the inter-particle forces in the agglomerates. In addition, the insulin raw material requires refrigerated storage, while these insulin spray-dried microparticles remain stable at room temperature up to several months (Balducci et al., 2014).

CHAPTER 5
COMBINATION OF FLURBIPROFEN AND INSULIN MICROPARTICULATE POWDERS FOR NASAL DELIVERY

In the previous research phases, flurbiprofen and insulin were transformed into spray-dried microparticulate powders, which demonstrated biopharmaceutical properties *in vitro* and, for flurbiprofen only, also *in vivo*, suitable aiming to their nose-to-brain delivery. Their combination could benefit the management of Alzheimer's disease (AD) by addressing different factors of AD's pathogenesis at the same time. The choice of a flurbiprofen+insulin combination was based on each of them, individually, showing both *in vitro* and *in vivo* to effectively address pathological factors of AD acting as disease-modifying compounds (Eriksen et al., 2003; Gasparini et al., 2002; Meister et al, 2013; Solano et al., 2000).

Thus, the last phase of the research started to study the blending of the flurbiprofen and insulin spray-dried microparticles, produced and characterized separately in the previous phases, to construct the agglomerate powder to be proposed as multi-drug dosage form for nasal administration. In case of flurbiprofen, F3, F13_70 and F13_40 spray-dried microparticles were used for the combination according to their availability. In order to define the ratio of the two drugs in the blend, it was recalled that 20 mg/day of the 2-drug powder formulation could suit for nasal administration in adults (divided in two 10 mg-shots, one per nostril). The anatomy of the human nasal cavity allows such amount of powder to be deposited and cover the nasal mucosa (a true density around 1.2 -1.5 g/cm^3 is reasonable for spray-dried microparticles, as reported by Balducci et al., 2014 and Belotti et al., 2015 respectively for insulin and amikacin). This nasal powder mass is in line with that of powder products already on the market (e.g. sumatriptan nasal powder for migraine relieve, 22 mg powder divided into 2 nosepieces; Tepper, 2016).

In the 20 mg 2-drug powder dose, the insulin dose was fixed at 20 UI (0.7 mg). The choice was guided in light of the clinical trials reporting that nasal insulin administered in solution at 20 UI dose (daily or twice-a-day) was effective in preserving the cognitive functions, improving memory and preserving functional abilities in mild and moderate AD patients.

Flurbiprofen is not as potent as insulin. It is used in oromucosal sprays for topical action in the oral cavity (e.g. Benactivdol® Gola spray solution, 8.75 mg flurbiprofen dose per shot). Having fixed that 0.7 mg insulin were to be in the 20 mg 2-drug powder dose, there would be room for 19.3 mg FB-COONa powder. These amounts would correspond to a 3.5:96.5 (% w/w) insulin/FB-COONa ratio in the mass for daily i.n. insufflation.

5.1 MATERIALS AND EQUIPMENT

Materials

FB-COOH material (batch n° T17121044) was kindly donated by Recordati S.p.A. (I-Milano). It was used for the preparation of the HPLC analytical standards and for the manufacturing of the flurbiprofen spray-dried microparticles as described in chapter 2. In particular, the flurbiprofen spray-dried microparticles were Mini B-191 spray-dried FB-COOH microparticles (F2, containing 99% FB-COOH), and Nano B-90 spray-dried FB-COONa microparticles (F13_40, containing 78.7% FB-COOH) (Tab. 2.II).

Insulin powder raw material (human recombinant, batch n° 15G629-B) was supplied by Sigma-Aldrich. It was used for the preparation of the HPLC analytical standards, the *in vitro* stability/compatibility tests and also for the manufacturing of the insulin spray-dried microparticles according to Balducci et al., 2014 (chapter 4).

Mannitol (Ph. Eur.) was supplied by Lisapharma S.p.A. (I-Erba) and lecithin (Lipoid® S45) by Lipoid AG (CH-Steinhausen). They were employed for the preparation of the excipient (mannitol/lecithin) spray-dried microparticles (previously referred to as Nano_ML_iPr, chapter 2). Kunitz-type protease inhibitor (i.e., enzymatic inhibitor for protease, specific for trypsin), acetonitrile, ethanol, isopropanol and methanol were also supplied by Sigma-Aldrich® (St. Louis, MO, USA). All other reagents and solvents were HPLC grade.

Equipment

- Gibertini Crystal 500CAL analytical balance (max weight 510 g, d=1 mg)
- Kern ALS 120-4 (max weight 120 g, d= 0.1 mg, reproducibility =0.2 mg, linearity = +/- 0.2 mg) analytical balance
- Mini Spray Dryer B-191 (Büchi Labortechnik, CH-Flawil)
- Nano Spray Dryer B-90 (Büchi Labortechnik, CH-Flawil)
- Branson 2510 Ultrasonic Bath (Emerson, St. Louis MO, USA)

5.2 METHODS

5.2.1 HPLC-UV method for insulin and flurbiprofen determination

When flurbiprofen and insulin were both present in the sample, their quantification was performed by reverse phase high performance liquid chromatography (HPLC) with UV-Vis detection (Agilent 1100 series, Santa Clara, CA, USA) and gradient elution as reported in chapter 4 for the analysis of insulin alone. With this method flurbiprofen

retention time was around 10 min (Fig. 5.1); the flurbiprofen linearity range was found in the concentration range 0.10 – 0.25 mg/ml (y= 16265x + 120.3, media of n=2 lines). Repeatability was 1.62 RSD(%) for peak area.

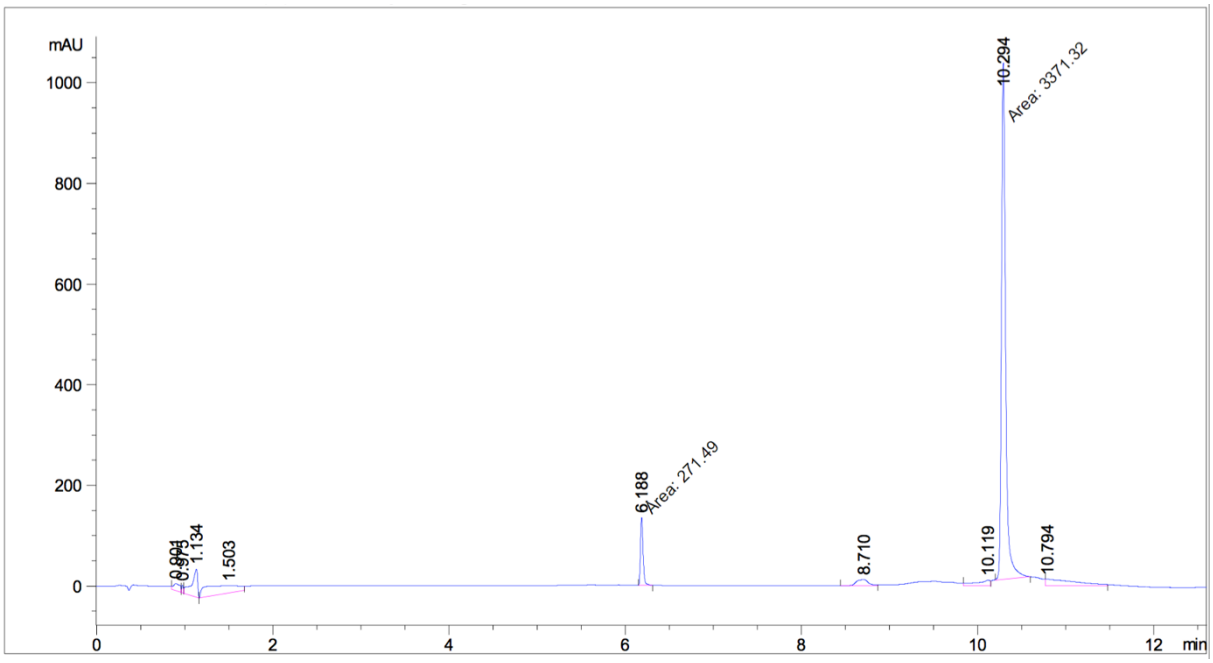

Figure 5.1. *HPLC-UV chromatogram of insulin (rt= 6 min) and flurbiprofen (rt= time 10 min) (rt: Retention Time).*

The analytical standard solution containing both substances was prepared from a 0.4 mg/ml stock solution of insulin dissolved in HCl 0.01 M and a 1 mg/ml stock solution of flurbiprofen dissolved in methanol. These stock solutions were stored at 2-8 °C for up to one month after preparation. In these conditions they both remained stable. On each day of analysis an aliquot of insulin stock solution was added to an aliquot of flurbiprofen stock solution and diluted with the mobile phase A to a final concentration of about 0.04 mg/ml insulin and 0.1 mg/ml flurbiprofen, i.e., within the method's linearity range for the two drugs.

5.2.2 *In vitro* study of insulin and flurbiprofen compatibility

Insulin chemical stability and compatibility with flurbiprofen when blended, were investigated *in vitro* as a function of the following variables:

- presence of flurbiprofen (as FB-COOH and FB-COONa)
- insulin to flurbiprofen mass ratio (% w/w)
- solvent for powder wetting/dissolution (PBS pH 7.4 or water)
- temperature

- contact time
- presence of biological material (nasal mucosa).

The compatibility after combination with flurbiprofen was studied on various blends between insulin raw material and flurbiprofen spray-dried microparticles (F2, F13_70 and F13_40). The insulin powder/flurbiprofen powder ratio considered was 14:86 (% w/w). Powder blending (100 mg) was carried out manually with a spatula in a 5 ml glass vial. The blending action was applied for 15 min, executing approximately 60 spatula movements per min. Before agglomeration, the blends were sampled (5 mg samples, randomly collected on the top, center and bottom of the vial, n=3) to assess homogeneous drug distribution by the HPLC-UV method described in paragraph 5.2.1. The stability of insulin alone was studied as reference, always using the raw material. The same Franz-type cells (permeation area 0.58 cm^2) described in the previous chapters were used for the stability experiments. However, a layer of Parafilm® was inserted between the barrier (artificial or mucosa) and the receptor compartment to create a seal and avoid drug diffusion to the receptor compartment. 5.0 mg of insulin powder or of blend were loaded in the donor and wet with 100 µl of the following solvents:

- HPLC-grade water (pH 5.8)
- PBS pH 7.4
- 1 mg/ml solution of Kunitz-type trypsin inhibitor in PBS pH 7.4.

Experiments lasted 30, 60 or 240 min. At the end, the donor compartment was rinsed with HPLC mobile phase A to recover the residue and quantify the two drugs. The amounts of both accumulated within the tissue thickness (artificial or biological) were extracted as well in order to calculate the mass balance. The extraction procedure is described in chapter 4 and chapter 2 for the artificial and the biological tissue, respectively. The generated samples were sonicated for 10 min, then centrifuged (10 min, 7500 x g). The supernatant was diluted with mobile phase A and injected onto HPLC-UV. A minimum of 3 replicates was carried out.

5.2.3 Ex vivo transport of insulin and flurbiprofen across rabbit nasal mucosa

Applying the same experimental conditions described in chapter 2 for the experiments with flurbiprofen powders, *ex vivo* (co)transport of flurbiprofen and insulin across rabbit nasal mucosa was studied from the insulin-flurbiprofen powder blends. The blends

contained insulin as raw material or spray-dried microparticles, and flurbiprofen spray-dried microparticles of FB-COOH (F2) or FB-COONa (F3 or F13_40). The ratio between the two drug powders was 14:86 (% w/w), for insulin and flurbiprofen, respectively. The homogeneous distribution of the two compounds was determined before using them. The transport experiments lasted 30 or 240 min. The mass balance was determined as described in chapter 2, after collecting the residual drugs from the donor compartment and the membrane. A minimum of 3 replicates was carried out.

5.2.4 Manufacturing of agglomerates of flurbiprofen and insulin spray-dried microparticles with excipients spray-dried microparticles

Agglomerates of insulin and flurbiprofen spray-dried microparticles were prepared by the tumbling method described for the flurbiprofen agglomerates (chapter 2). Before tumbling, a blend of insulin spray-dried microparticles, FB-COONa spray-dried microparticles (F13_40) and mannitol/lecithin spray-dried microparticles (Nano ML_iPr) was prepared in a 5 ml glass container by manual mixing with a spatula. The total blend mass was 0.5 g and the components' ratios were 14:43:43, respectively for insulin, FB-COONa and mannitol/lecithin spray-dried microparticles. Blend homogeneity was determined before agglomeration. The agglomeration yield was calculated from the ratio between the weight of the agglomerates collected and the total amount of spray-dried microparticles processed per cent.

5.2.4 Data analysis

Statistical analysis of data was performed by applying unpaired two-tailed Student's test. Significance was accepted at $P < 0.05$.

5.3 RESULTS AND DISCUSSION

5.3.1 Chemical stability of insulin in the presence of flurbiprofen

The construction of a solid combination product in the form of nasal agglomerates of microparticulate powders require that the two drugs are stable when intimately mixed. Stability is required for both drugs (1) in the solid state for the multi-drug powder during manufacturing and storage and (2) in the conditions of the nasal administration. Thus, the stability and compatibility of the two drugs in a blend (physical mixture) was determined with a special focus on insulin, which is the most delicate among the two compounds. In the blends prepared for the purpose, insulin raw material was used as

it was available in larger quantity. Moreover, the comparative study carried out in the previous phase (chapter 4) had shown no substantial differences between the two microparticulate powders, raw and spray-dried. The other powder was FB-COONa spray-dried microparticles as FB-COONa was available only as spray-dried microparticles. The first blend considered contained insulin raw material and FB-COONa at 14:86 mass powder ratio.

First of all, we assessed the stability of insulin and FB-COONa in the blend in solid state, based on the respective insulin and flurbiprofen contents measured by HPLC-UV (chemical stability). The blend was homogenous at time zero and the drugs' content complied with the theoretical ratio. Insulin and flurbiprofen contents did not vary upon storage at -18 °C for 3 weeks, confirming the stability of both. The blend was not followed beyond the 3rd week from preparation.

Getting one step closer to the *in vivo* conditions of the powder nasal administration, the blend was introduced into a closed environment and wet with a small volume of PBS pH 7.4. This mimics the fact that *in vivo*, after deposition on the mucosa surface, the powder finds the aqueous nasal secretion as solvent for dissolution. The intranasal pH is slightly lower than 7.4 (Washington et al., 2000), but this solvent was preferred for the solubility of both FB-COONa and insulin. After 4 h at 37 °C (body temperature), both drugs were recovered from the vial in amounts corresponding to the initial loading (95 $\pm$ 4% and 99 $\pm$ 5% recovered insulin and flurbiprofen, respectively). Hence, insulin and flurbiprofen did not show evidence of incompatibility leading to a decrease of their respective amounts, after dispersion and dissolution in the phosphate buffered saline solution. Being FB-COONa the salt of a weak acid with a strong base, a solution of it can see the reaction of the ionized flurbiprofen with water and increase the concentration of hydroxide ion. The resulting pH increase could be detrimental for insulin (Brange et al., 1993). However, the solvent used was a buffer solution, which in principle keep the pH stable.

In the next step, the biological variable was added, when the insulin/flurbiprofen blend was put in contact with the nasal mucosa and wet with PBS pH 7.4 at body temperature. The addition of the mucosa completely changed the picture: only 20% of the loaded insulin was recovered from the system after 4 h contact in the presence of flurbiprofen. This very low recovery of insulin was attributed to a chemical degradation and process was time-dependent (Fig. 5.2). Indeed, a 1st order relationship was found between the amount of drug recovered and the contact time ($y= 101{,}99e^{-0{,}007x}$, $R^2=$

0.9948). The shorter the contact, the higher the insulin recovery (85% and 60% recovered after 30 minutes and 1 hour, respectively).

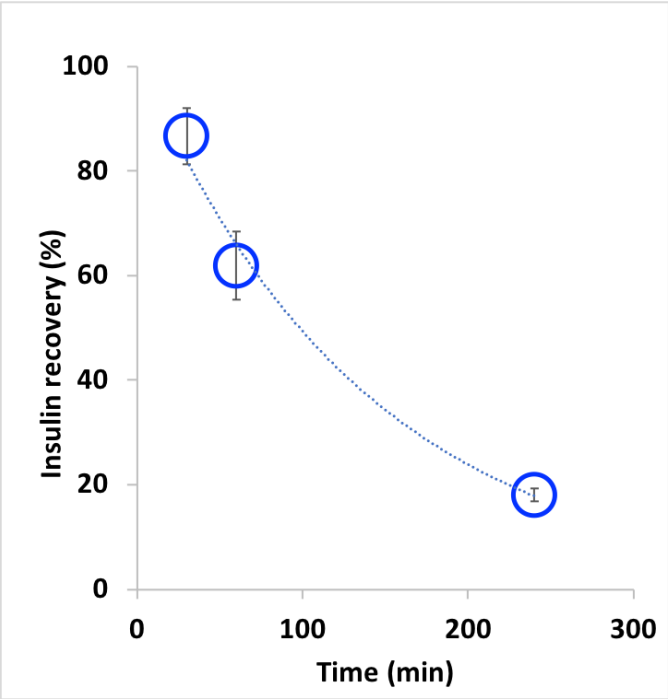

***Figure 5.2**. Insulin recovery as a function of the contact time between the blend 14:86 insulin raw material:FB-COONa spray-dried microparticle blend and the nasal mucosa (mean ± SEM, n≥3).*

The observed chemical degradation of insulin in the *ex vivo* conditions was linked to the presence of flurbiprofen. In fact, when insulin raw material was tested in the same conditions of solvent, mucosa and temperature, in the absence of FB-COONa, its recovery at 4 h was complete (97 ± 1%). This recovery was in line with the mass balance calculated at the end of the *ex vivo* transport experiments across rabbit nasal mucosa of insulin alone (chapter 4).

Thus, insulin degradation occurred in an environment where FB-COONa was contemporarily present and likely dissolving in contact with the nasal mucosa. Recalling the hypothesis of FB-COO^- hydrolysis increasing the pH that the buffer could neutralize, PBS pH 7.4 was substituted with water. Insulin recovery was not improved (Fig. 5.3). The hypothesized pH increase was not measured either.

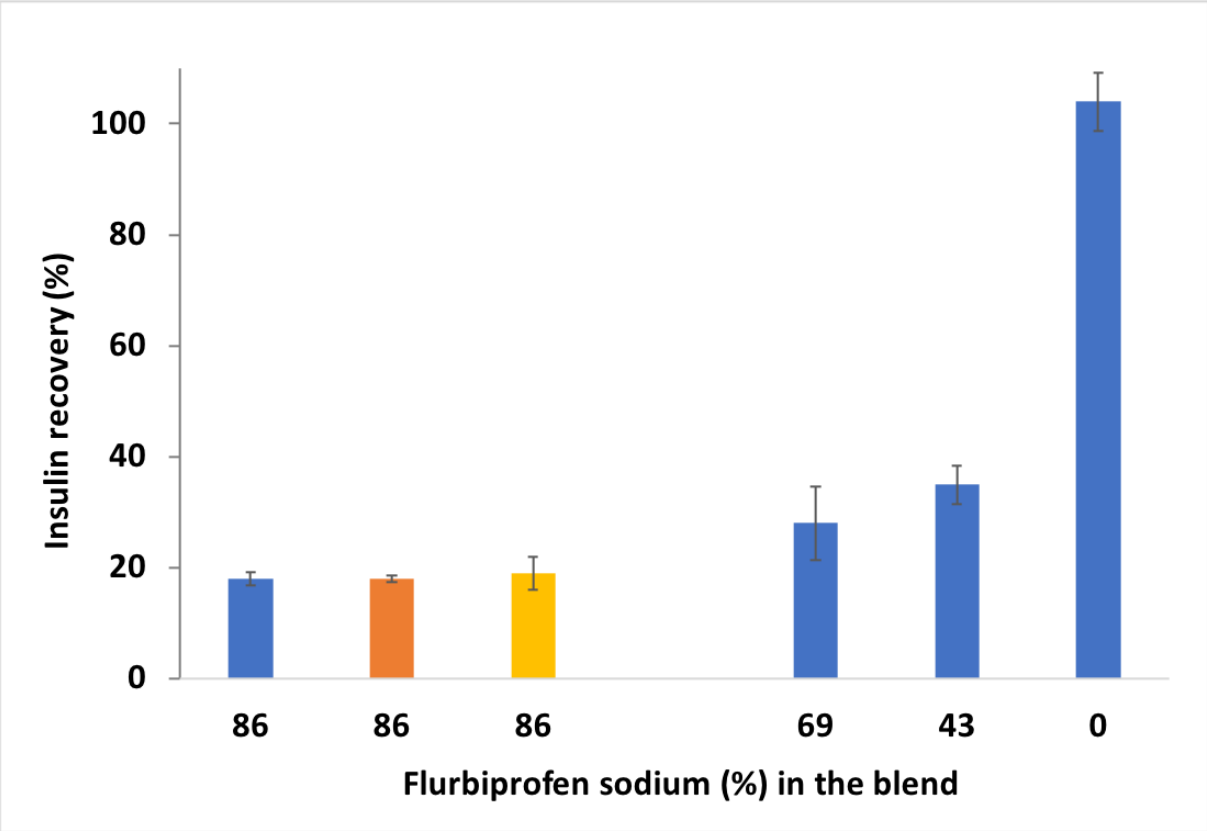

***Figure 5.3**. Insulin recovery after 4 hours in contact with the nasal mucosa from insulin powder raw material alone in comparison with blends with flurbiprofen spray-dried microparticles. In the blends, insulin:FB-COONa:FB-COOH powder ratio was 14:69:17 (i.e., 80:20 FB-COONa:FBCOOH microparticles), 14:43:43 (i.e., 50:50 FB-COONa:FBCOOH microparticles), 14:0:86 (1:0 FB-COONa:FBCOOH microparticles) (% w/w). Powders were wet with PBS pH 7.4 (blue), water (orange) or a solution of Kunitz-type trypsin inhibitor (1 mg/ml) in PBS pH 7.4 (yellow). Data are expressed as mean* ± SEM (n≥*3)*.

The flurbiprofen part of the blend (86% w/w) was modified by gradually substituting FB-COONa spray-dried microparticles with FB-COOH spray-dried microparticles at 3 salt/acid ratios, namely 50:50, 20:80 and 0:100. As shown in Fig. 5.3, the recovery of insulin after 4 h depended on the sodium salt content: insulin recovery increased as FB-COONa percentage in the blend decreased until complete recovery when the blend contained only FB-COOH. In all these experiments, flurbiprofen was always completely recovered (>98% drug recovered).

We tried to substitute a fraction of FB-COONa in the blend with a different component, namely with the mannitol/lecithin excipient spray-dried microparticles (14:43:43 insulin: FB-COONa:excipients). The insulin recovery after 4 h was 24 ± 1%, i.e., as low as in the blend containing 43% of FB-COOH. This confirmed that FB-COONa was the

“degrading element”, but only when the blend was in contact with nasal mucosa. Degradation was a function of FB-COONa percentage in the blend and no matter what third component was added to the blend. The excipients did not protect insulin against chemical degradation.

Explaining the observed insulin degradation is not easy, but the metabolic activity of the excised rabbit nasal mucosa could be one factor to consider. In the early ‘90, Sarkar reviewed the literature and reported that the nasal mucosa is a pseudo first-pass barrier for drugs nasally administered, both in humans and in animals for pre-clinical studies. The nasal mucosa contains cytochrome P-450 and cytochrome P-450-dependent enzymes, whose catalytic activity in the nasal tissue is remarkably higher than in any other tissues including the liver (i.e., three- to four-folds higher NADPH-cytochrome P-450 reductase content in the nasal mucosa *versus* liver). Among other mammals, including human, the rabbit has the highest concentration of cytochrome P-450 enzyme in nasal tissue (approximately 350 pmol/mg microsomal proteins). These enzymes are responsible of phase I metabolism (oxidative reactions), which in the nasal tissue is generally higher in the olfactory region than in the respiratory one. Moreover, the nasal mucosa contains protease and proteinase enzymes, including exo- and endo-peptidases: the proteolytic activity of the nasal mucosa was demonstrated in homogenates of albino rabbit’s nasal mucosa against several proteins, including insulin. In rabbit nasal mucosa, the proteolytic enzymes are half cytosolic and half membrane-bound, thus the metabolism of proteins could happen both inside and the surface of nasal cells (Sarkar, 1992).

It is interesting that in experimental conditions similar to those applied in the present study of insulin stability/compatibility with flurbiprofen, another peptide (desmopressin) was reported subjected to enzymatic degradation by the tissue (Balducci et al., 2013). Desmopressin is a peptide like insulin and peptides can be degraded by proteolytic enzymes of the excised rabbit nasal mucosa. As proteases are numerous in the nasal tissue, it is complicate to recognize which enzyme(s) is involved. We checked whether trypsin may be responsible of the observed degradation of insulin. Trypsin is known to reduce peptide drugs’ availability after nasal administration (Morimoto et al., 1995). Thus, a test was carried out in which the Kunitz inhibitor of trypsin was dissolved in the solvent used to wet the powder, but insulin recovery after the 4 h was equivalent to that in absence of the enzymatic inhibitor (Fig. 5.3). Either trypsin was not the right enzyme or insulin was not degraded enzymatically. In other words, this result may be

due to the fact that trypsin is only one of many enzymes capable to metabolize insulin. If in our *in vitro* experimental set-up, the presence and action of trypsin were minor and other enzymes were involved, the use of the trypsin inhibitor would make no difference. While the hypothesis of enzymatic degradation is uncertain based on the available data, FB-COONa definitely favored the degradation. In fact, when insulin was alone in contact with the nasal mucosa, no degradation was observed. A pH effect is as uncertain as the enzymatic hypothesis, as proved when substituting it with FB-COOH or changing the solvent from PBS to water.

In summary, the results the of the compatibility studies taken together, show that insulin was unstable in the *ex vivo* conditions in presence of FB-COONa. This should not be considered a limiting factor of the further development of the nasal 2-drug combination of insulin and FB-COONa. In fact, when the test time was reduced to 30 min, insulin degradation was lower (<15%). Transposing to the *in vivo* situation, the amount of insulin degraded before nasal absorption could be not as detrimental. In fact nasal drug absorption generally happens in the first 15 minutes after drug administration, while the nasal mucociliary clearance removes the drug from the absorption site (Illum et al., 2001). The tests here performed lasted 4 h to characterize the stability profile, but the 30 min time point should be considered the most relevant for the purpose of nasal delivery.

5.3.2 *Ex vivo* drug transport across rabbit nasal mucosa

In spite of the discovered chemical instability of insulin blended with flurbiprofen, the *ex vivo* transport of the two drugs was studied across excised rabbit nasal mucosa from the 14:86 (% w/w) powder blend. This mass ratio was different from the 3.5:96.5 (% w/w) ratio discussed at the beginning of this chapter. As the typical amount of powder loaded was 5 mg in all the *ex vivo* experiments with spray-dried microparticles. Having fixed 5 mg as the total amount of powder for the tests, the 0.7 mg insulin dose (14% of the blend) was maintained and the remaining “space” up to 5 mg was filled by FB-COONa (and/or the other components). With FB-COOH, a 50:50 blend was also considered.

The blends contained either insulin raw material or the spray-dried microparticles. The study aimed to assess whether the transport profiles of the two drugs measured individually, changed being the two together. Moreover, since insulin degradation occurred in *in vitro* tests without permeation, we checked whether the transport across

the nasal mucosa modified the interaction between the two drugs in the donor compartment or between the drug and the mucosa. As shown in Fig. 5.4A, there was no difference in the transmucosal insulin transport from the spray-dried microparticles and the insulin raw material. Flurbiprofen spray-dried microparticles were the second component, either FB-COOH (F2) or FB-COONa (F3 and F13_40). While the salt form was preferred for its extensive permeation across the mucosa *ex vivo* (chapter 2), the acid form was safer for insulin stability. The transport profiles of insulin and flurbiprofen were followed up to 4 h, but with a particular focus on the first 30 minutes.

Blends insulin/FB-COONa

Using the 14:86 (% w/w) powder blend of insulin raw material and FB-COONa spray-dried microparticles (F13_40), after 30 min the amount of insulin transported per unit area was 0.015 ± 0.005 mg cm^{-2}, corresponding to 1.2 ± 0.4% of the initial loading (mean ± SEM) (Fig. 5.4A). Insulin accumulation inside the mucosa was 0.009 ± 0.002 mg, which was not significantly different from the amount accumulated after 4 h of permeation from the raw material alone (see chapter 4). This indicates that insulin started early to interact with the biological tissue, just after its dissolution and despite its molecular weight. The insulin mass balance after 30 min was close to 70% (Fig. 5.4B), thus in line with what found in the stability test at 30 minutes.

As for flurbiprofen, the amount transported in 30 min across the nasal mucosa was 0.50 ± 0.10 mg cm^{-2} (corresponding to 8.4 ± 1.7% of the initial loading). FB-COOH accumulation inside the mucosa was 0.15 ± 0.03 mg, not significantly different from the accumulation after 4 h from the F13_40 spray-dried microparticles (chapter 2).

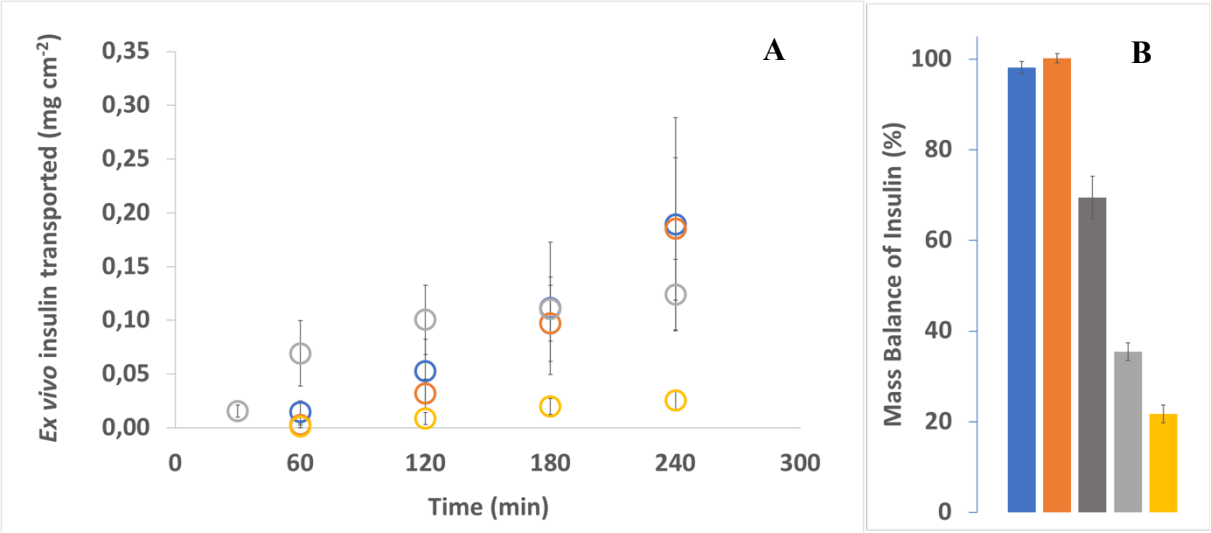

Figure 5.4. *(A) Insulin transport across rabbit nasal mucosa from: insulin raw material (blue), insulin spray-dried microparticles (orange), 14:86 insulin raw material/FB-COONa (F13_40) blend (grey), and 14:86 insulin spray-dried microparticles/FB-COONa (F3) blend (yellow). (B) Insulin mass balance after 4 h of ex vivo transport, the color code is the same of panel A, except for dark grey that shows the mass balance after 0.5 h. Data expressed as mean* ± SEM (*n≥3)*.

By prolonging the experiment, it was found that insulin continued to be transported beyond 30 min from the 14:86 powder blend: at the end of the 4th h, the insulin transported per unit area was 0.12 ± 0.03 mg cm^{-2} (corresponding to 9.3 ± 2.3% of insulin initial loading) (Fig. 5.4A). It is interesting to note that the 4 h permeation profile of insulin from this blend was not significantly different from the permeation of insulin from the raw material alone (P >0.05). This result is important because (1) we know that insulin was degraded in presence of FB-COONa and (2) the insulin initial loading ("dose") was lower with the blend. Since drug transport across the tissue is dependent on the drug concentration gradient, despite insulin powder dose was much lower when using the blend, in these conditions insulin may have reached and maintained the saturation in contact with the mucosa. However, a slow decrease in insulin transport was noticed after the 2nd hour (Fig. 5.4A), which was attributed to the progressive degradation of the peptide. In fact, at the end of 4 h-experiment the insulin mass balance was around 35% (Fig. 5.4B), matching the results of the stability test.

When the blend 14:86 blend contained insulin spray-dried microparticles instead of the raw material and F3 FB-COONa spray-dried microparticles instead of F13_40, the insulin *ex vivo* transport was lower compared to the transport from insulin spray-dried microparticles without flurbiprofen and the difference became statistically significant

from the 2nd h on. The amount of insulin transported per unit area after 4 h was 0.026 ± 0.009 mg cm^{-2} (corresponding to 2.1 ± 0.8% of the initial loading) (Fig. 5.4A). The accumulation inside the mucosa (0.008 ± 0.014 mg insulin) was in line with that produced by the insulin spray-dried microparticles alone and by the insulin raw material blended with F13_40. Insulin recovery at the end of the experiment was 21.7 ± 1.9%, significantly lower compared to the recovery obtained from the 14:86 blend insulin raw material:F13_40 (Fig. 5.4B). These results suggest that when insulin was in the blend in the form of microparticulate powder, the interaction with FB-COONa in contact with the nasal mucosa was somehow facilitated and insulin degradation was more intense, which also negatively affected diffusion.

FB-COOH transported per unit area from the blend with insulin spray-dried microparticles was 3.93 ± 0.19 mg cm^{-2} (corresponding to 64 ± 3% of the initial loading). Compared to the transport profile of Mini B-191 FB-COONa microparticles (F3; Fig. 2.7), the presence of insulin made a difference as the drug transported across the mucosa was significantly lower from the 2nd h on ($P < 0.05$). Conversely, flurbiprofen accumulation inside the mucosa was 25% higher (0.35 ± 0.01 mg as FB-COOH, $P < 0.05$)

Blends insulin/ FB-COOH

Considering the 14:86 blend of insulin spray-dried microparticles with FB-COOH spray-dried microparticles (F2), the insulin transported across the nasal mucosa in 4 hours was extremely low and variable, namely 0.001 ± 0.002 mg cm^{-2} (corresponding to 0.10 ± 0.13% of initial insulin loading). Insulin transport in the presence of F2 differed much from the behavior of insulin spray-dried microparticles alone. Presumably, none of the molecules was easy to dissolve in the small volume of PBS. In addition, FB-COOH was more abundant than insulin and may have competed with insulin for the solvent. Limited dissolution would result in lower permeation. Indeed, the increase of insulin content in the blend with F2 to 50% (w/w), increased insulin permeation (0.032 ± 0.004 mg cm^{-2}, corresponding to 0.37 ± 0.04 of initial insulin loading). Moreover, the blend with F2 allowed for complete recovery of insulin at the end of the experiment (96.8% ± 4.6 and 97.3 ± 1.6 for the 14:86 and 50:50 blends, respectively), confirming that the peptide did not degrade as seen in stability test *in vitro*.

As for FB-COOH, the amount transported per unit area in 4 h was 1.39 ± 0.22 mg cm^{-2} (corresponding to 18.5 ± 2.7% of the initial loading). This amount was significantly lower than what seen for F2 alone from the 1st hour on ($P < 0.05$) (Fig. 2.7). This could be due to the lower FB-COOH loading at time zero. However, the 50:50 blend (which increased FB-COOH loading) gave a similar transport of FB-COOH (1.29 ± 0.10 mg cm^{-2}).

Thinking to the 2-drug combination for nose-to-brain delivery, the results suggest that the advantage offered by FB-COONa in terms of transmucosal transport is counteracted by the degradation of insulin issue in contact with the mucosa. The diffusion across the tissue did not modify the degradation compared to the situation in which diffusion was impeded. The understanding of the mechanism underlying this degradation is fundamental to possibly find a solution to the problem.

5.3.3 Agglomerates of insulin and flurbiprofen spray-dried microparticles

The insulin spray-dried microparticles and FB-COONa spray-dried microparticles (F13_40) were agglomerated by tumbling to create the actual nasal dosage form. Excipient spray-dried microparticles (Nano ML_iPr) were added to facilitate agglomerate formation, as discussed for flurbiprofen and excipient agglomerates in chapter 2. The blend was prepared to contain 14:43:43 (% w/w) insulin spray-dried microparticles + F13_40 + excipient spray-dried microparticles. Since F13_40 contained 78.7 % FB-COOH (Tab. 2.II), its content in the pre-agglomeration blend was 34%. The blend was homogenous with respect to both drugs before agglomeration.

Agglomeration yield and drug content of two agglomerate size fractions (fraction 1: d >500 µm; fraction 2: 106 < d < 500 µm) are shown in Tab. 5.I. The total yield was 93%, comparable to that of the best agglomerates of FB-COONa spray-dried microparticles discussed in chapter 2.

Insulin content in the insulin- FB-COONa -excipient agglomerates corresponded to the theoretical value (14%) in each agglomerate fraction, meaning that the drug was homogeneously distributed. In contrast, flurbiprofen content was lower than the theoretical value in fraction 1 agglomerates and consequently higher in the smaller-size agglomerates (Tab. %.I).

Table 5.I. *Agglomerates of insulin,* FB-COONa *and excipient spray-dried microparticles (powder ratio 14:43:43) manufactured by tumbling. In each fraction insulin content was expected to be 14% (w/w) and flurbiprofen 34% as FB-COOH (% w/w). Data expressed as mean ± standard deviation.*

Agglomerate Fraction (μm)	Yield (%)	INS content (% w/w)	FB-COOH content (% w/w)
>500	8.1	14.4 ± 2.0	20.6 ± 3.1
106-500	84.7	11.5 ± 0.1	55.3 ± 2.8

5.4 CONCLUSIONS

The combination of FB-COONa and insulin was feasible from a physical perspective. In fact, a blend of FB-COONa spray-dried microparticles and insulin spray-spray-dried microparticles with excipient spray-dried microparticles was agglomerated in a 2-drug powder dosage form. The knowledge acquired in chapter 2 allowed here to obtain agglomerates at high yield and good content of both drugs. However, in contact with the nasal mucosa, insulin was found chemically unstable in a time-dependent manner only in presence of FB-COONa. Anyway, even in presence of FB-COONa, insulin was still able to be transported across the nasal mucosa *ex vivo*. The mechanism underlying the observed insulin degradation must be understood in order for the 2-drug powder of FB-COONa and insulin to be finalized into the nasal product for AD.

FINAL CONCLUSIONS

This Ph.D. research started from the choice of flurbiprofen and insulin as molecules of interest for the management of AD, possibly in its early phases. In three years of work, two types of nasal powders have been constructed, i.e., spray-dried microparticles and agglomerates. Flurbiprofen and insulin have been separately transformed by spray drying into microparticulate powders with size, dissolution and transmucosal transport *ex vivo* favorable to the intended i.n. application. In the case of flurbiprofen, the spray-dried microparticles could be obtained as either the acid form of the drug (FB-COOH) or its sodium salt (FB-COONa). Although characterized by different aqueous solubility and dissolution rate, both provide an interesting option, particularly for the subsequent combination with insulin.

The agglomerates of FB-COONa spray-dried microparticles with excipient spray-dried microparticles represent the second type of nasal powder resulting from this research. Recalling the Ph. Eur., both the flurbiprofen spray-dried microparticles and agglomerates comply with definition of nasal powder as long as they are combined with the UDS powder insufflator device for the purpose of administration and deposition into the nasal cavities. The two powder-device combinations studied, have led to the observation of the different behavior of the two powders when insufflated: the powder delivery with the agglomerates was more efficient than with the microparticles, emitting more than 80% of the amount of powder loaded in the device's reservoir. Thus, the agglomeration has solved one the problems that fine microparticles pose when constructing a product for i.n. drug delivery. Powder density, packing and flow are improved with the agglomerates, while the potential risk for lung inhalation of microparticles smaller than 10 μm is substantially reduced.

In light of these results, agglomerates should be preferred over spray-dried microparticles for i.n. flurbiprofen delivery. However, no system is perfect and flurbiprofen agglomerate manufacturing has been shown critical with respect to the homogeneous distribution of the drug within the powder. The agglomeration method is one variable influencing this aspect, which needs to be improved to provide the correct drug dosage. In addition, the agglomerates are less efficient than the spray-dried microparticles in terms of drug transport *ex vivo* and also *in vivo*, possibly due to a different distribution and coverage of the mucosal surface.

Similarly, insulin has been made available as microparticulate powder suitable for inhalation, but at present is not yet a nasal powder. There is necessary work to carry out in order to transform the insulin spray-dried microparticles into a nasal powder, including the combination with the nasal insufflator.

The availability of the nasal product has enabled the intranasal administration of the flurbiprofen powders (microparticles and agglomerates) *in vivo* to rats: the first positive result is the benefit of the i.n. powders over the i.n. solution, particularly in terms of brain disposition more than systemic absorption. With the powders a much higher drug dose per shot can be insufflated, which likely sustains the transport of flurbiprofen to the brain *via* the nose-to-brain pathway. The exploitation of this pathway by the powders has been evidenced by two specific indexes calculated from the serum and brain AUCs after i.n. and i.v. administration. The efficiency of brain targeting is higher using the powders (microparticles > agglomerates) compared to the solution, in light of the different doses and the surface area for formulation deposition, which was double with the solution. The second positive result is that flurbiprofen reaches the brain at higher levels after i.n. administration as powder compared to i.v. injection of a similar dose. Whether the observed brain levels are relevant for management of early inflammation in AD requires to be investigated.

Finally, the combination of insulin and flurbiprofen microparticulate powders has moved the first steps and the study of the 2-drug powder remains incomplete. It is mandatory to find a way to blend and agglomerate the small amount of insulin with flurbiprofen and excipient (all in the form or spray-dried microparticulate powder) in a nasal powder, requiring the homogeneous distribution of both drugs, not only one. The construction and use of this powder is currently challenged by the observation that insulin is chemically unstable in contact with the nasal mucosa together with FB-COONa. The prosecution of the work is encouraged by the most recent observation that there is no insulin loss in presence of FB-COOH. FB-COOH spray-dried microparticles are available and have shown, although preliminarily, a non-dissimilar performance *in vivo* compared to the FB-COONa spray-dried microparticles.

BIBLIOGRAPHY

- Abdel Mouez M, Zaki NM, Mansour S, Geneidi AS. Bioavailability enhancement of verapamil HCl via intranasal chitosan microspheres. Eur. J. Pharm. Sci. 2014; 51, 59–66. https://doi.org/10.1016/j.ejps.2013.08.029.
- Adi S, Adi H, Chan HK, Finlay WH, Tong Z, Yang R, Yu A. (2011). Agglomerate strength and dispersion of pharmaceutical powders. Pharm Res. 2006;23(11):2556-65.
- Agrawal M, Saraf S, Saraf S, Antimisiaris SG, Chougule MB, Shoyele SA, Alexander A. Nose-to-brain drug delivery: An update on clinical challenges and progress towards approval of anti-Alzheimer drugs. J Control Release. 2018;281:139-177. doi: 10.1016/j.jconrel.2018.05.011.
- Aisen PS., Tarenflurbil: a shot on goal. Lancet Neurol. 2008;7(6):468-9. doi: 10.1016/S1474-4422(08)70091-7.
- Alvarez XA, Cacabelos R, Sampedro C, Couceiro V, Aleixandre M, Vargas M, Linares C, Granizo E, García-Fantini M, Baurecht W, Doppler E, Moessler H. Combination treatment in Alzheimer's disease: results of a randomized, controlled trial with cerebrolysin and donepezil. Curr Alzheimer Res. 2011;8(5):583-91.
- Annweiler C, Herrmann FR, Fantino B, Brugg B, Beauchet O. Effectiveness of the combination of memantine plus vitamin D on cognition in patients with Alzheimer disease: a pre-post pilot study. Cogn Behav Neurol. 2012;25(3):121–127.
- AptarGroup I., 2017. Aptargroup [WWW document]. https://pharma.aptar.com/en-us.
- Aquino RP, Stigliani M, Del Gaudio P, Mencherini T, Sansone F, Russo P. Nanospray drying as a novel technique for the manufacturing of inhalable NSAID powders. ScientificWorldJournal. 2014;2014:838410. doi: 10.1155/2014/838410.
- Atri A, Shaughnessy LW, Locascio JJ, Growdon JH. Long-term course and effectiveness of combination therapy in Alzheimer disease. Alzheimer Dis Associ Disord. 2008;22(3):209–221.
- Balducci AG, Cagnani S, Sonvico F, Rossi A, Barata P, Colombo G, Colombo P, Buttini F. Pure insulin highly respirable powders for inhalation. Eur J Pharm Sci. 2014;51:110-7. doi: 10.1016/j.ejps.2013.08.009.

- Balducci AG, Ferraro L, Bortolotti F, Nastruzzi C, Colombo P, Sonvico F, Russo P, Colombo G. Antidiuretic effect of desmopressin chimera agglomerates by nasal administration in rats. Int. J. Pharm 2013; 440, 154–160. https://doi.org/10.1016/j.ijpharm.2012.09.049
- Banks, W. A. Characteristics of compounds that cross the blood-brain barrier. BMC Neurol. 2009; 12;9 Suppl 1:S3. doi: 10.1186/1471-2377-9-S1-S3.
- Bedse G, Di Domenico F, Serviddio G, Cassano T. Aberrant insulin signaling in Alzheimer's disease: current knowledge. Front Neurosci. 2015;9:204. doi: 10.3389/fnins.2015.00204.
- Belgamwar VS, Patel HS, Joshi AS, Agrawal A, Surana SJ, Tekade AR. Design and development of nasal mucoadhesive microspheres containing tramadol HCl for CNS targeting. Drug Deliv. 2011;18(5):353-60. doi: 10.3109/10717544.2011.557787.
- Belgi A, Akhter Hossain MW, Tregear G, D Wade J. The chemical synthesis of insulin: from the past to the present. Immunology, Endocrine & Metabolic Agents in Medicinal Chemistry (Formerly Current Medicinal Chemistry-Immunology, Endocrine and Metabolic Agents), 2011; 11(1), 40-47. DOI: 10.2174/187152211794519412.
- Belotti S, Rossi A, Colombo P, Bettini R, Rekkas D, Politis S, Colombo G, Balducci AG, Buttini F. Spray dried amikacin powder for inhalation in cystic fibrosis patients: a quality by design approach for product construction. Int J Pharm. 2014; 471(1-2):507-15. doi: 10.1016/j.ijpharm.2014.05.055.
- Belotti S, Rossi A, Colombo P, Bettini R, Rekkas D, Politis S, Colombo G, Balducci AG, Buttini F. Spray-dried amikacin sulphate powder for inhalation in cystic fibrosis patients: the role of ethanol in particle formation. Eur J Pharm Biopharm. 2015 Jun;93:165-72. doi: 10.1016/j.ejpb.2015.03.023.
- Benedict C, Hallschmid M, Hatke A, Schultes B, Fehm HL, Born J, Kern W. Intranasal insulin improves memory in humans. Psychoneuroendocrinology. 2004;29(10):1326-34. doi: 10.1016/j.psyneuen.2004.04.003.
- Benedict C, Kern W, Schultes B., Born J, Hallschmid M. Differential sensitivity of men and women to anorexigenic and memory- improving effects of intranasal insulin. J. Clin. Endocrinol. Metab. 2008; 93, 1339–1344. doi: 10.1210/jc.2007-2606.

- Birch AM, Katsouri L, Sastre M. Modulation of inflammation in transgenic models of Alzheimer's disease. J Neuroinflammation. 2014;11:25. doi: 10.1186/1742-2094-11-25.
- Bitter C, Suter-Zimmermann K, Surber C. Nasal drug delivery in humans. I Curr Probl Dermatol. 2011;40:20-35. doi: 10.1159/000321044.
- Bortolotti F, Balducci AG, Sonvico F, Russo P, Colombo G. In vitro permeation of desmopressin across rabbit nasal mucosa from liquid nasal sprays: the enhancing effect of potassium sorbate. Eur J Pharm Sci. 2009;37(1):36-42. doi: 10.1016/j.ejps.2008.12.015.
- Bottom R. The role of modulated temperature differential scanning calorimetry in the characterisation of a drug molecule exhibiting polymorphic and glass forming tendencies. Int J Pharm. 1999;192(1):47-53.
- Brange J, Langkjœr L. Insulin Structure and Stability. Pharm Biotechnol. 1993;5:315-50.
- Brange J, Langkj L, Havelund S, Vølund A. Chemical stability of insulin. 1. Hydrolytic degradation during storage of pharmaceutical preparations. Pharm Res. 1992 Jun;9(6):715-26.
- Broadhead J, Edmond Rouan SK, Rhodes CT. The spray driying of pharmaceuticals. Drug Dev Ind Pharm, 1992; 18.11-12: 1169-1206.
- Buchi Labortechnic, 2017. B CHI Labortechnik AG [WWW document]. https:// www.buchi.com/en. In: www.buchi.com.
- Burki K, Jeon I, Arpagaus C, Betz G. New insights into respirable protein pow- der preparation using a nano spray dryer. Int. J. Pharm. 2011; 408, 248–256. https://doi.org/10.1016/j.ijpharm.2011.02.012.
- Buttini F, Colombo P, Rossi A, Sonvico F, Colombo, G. Particles and powders: tools of innovation for non-invasive drug administration. J Control Release. 2012;161(2):693-702. doi: 10.1016/j.jconrel.2012.02.028.
- Callens C, Ceulemans J, Ludwig A, Foreman P, Remon JP. Rheological study on mucoadhesivity of some nasal powder formulations. Eur J Pharm Biopharm. 2003;55(3):323-8.
- Callens C, Remon JP. Evaluation of starch-maltodextrin-Carbopol 974 P mixtures for the nasal delivery of insulin in rabbits. J Control Release. 2000;66(2-3):215-20.

- Cano-Cuenca N, Solis-Garcia Del Pozo JE, Jordan J. Evidence for the efficacy of latrepirdine (Dimebon) treatment for improvement of cognitive function: a meta-analysis. J Alzheimers Dis. 2014;38: 155–164.
- Chapman CD, Frey WH, Craft S, Danielyan L, Hallschmid M, Schiöth HB, Benedict C. Intranasal treatment of central nervous system dysfunction in humans. Pharm Res. 2013;30(10):2475-84. doi: 10.1007/s11095-012-0915-1.
- Chaturvedi M, Kumar M, Pathak K. A review on mucoadhesive polymer used in nasal drug delivery system. J Adv Pharm Technol Res. 2011;2(4):215-22. doi: 10.4103/2231-4040.90876.
- Chen R, Chan PT, Chu H, Lin YC, Chang PC, Chen CY, Chou KR. Treatment effects between monotherapy of donepezil versus combination with memantine for Alzheimer disease: A meta-analysis. PLoS One. 2017;12(8):e0183586. doi: 10.1371/journal.pone.0183586. eCollection 2017.
- Chien Y., Su K., Chang S. Nasal Systemic Drug Delivery, 1989. ISBN: 978-0824780937, Publisher: Marcel Dekker Inc.
- Cho W, Kim MS, Jung MS, Park J, Cha KH, Kim JS, Park HJ, Alhalaweh A, Velaga, SP, Hwang SJ. Design of salmon calcitonin particles for nasal delivery using spray-drying and novel supercritical Wuid-assisted spray-drying processes. Int. J. Pharm. 2015; 478, 288–296. https://doi.org/10.1016/j.ijpharm.2014.11.051.
- Christodoulou E, Kechagia IA, Tzimas S, Balafas E, Kostomitsopoulos N, Archontaki H, Dokoumetzidis A, Valsami G. Serum and tissue pharmacokinetics of silibinin after per os and i.v. administration to mice as a HP-β-CD lyophilized product. Int J Pharm. 2015;493(1-2):366-73. doi: 10.1016/j.ijpharm.2015.07.060.
- Claxton A, Baker LD, Hanson A, Trittschuh EH, Cholerton B, Morgan A, Callaghan M, Arbuckle M, Behl C, Craft S. Long-acting intranasal insulin detemir improves cognition for adults with mild cognitive impairment or early-stage Alzheimer's disease dementia. J Alzheimers Dis. 2015;44(3):897-906. doi: 10.3233/JAD-141791.
- Claxton A, Baker LD, Wilkinson CW, et al. Sex and ApoE genotype differences in treatment response to two doses of intranasal insulin in adults with mild cognitive impairment or Alzheimer’s disease. J Alzheimers Dis. 2013;35(4):789-497.
- Colombo P., Alhaique F., Caramella C., et al., Principi di tecnologia farmaceutica-Seconda edizione, 2015. Publisher: Casa Editrice Ambrosiana.

- Colombo G, Bortolotti F, Chiapponi V, Buttini F, Sonvico F, Invernizzi R, Quaglia F, Danesino C, Pagella F, Russo P, Bettini R, Colombo P, Rossi A. Nasal powders of thalidomide for local treatment of nose bleeding in persons affected by hereditary hemorrhagic telangiectasia. Int. J. Pharm. 2016; 514, 229–237. https://doi.org/10.1016/j.ijpharm.2016.07.002.
- Colombo G, Lorenzini L, Zironi E, Galligioni V, Sonvico F, Balducci AG, Pagliuca G, Giuliani A, Calzà L, Scagliarini A. Brain distribution of ribavirin after intranasal administration. Antivir. Res. 2011; 92, 408–414. https://doi.org/10.1016/j.antiviral.2011.09.012.
- Colombo P, Traini D, Buttini F. Inhalation Drug Delivery: Techniques and Products; ISBN: 978-1-118-35412-4 2013, Publisher: Wiley-Blackwell.
- Connelly PJ, Prentice NP, Cousland G, Bonham J. A randomised double-blind placebo-controlled trial of folic acid supplementation of cholinesterase inhibitors in Alzheimer's disease. Int J Geriat Psychiatry. 2008;23(2):155–160.
- Costantino HR, Illum L, Brandt G, Johnson PH, Quay SC. Intranasal delivery: physicochemical and therapeutic aspects. Int J Pharm. 2007;337(1-2):1-24.
- Coucke D, Pringels E, Foreman P, Adriaensens P, Carleer R, Remon JP, Vervaet, C. Infuence of heat treatment on spray-dried mixtures of Amioca starch and Carbopol 974P used as carriers for nasal drug delivery. Int. J. Pharm. 2009; 378, 45–50. https://doi.org/10.1016/j.ijpharm.2009.05.041.
- Craft S, Baker LD, Montine TJ, Minoshima S, Watson GS, Claxton A, Arbuckle M, Callaghan M, Tsai E, Plymate SR, Green PS, Leverenz J, Cross D, Gerton B. Intranasal insulin therapy for Alzheimer disease and amnestic mild cognitive impairment: a pilot clinical trial. Arch Neurol. 2012;69(1):29-38. doi: 10.1001/archneurol.2011.233.
- Cuello AC. Early and late CNS inflammation in Alzheimer's disease: two extremes of a continuum?. Trends Pharmacol Sci. 2017;38(11):956-966. doi: 10.1016/j.tips.2017.07.005.
- Cummings J. Lessons learned from Alzheimer disease: Clinical trials with negative outcomes. Clin Transl Sci. 2018;11(2):147-152. doi: 10.1111/cts.12491.
- Dalpiaz A, Fogagnolo M, Ferraro L, Capuzzo A, Pavan B, Rassu G, Salis A, Giunchedi P, Gavini E. Nasal chitosan microparticles target a zidovudine pro- drug to brain HIV sanctuaries. Antivir. Res. 2015; 123, 146–157. https://doi.org/10.1016/j.antiviral.2015.09.013.

- Dalpiaz, A., Pavan, B. (2018). Nose-to-Brain Delivery of Antiviral Drugs: A Way to Overcome Their Active Efflux?. Pharmaceutics. 2018;10(2). pii: E39. doi: 10.3390/pharmaceutics10020039.
- David SE, Timmins P, Conway BR. Impact of the counterion on the solubility and physicochemical properties of salts of carboxylic acid drugs. Drug Dev Ind Pharm. 2012;38(1):93-103. doi: 10.3109/03639045.2011.592530.
- Davis TD, Peck GE, Stowell JG, Morris KR, Byrn SR. Modeling and monitoring of polymorphic transformations during the drying phase of wet granulation. Pharm Res. 2004;21(5):860-6.
- Dean RL. The preclinical development of Medisorb Naltrexone, a once a month long acting injection, for the treatment of alcohol dependence. Front Biosci, 2005; 10, 643-655.
- de la Monte, S. M., & Wands, J. R. Alzheimer's disease is type 3 diabetes-evidence reviewed. J Diabetes Sci Technol. 2008;2(6):1101-13.
- de Lange EC. PKPD aspects of brain drug delivery in a translational perspective. In Drug Delivery to the Brain (pp. 233-268). Springer, New York, NY. 2014.
- Del Gaudio P, Sansone F, Mencherini T, De Cicco F, Russo P, Aquino RP. Nanospray drying as a novel tool to improve technological properties of soy IsoWavone extracts. Planta Med. 2017; 83, 426–433. https://doi.org/10.1055/s-0042-110179.
- Deli MA. Potential use of tight junction modulators to reversibly open membranous barriers and improve drug delivery. Biochim Biophys Acta. 2009;1788:892–910.
- Dhakar RC, Maurya SD, Tilak VK, Gupta AK. A review on factors affecting the design of nasal drug delivery system. International journal of drug delivery. 2011; 3(2), 194-208.
- Dhuria SV, Hanson LR, Frey II WH. Intranasal delivery to the central nervous system: mechanisms and experimental considerations. J Pharm Sci. 2010;99(4):1654-73. doi: 10.1002/jps.21924.
- Djupesland PG. Nasal drug delivery devices: characteristics and performance in a clinical perspective a review. Drug Deliv. Transl. Res. 2013; 3, 42–62. https://doi.org/10. 1007/s13346-012-0108-9.
- Djupesland PG, Messina JC, Mahmoud RA. The nasal approach to delivering treatment for brain diseases: an anatomic, physiologic, and delivery technology overview. Ther Deliv. 2014;5(6):709-33. doi: 10.4155/tde.14.41.

- Djupesland PG, Skretting A, Winderen M, Holand T. Breath actuated device improves delivery to target sites beyond the nasal valve. Laryngo- scope. 2006; 116:466–472.
- Dong J, Shang Y, Inthavong K, Chan HK, Tu J. Numerical Comparison of Nasal Aerosol Administration Systems for Efficient Nose-to-Brain Drug Delivery. Pharmaceutical research, 2018;35(1), 5.
- Dunn MF. Zinc–ligand interactions modulate assembly and stability of the insulin hexamer – a review. BioMetals 2005; 18:295–303.
- Elmowafy E, Osman R, El-Shamy Ael-H, Awad GA. Nasal polysaccharides-glucose regulator microparticles: optimization, tolerability and antidiabetic activity in rats. Carbohydr Polym. 2014;108:257-65. doi: 10.1016/j.carbpol.2014.02.064.
- England RJA, Homer JJ, Knight LC, Ell SR. Nasal pH measurement: a reliable and repeatable parameter. Clin Otolaryngol Allied Sci. 1999;24(1):67-8.
- Eriksen JL, Sagi SA, Smith TE, Weggen S, Das P, McLendon DC, Ozols VV, Jessing KW, Zavitz KH, Koo EH, Golde TE. NSAIDs and enantiomers of flurbiprofen target γ-secretase and lower Aβ42 in vivo. J Clin Invest. 2003;112(3):440-9.
- Fan LY, Chiu MJ. Combotherapy and current concepts as well as future strategies for the treatment of Alzheimer's disease. Neuropsychiatr Dis Treat. 2014;10:439-51. doi: 10.2147/NDT.S45143
- Farraj NF, Johansen BR, Davis SS, Illum L. Nasal administration of insulin using bioadhesive microspheres as a delivery system. J Controlled Release. 1990;13(2-3), 253-261.
- Field PLY, Raisman G. Ensheathment of the olfactory nerves in the adult rat. J Neurocytol. 2003;32(3), 317-324.
- Floroiu A, Klein M, Krämer J, et al. Towards Standardized Dissolution Techniques for In Vitro Performance Testing of Dry Powder Inhalers. Dissolut Technol. 2018;25(3).
- Food and Drug Administration (FDA), (2016). Use of International Standard ISO 10993-1, "Biological evaluation of medical devices - Part 1: Evaluation and testing within a risk management process; Guidance for Industry and Food and Drug Administration Staff, CDRH, 2016.
- Fortuna A, Alves G, Serralheiro A, Sousa J, Falcão A. Intranasal delivery of systemic-acting drugs: small-molecules and biomacromolecules. Eur J Pharm Biopharm. 2014;88(1):8-27. doi: 10.1016/j.ejpb.2014.03.004.

- Garcia-Arieta A, Torrado-Santiago S, Goya L, Torrado JJ. Spray-dried powders as nasal absorption enhancers of cyanocobalamin. Biol Pharm Bull. 2001;24(12):1411-6.
- Garmise, R.J., Mar, K., Crowder, T.M., Hwang, C.R., Ferriter, M., Huang, J., Mikszta, J.A., Sullivan, V.J., Hickey, A.J., 2006. Formulation of a dry powder in uenza vac- cine for nasal delivery. AAPS PharmSciTech 7, E131–E137. https://doi.org/10.1208/pt070119.
- Garmise, R.J., Staats, H.F., Hickey, A.J. Novel dry powder preparations of whole inactivated influenza virus for nasal vaccination. AAPS PharmSciTech. 2007; 8, 2–10. https: //doi.org/10.1208/pt0804081.
- Gasparini, L, Netzer WJ, Greengard P, Xu H. Does insulin dysfunction play a role in Alzheimer's disease? Trends Pharmacol. Sci. 2002.23, 288–293. doi: 10.1016/S0165-6147(02)02037-0
- Gavini E, Hegge AB, Rassu G, Sanna V, Testa C, Pirisino G, Karlsen J, Giunchedi P. Nasal administration of carbamazepine using chitosan microspheres: in vitro/in vivo studies. Int. J. Pharm. 2006; 307, 9–15. https://doi.org/10.1016/j.ijpharm. 2005.09.013.
- Gavini E, Rassu G, Ferraro L, Generosi A, Rau JV, Brunetti A, Giunchedi P, Dalpiaz A, Antonelli T, Giunchedi P, Buniatian GH, Gleiter CH, Frey WH. Influence of chitosan glutamate on the in vivo intranasal absorption of roki- tamycin from microspheres. J. Pharm. Sci. 2011;100, 1488–1502. http://dx.doi.org/10. 1002/jps.22382.
- Gavini E, Rassu G, Sanna V, Cossu M, Giunchedi P. Mucoadhesive microspheres for nasal administration of an antiemetic drug, metoclopramide: in-vitro/ ex-vivo studies. J. Pharm. Pharmacol. 2005; 57, 287–294. https://doi.org/10.1211/ 0022357055623.
- Geldenhuys WJ, Darvesh AS. Pharmacotherapy of Alzheimer's disease: current and future trends. Expert Rev Neurother. 2015, 15(1):3-5. doi: 10.1586/14737175.2015.990884.
- Giuliani A, Balducci AG, Zironi E, Colombo G, Bortolotti F, Lorenzini L, Galligioni V, Pagliuca G, Scagliarini A, Calzà L, Sonvico F. In vivo nose-to-brain delivery of the hydrophilic antiviral ribavirin by microparticle agglomerates. Drug Deliv. 2018; 25(1):376-387 doi: 10.1080/10717544.2018.1428242.

- Gomez-Nicola D, Boche D. Post-mortem analysis of neuroinflammatory changes in human Alzheimer's disease. Alzheimers Res Ther. 2015;7(1):42. doi: 10.1186/s13195-015-0126-1.
- Graff CL, Pollack GM. Functional evidence for P-glycoprotein at the nose brain barrier. Pharm. Res. 2005; 22:86Y93.
- Graff CL, Pollack GM. P-glycoprotein attenuates brain uptake of substrates after nasal instillation. Pharm. Res. 2003; 20:1225Y1230.
- Green RC, Schneider LS, Amato DA, Beelen AP, Wilcock G, Swabb EA, Zavitz KH. Effect of tarenflurbil on cognitive decline and activities of daily living in patients with mild Alzheimer disease: a randomized controlled trial. JAMA. 2009; 302(23):2557-64. doi: 10.1001/jama.2009.1866.
- Gupta PP, Pandey RD, Jha D, Shrivastav V, Kumar S., Role of traditional nonsteroidal anti-inflammatory drugs in Alzheimer's disease: a meta-analysis of randomized clinical trials. Am J Alzheimers Dis Other Demen. 2015, 30(2):178-82. doi: 10.1177/1533317514542644.
- Haggag YA, Faheem AM. Evaluation of nano spray drying as a method for dry- ing and formulation of therapeutic peptides and proteins. Front. Pharmacol. 2015; 6, 140. https://doi.org/10.3389/fphar.2015.00140.
- Hallschmid M, Benedict C, Schultes B, Perras B, Fehm HL, Kern W, Born J. (2008). Towards the therapeutic use of intranasal neuropeptide administration in metabolic and cognitive disorders. Regul Pept. 2008;149(1-3):79-83. doi: 10.1016/j.regpep.2007.06.012.
- Hansen FS, Djupesland PG, Fokkens WJ. Preliminary efficacy of fluticasone delivered by a novel device in recalcitrant chronic rhinosinusitis. Rhinology. 2010;48(3):292-9. doi: 10.4193/Rhin09.178.
- Hartmann S, Mobius HJ. Tolerability of memantine in combina- tion with cholinesterase inhibitors in dementia therapy. Int Clin Psychopharmacol. 2003;18(2):81–85.
- Hasçiçek C, Gönül N, Erk N. Mucoadhesive microspheres containing gentamicin sulfate for nasal administration: preparation and in vitro characterization. Farmaco. 2003;58(1):11-6.
- Heneka MT, Carson MJ, El Khoury J, Landreth GE, Brosseron F, Feinstein DL, Jacobs AH, Wyss-Coray T, Vitorica J, Ransohoff RM, Herrup K, Frautschy SA, Finsen B, Brown GC, Verkhratsky A, Yamanaka K, Koistinaho J, Latz E, Halle A,

Petzold GC, Town T, Morgan D, Shinohara ML, Perry VH, Holmes C, Bazan NG, Brooks DJ, Hunot S, Joseph B, Deigendesch N, Garaschuk O, Boddeke E, Dinarello CA, Breitner JC, Cole GM, Golenbock DT, Kummer MP.Neuroinflammation in Alzheimer's disease. Lancet Neurol. 2015;14(4):388-405. doi: 10.1016/S1474-4422(15)70016-5.

- Hirlekar RS, Momin AM. Advances in Drug Delivery from Nose to Brain: An Overview. Current Drug Therapy. 2018;13(1), 4-24.10.2174/1574885512666170921145204
- Holmes C, Boche D, Wilkinson D, Yadegarfar G, Hopkins V, Bayer A, Jones RW, Bullock R, Love S, Neal JW, Zotova E, Nicoll JA. Long-term effects of Aβ42 immunisation in Alzheimer's disease: follow-up of a randomised, placebo- controlled phase I trial. Lancet. 2008;372(9634):216-23. doi: 10.1016/S0140-6736(08)61075-2.
- Howard R, McShane R, Lindesay J, Ritchie C, Baldwin A, Barber R, Burns A, Dening T, Findlay D, Holmes C, Hughes A, Jacoby R, Jones R, Jones R, McKeith I, Macharouthu A, O'Brien J, Passmore P, Sheehan B, Juszczak E, Katona C, Hills R, Knapp M, Ballard C, Brown R, Banerjee S, Onions C, Griffin M, Adams J, Gray R, Johnson T, Bentham P, Phillips P. Donepezil and memantine for moderate-to-severe Alzheimer's disease.N Engl J Med. 2012;366(10):893-903. doi: 10.1056/NEJMoa1106668.
- Huang D. Modeling of particle formation during spray drying. In: Palma, Spain: Eur. Dry. Conf. 2011.
- Illum, L. Nasal drug delivery: new developments and strategies. Drug Discov Today. 2002;7(23):1184-9.
- Illum L. Nasal drug delivery-possibilities, problems and solutions. Journal of controlled release2003; 87(1-3), 187-198.
- Illum L, Farraj NF, Davis SS. Chitosan as a novel nasal delivery system for peptide drugs. Pharm Res. 1994;11(8):1186-9.
- Illum L, Fisher AN, Jabbal-Gill I, Davis SS. Bioadhesive starch microspheres and absorption enhancing agents act synergistically to enhance the nasal absorption of polypeptides. Int. J. Pharm. 2001; 222, 109–119.
- Imbimbo BP. Why did tarenflurbil fail in Alzheimer's disease?. J Alzheimers Dis. 2009;17(4):757-60. doi: 10.3233/JAD-2009-1092.

- Ishwarya SP, Anandharamakrishnan C, Stapley AGF. Spray-freeze-drying: a novel process for the drying of foods and bioproducts. Trends Food Sci. Technol. 2015; 41, 161–181. https://doi.org/10.1016/j.tifs.2014.10.008.
- Jadhav KR, Gambhire MN, Shaikh IM, Kadam VJ, Pisal SS. Nasal drug delivery system-factors affecting and applications. Current drug therapy, 2007; 2(1), 27-38.
- Jain SK, Chourasia MK, Jain AK, Jain RK, Shrivastava AK. Development and characterization of mucoadhesive microspheres bearing salbutamol for nasal delivery. Drug Deliv. 2004; 11, 113–122. https://doi.org/10.1080/10717540490280750.
- Kandimalla, KK, Donovan MD (a). Carrier mediated transport of chlorpheniramine and chlorcyclizine across bovine olfactory mucosa: implications on nose-to-brain transport. J. Pharm. Sci. 2005; 94:613Y624.
- Kandimalla, KK, Donovan MD (b). Localization and differential activity of P-glycoprotein in the bovine olfactory and nasal respiratory mucosae. *Pharmaceutical research*, 2005; *22*(7), 1121-1128.
- Karavasili C, Bouropoulos N, Sygellou L, Amanatiadou EP, Vizirianakis IS, Fatouros DG. PLGA/DPPC/trimethylchitosan spray-dried microparticles for the nasal delivery of ropinirole hydrochloride: in vitro, ex vivo and cytocompatibility assessment. Mater. Sci. Eng. C. 2016; 59, 1053–1062. https://doi.org/10.1016/j.msec.2015.11. 028.
- Katsarov P, Pilicheva B, Uzunova Y, Gergov G, Kassarova M. Chemical cross-linking: A feasible approach to prolong doxylamine/pyridoxine release from spray-dried chitosan microspheres. Eur J Pharm Sci. 2018;123:387-394. doi: 10.1016/j.ejps.2018.07.059.
- Kim Y, Wellum G, Mello K, Strawhecker KE, Thoms R, Giaya A, Wyslouzil BE. Effects of relative humidity and particle and surface properties on particle resuspension rates. Aerosol Science and Technology, 2016; 50(4), 339-352.
- Kozlovskaya L, Abou-Kaoud M, Stepensky D. Quantitative analysis of drug delivery to the brain via nasal route. J Control Release. 2014;189:133-40. doi: 10.1016/j.jconrel.2014.06.053.
- Krauland AH, Leitner VM, Grabovac V, Bernkop-Schnürch A. In vivo evalua- tion of a nasal insulin delivery system based on thiolated chitosan. J. Pharm. Sci. 2006; 95, 2463–2472 https://doi.org/10.1002/jps.20700.

- Kulkarni AD, Bari DB, Surana SJ, Pardeshi CV. In vitro, ex vivo and in vivo performance of chitosan-based spray-dried nasal mucoadhesive microspheres of diltiazem hydrochloride. Journal of Drug Delivery Science and Technology, 2016; 31, 108-117.
- Lee CH, Chien W. Development and evaluation of a mucoadhesive drug delivery system for dual-controlled delivery of nonoxynol-9. J Control Release, 1996; 39(1), 93-103.
- Lee HB, Blaufox MD. Blood volume in the rat. J Nucl Med. 1985;26(1), 72-76.
- Lee SH, Heng D, Ng WK, Chan HK, Tan RB. Nano spray drying: a novel method for preparing protein nanoparticles for protein therapy. Int J Pharm. 2011;403(1-2):192-200. doi: 10.1016/j.ijpharm.2010.10.012.
- Lehrer S. Nasal NSAIDs for Alzheimer's disease. Am J Alzheimers Dis Other Demen. 2014;29(5):401-3. doi: 10.1177/1533317513518658.
- Lewis AL, Jordan F, Patel T, Jeffery K, King G, Savage M, Shalet S, Illum L. Intranasal Human Growth Hormone (hGH) Induces IGF-1 Levels Comparable With Subcutaneous Injection With Lower Systemic Exposure to hGH in Healthy Volunteers. J Clin Endocrinol Metab. 2015;100(11):4364-71. doi: 10.1210/jc.2014-4146.
- Lim ST, Martin GP, Berry DJ, Brown MB. Preparation and evaluation of the in vitro drug release properties and mucoadhesion of novel microspheres of hyaluronic acid and chitosan. J Control Release. 2000;66(2-3):281-92.
- Liu Q, Shen Y, Chen J, Gao X, Feng C, Wang L, Zhang Q, Jiang X. Nose-to-brain transport pathways of wheat germ agglutinin conjugated PEG-PLA nanoparticles. Pharm Res. 2012 Feb;29(2):546-58. doi: 10.1007/s11095-011-0641-0.
- Lochhead JJ, Thorne RG. (2012). Intranasal delivery of biologics to the central nervous system. Adv Drug Deliv Rev. 2012;64(7):614-28. doi: 10.1016/j.addr.2011.11.002.
- Lopez OL, Becker JT, Wahed AS, et al. Long-term effects of the concomitant use of memantine with cholinesterase inhibition in Alzheimer disease. J Neurol Neurosurg Psychiatry. 2009;80(6): 600–607.
- Lundbeck H A/S. Study of Lu AE58054 in Patients with Mild - Moderate Alzheimer's Disease Treated with Donepezil (STARSHINE). In: ClinicalTrials.gov [website on the Internet]. Bethesda, MD: US National Library of Medicine; 2013[updated October 10, 2013]. Available from

http://clinicaltrials.gov/ct2/show/NCT01955161?term=NCT01955161& rank 1. NLM identifier: NCT01955161.

- Mahajan HS, Gattani SG. Nasal administration of ondansetron using a novel microspheres delivery system part II: ex vivo and in vivo studies. Pharm. Dev. Technol. 2010;15, 653–657. https://doi.org/10.3109/10837450903479970.
- Mahajan HS, Tatiya BV, Nerkar PP. Ondansetron loaded pectin based microspheres for nasal administration: in vitro and in vivo studies. Powder Technol. 2012; 221, 168–176. https://doi.org/10.1016/j.powtec.2011.12.063.
- Martinac A, Filipović-GrčićJ., Perissutti, B., Voinovich, D., Paveli. Spray-dried chitosan/ethylcellulose microspheres for nasal drug delivery: swelling study and eval- uation of in vitro drug release properties. J. Microencapsul. 2005;22, 549–561. https://doi. org/10.1080/02652040500098960.
- Manniello MD, Del Gaudio P, Porta A, Aquino RP, Russo P. Aerodynamic properties, solubility and in vitro antibacterial efficacy of dry powders prepared by spray drying: Clarithromycin versus its hydrochloride salt. Eur J Pharm Biopharm. 2016;104:1-6. doi: 10.1016/j.ejpb.2016.04.009.
- Martignoni I, Trotta V, Lee WH, Loo CY, Pozzoli M, Young PM, Scalia S, Traini D. Resveratrol solid lipid microparticles as dry powder formulation for nasal delivery, characterization and in vitro deposition study. J. Microencapsul. 2016;33, 735–742. https://doi.org/10.1080/02652048.2016.1260659.
- Masters K. Scale-up of spray dryers. Drying technology, 1994;12(1-2), 235-257.
- McGeer PL, Guo JP, Lee M, Kennedy K, McGeer EG, Alzheimer's Disease Can Be Spared by Nonsteroidal Anti-Inflammatory Drugs. J Alzheimers Dis. 2018;62(3):1219-1222. doi: 10.3233/JAD-170706.
- Meister S, Zlatev I, Stab J, Docter D, Baches S, Stauber RH, Deutsch M, Schmidt R, Ropele S, Windisch M, Langer K, Wagner S, von Briesen H, Weggen S, Pietrzik CU. Nanoparticulate flurbiprofen reduces amyloid-β 42 generation in an in vitro blood–brain barrier model. Alzheimers Res Ther. 2013;5(6):51. doi: 10.1186/alzrt225.
- Meredith ME, Salameh TS, Banks WA. Intranasal delivery of proteins and peptides in the treatment of neurodegenerative diseases. AAPS J. 2015;17(4):780-7. doi: 10.1208/s12248-015-9719-7.
- Miguel-Álvarez M, Santos-Lozano A, Sanchis-Gomar F, Fiuza-Luces C, Pareja-Galeano H, Garatachea N, Lucia A., Non-steroidal anti-inflammatory drugs as a

treatment for Alzheimer's disease: a systematic review and meta-analysis of treatment effect. Drugs Aging. 2015;32(2):139-47. doi: 10.1007/s40266-015-0239-z.

- Milewski M, Goodey A, Lee D, Rimmer E, Saklatvala R, Koyama S, Iwashima M, Haruta S. Rapid absorption of dry-powder intranasal oxytocin. Pharm. Res. 2016;33, 1936–1944. https://doi.org/10.1007/s11095-016-1929-x.
- Mikszta, J.A., Sullivan, V.J., Dean, C., Waterston, A.M., Alarcon, J.B., Dekker III, J.P., Brittingham, J.M., Huang, J., Hwang, C.R., Ferriter, M., Jiang, G., Mar, K., Saikh, K.U., Stiles, B.G., Roy, C.J., Ulrich, R.G., Harvey, N.G.. Protective immunization against inhalational anthrax: a comparison of minimally invasive delivery platforms. J Infect Dis. 2005; 191, 278–288. https://doi.org/10.1086/426865.
- Morimoto K, Miyazaki M, Kakemi M. Effects of proteolytic enzyme inhibitors on nasal absorption of salmon calcitonin in rats. International journal of pharmaceutics, 1995; 113(1), 1-8.
- Muntimadugu E, Dhommati R, Jain A, Challa VG, Shaheen M, Khan W. Intranasal delivery of nanoparticle encapsulated tarenflurbil: a potential brain targeting strategy for Alzheimer's disease, Eur J Pharm Sci. 2016;92:224-34. doi: 10.1016/j.ejps.2016.05.012.
- Mygind N, Dahl, R. Anatomy, physiology and function of the nasal cavities in health and disease. Adv Drug Deliv Rev. 1998;29(1-2):3-12.
- Myriad Genetics Reports Results of U.S., Phase 3 Trial of FlurizanTMin Alzheimer's Disease, (2008). http://investor.myriad.com/news-releases/news-release-details/myriad-genetics-reports-results-us-phase-3-trial-flurizantm.
- Nagda CD, Chotai NP, Nagda DC, Patel SB, Patel UL. Development and characterization of mucoadhesive microspheres for nasal delivery of ketorolac. Pharmazie. 2011 Apr;66(4):249-57.
- Nema T, Jain A, Jain A, Shilpi S, Gulbake A, Hurkat P, Jain SK. Insulin delivery through nasal route using thiolated microspheres. Drug Deliv. 2013;20(5):210-5. doi: 10.3109/10717544.2012.746401.
- Oliveira P, Fortuna A, Alves G, Falcao A. Drug-metabolizing Enzymes and Efflux Transporters in Nasal Epithelium: Influence on the Bioavailability of Intranasally Administered Drugs. Curr Drug Metab. 2016;17(7):628-47.

- Ozsoy Y, Gungor S, Cevher, E. Nasal delivery of high molecular weight drugs. Molecules, 2009; 14(9), 3754-3779.
- Pardeshi CV, Belgamwar VS. Direct nose to brain drug delivery via integrated nerve pathways bypassing the blood–brain barrier: an excellent platform for brain targeting. Expert Opin Drug Deliv. 2013;10(7):957-72. doi:10.1517/17425247.2013.790887
- Pardeshi CV, Rajput PV, Belgamwar VS, Tekade AR. Formulation, optimization and evaluation of spray-dried mucoadhesive microspheres as intranasal carriers for valsartan. J. Microencapsul. 2012; 29, 103–114. https://doi.org/10.3109/02652048.2011.630106.
- Pardridge, WM. Drug transport across the blood–brain barrier. J Cereb Blood Flow Metab. 2012; 32(11): 1959–1972.
- Parepally JM, Mandula H, Smith QR. Brain uptake of nonsteroidal anti-inflammatory drugs: ibuprofen, flurbiprofen, and indomethacin. Pharm Res. 2006;23(5):873-81.
- Parlati C, Colombo P, Buttini F, Young PM, Adi H, Ammit AJ, Traini D. Pulmonary spray dried powders of tobramycin containing sodium stearate to improve aerosolization efficiency. Pharm Res. 2009;26(5):1084-92. doi: 10.1007/s11095-009-9825-2.
- Patel BB, Patel JK, Chakraborty S, Shukla D. Revealing facts behind spray dried solid dispersion technology used for solubility enhancement. Saudi Pharm J. 2015;23(4):352-65. doi: 10.1016/j.jsps.2013.12.013.
- Patel JK, Chavda JR. Formulation and evaluation of stomach-specific amoxicillin-loaded carbopol-934P mucoadhesive microspheres for anti-Helicobacter pylori therapy. Journal of Microencapsulation, 2009; 26(4), 365-376.
- PATENT: US9339456B2 Inhalation-type pharmaceutical composition for the treatment of arthritis and preparation method thereof
- Patil S, Babbar A, Mathur R, Mishra A, Sawant K. Mucoadhesive chitosan microspheres of carvedilol for nasal administration. J. Drug Target. 2010; 18, 321–331. https: //doi.org/10.3109/10611861003663523.
- Paudel A, Worku ZA, Meeus J. et al. Manufacturing of solid dispersions of poorly water soluble drugs by spray drying: formulation and process considerations. Int. J. Pharm. 2013, 453, 253-284.

- Pereswetoff-Morath L, Edman P. Dextran microspheres as a potential nasal drug delivery system for insulin-in vitro and in vivo properties. Int J Pharm, 1995;124(1), 37-44.
- Pilcer G, Amighi K. Formulation strategy and use of excipients in pulmonary drug delivery. Int. J. Pharm. 2010;392,1–19. https://doi.org/10.1016/j.ijpharm.2010.03.017.
- Picone P, Sabatino MA, Ditta LA, Amato A, San Biagio PL, Mulè F, Giacomazza D, Dispenza C, Di Carlo M. Nose-to-brain delivery of insulin enhanced by a nanogel carrier. J Control Release. 2018;270:23-36. doi: 10.1016/j.jconrel.2017.11.040.
- Pignatello R, Pantò V, Salmaso S, Bersani S, Pistarà V, Kepe V, Barrio JR, Puglisi G. Flurbiprofen derivatives in Alzheimer's disease: Synthesis, pharmacokinetic and biological assessment of lipoamino acid prodrugs. Bioconjug Chem. 2008;19(1):349-57.
- Pimplikar SW. Neuroinflammation in Alzheimer's disease: from pathogenesis to a therapeutic target. J Clin Immunol. 2014;34 Suppl 1:S64-9. doi: 10.1007/s10875-014-0032-5.
- Pires A, Fortuna A, Alves G, Falcão A.Intranasal drug delivery: how, why and what for?. J Pharm Pharm Sci. 2009;12(3):288-311.
- Pires PC, Santos AO. Nanosystems in nose-to-brain drug delivery: A review of non-clinical brain targeting studies. J Control Release. 2018;270:89-100. doi: 10.1016/j.jconrel.2017.11.047.
- Porsteinsson AP, Grossberg GT, Mintzer J, Olin JT. Memantine MEM-MD-12 Study Group. Memantine treatment in patients with mild to moderate Alzheimer's disease already receiving a cholinesterase inhibitor: a randomized, double-blind, placebo-controlled trial. Curr Alzheimer Res. 2008;5(1):83–89.
- Pozzoli M, Traini D, Young PM, Sukkar MB, Sonvico F. Development of a Soluplus budesonide freeze-dried powder for nasal drug delivery. Drug Dev. Ind. Pharm. 2017;1–9. http://dx.doi.org/10.1080/03639045.2017.1321659.
- Pringels E, Callens C, Vervaet C, Dumont F, Slegers G, Foreman P, Remon JP. Influence of deposition and spray pattern of nasal powders on insulin bioavailability. Int. J. Pharm. 2006; 310, 1–7. https://doi.org/10.1016/j.ijpharm.2005.10.049.
- Pringels E, Vervaet C, Verbeeck R, Foreman P, Remon JP. The addition of calcium ions to starch/Carbopol® mixtures enhances the nasal bioavailability of insulin. Eur.

J. Pharm. Biopharm. 2008; 68, 201–206. https://doi.org/10.1016/j.ejpb.2007.05.008.

- Raffin RP, Colombo P, Sonvico F, Polleto FS, Colombo G, Rossi A, Pohlmann AR, Guterres SS. Soft agglomerates of pantoprazole gastro-resistant microparticles for oral administration and intestinal release. J. Drug Del. Sci. Tech. 2017; 17, 407–413.
- Rapoport SI. Osmotic opening of the blood–brain barrier: principles, mechanism, and therapeutic applications. Cell Mol Neurobiol. 2000 Apr;20(2):217-30.
- Rassu G, Soddu E, Cossu M, Brundu A, Cerri G, Marchetti N, Ferraro L, Regan RF, Giunchedi P, Gavini E, Dalpiaz A. Solid microparticles based on chitosan or methyl--cyclodextrin: a Vrst formulative approach to increase the nose-to-brain transport of deferoxamine mesylate. J. Control. Release 2015;201, 68–77. https://doi.org/10.1016/j.jconrel.2015.01.025.
- Reger MA, Watson GS, Frey WH, et al. Effects of intranasal insulin on cognition in memory-impaired older adults: modulation by APOE genotype. Neurobiol Aging. 2006;27(3):451-458.
- Reger MA, Watson GS, Green PS, Wilkinson CW, Baker LD, Cholerton B, Fishel MA, Plymate SR, Breitner JC, DeGroodt W, Mehta P, Craft S. Intranasal insulin improves cognition and modulates beta-amyloid in early AD. Neurology. 2008; 70(6):440-448.
- Reno FE, Edwards CN, Bendix Jensen M, Török-Bathó M, Esdaile DJ, Piché C, Triest M, Carballo D. Needle-free nasal delivery of glucagon for treatment of diabetes-related severe hypoglycemia: toxicology of polypropylene resin used in de-livery device. Cutan. Ocul. Toxicol. 2016; 35, 242–247. https://doi.org/10.3109/15569527.2015.1089884.
- Rich S, Leverenz JB, Ramaswamy S, Hampel H. An analytical framework for projecting the cognitive effect of combination therapy with intepirdine (rvt-101) and donepezil versus placebo after 24 weeks in mild-moderate Alzheimer’s disease. Alzheimer's & Dementia: The Journal of the Alzheimer's Association, 2017; 13(7), P1262.
- Rubino JT. Solubilities and solid state properties of the sodium salts of drugs. J Pharm Sci. 1989 Jun;78(6):485-9.

- Rubio-Perez JM, Morillas-Ruiz JM. A review: inflammatory process in Alzheimer's disease, role of cytokines. ScientificWorldJournal. 2012;2012:756357. doi: 10.1100/2012/756357.
- Russo P, Buttini F, Sonvico F, Bettini R, Massimo G, Sacchetti C, Colombo P, Santi P. Chimeral agglomerates of microparticles for the administration of caffeine nasal powders. J. Drug Deliv. Sci. Technol. 2004; 14, 449–454. https://doi.org/10.1016/S1773-2247(04)50083-7.
- Russo P, Sacchetti C, Pasquali I, Bettini R, Massimo G, Colombo P, Rossi A. Primary microparticles and agglomerates of morphine for nasal insufWation. J. Pharm. Sci. 2006; 95, 2553–2561. https://doi.org/10.1002/jps.20604.
- Sacchetti C, Artusi M, Santi P, Colombo P. Caffeine microparticles for nasal administration obtained by spray drying. Int. J. Pharm. 2002; 242, 335–339. https://doi.org/ 10.1016/S0378-5173(02)00177-1.
- Saladini B, Bigucci F, Cerchiara T, Gallucci MC, Luppi B. Microparticles based on chitosan/pectin polyelectrolyte complexes for nasal delivery of tacrine hydrochloride. Drug Deliv. Transl. Res. 2013; 3, 33–41. https://doi.org/10.1007/s13346-012-0086-y.
- Sanabria-Castro A, Alvarado-Echeverría I, Monge-Bonilla C. Molecular pathogenesis of Alzheimer's disease: an update. Ann Neurosci. 2017;24(1):46-54. doi: 10.1159/000464422.
- Sansone F, Picerno P, Mencherini T, Russo P, Gasparri F, Giannini V, Lauro MR, Puglisi g, Aquino R. Enhanced technological and permeation properties of a microencapsulated soy isoflavones extract. J Food Eng., 2013, 115.3: 298-305.
- Santhalakshmy S, Bosco SJD, Francis S, Sabeena M. Effect of inlet temperature on physicochemical properties of spray-dried jamun fruit juice powder. Powder Technology, 2015; 274: 37-43.
- Sanz-Blasco S, Calvo-Rodriguez M, Caballero E, Garcia-Durillo M, Nunez L, Villalobos C. Is it All Said for NSAIDs in Alzheimer's Disease? Role of Mitochondrial Calcium Uptake. Curr Alzheimer Res. 2018;15(6):504-510. doi: 10.2174/1567205015666171227154016.
- Sarkar MA. Drug metabolism in the nasal mucosa. Pharm res. 1992; 9(1), 1-9.
- Scheibe M, Bethge C, Witt M, Hummel T. Intranasal administration of drugs. Archives of Otolaryngology–Head & Neck Surgery, 2008;134(6), 643-646.

- Schipper NG, Romeijn SG, Verhoef JC, Merkus FW. Nasal insulin delivery with dimethyl-beta-cyclodextrin as an absorption enhancer in rabbits: powder more effective than liquid formulations. Pharm Res.10(5):682-6.
- Schmid V, Kullmann S, Gfrörer W, Hund V, Hallschmid M, Lipp HP, Häring HU, Preissl H, Fritsche A, Heni M. Safety of intranasal human insulin: A review. Diabetes Obes Metab. 2018;20(7):1563-1577. doi: 10.1111/dom.13279.
- Schneider LS, Insel PS, Weiner MW; Alzheimer's Disease Neuroimaging I. Treatment with cholinesterase inhibitors and memantine of patients in the Alzheimer's Disease Neuroimaging Initiative. Arch Neurol. 2011;68(1):58–66.
- Sefton MV, Antonacci GM. Adsorption isotherms of insulin onto various materials. Diabetes. 1984;33(7), 674-680.
- Sironi D, Rosenberg J, Bauer-Brandl A, Brandl M. Dynamic dissolution-/permeation-testing of nano- and microparticle formulations of fenofibrate. Eur J Pharm Sci. 2017;96:20-27. doi: 10.1016/j.ejps.2016.09.001.
- Sironi D, Rosenberg J, Bauer-Brandl A, Brandl M. PermeaLoop™, a novel in vitro tool for small-scale drug-dissolution/permeation studies. J Pharm Biomed Anal. 2018 Jul 15;156:247-251. doi: 10.1016/j.jpba.2018.04.042.
- Smart JD. The basics and underlying mechanisms of mucoadhesion. Adv Drug Deliv Rev. 2005;57(11):1556-68.
- Solano DC, Sironi M, Bonfini C, Solerte SB, Govoni S, Racchi M. Insulin regulates soluble amyloid precursor protein release via phosphatidyl inositol 3 kinase-dependent pathway. FASEB J. 2002.14, 1015–1022
- Sosnik A, Seremeta KP. Advantages and challenges of the spray-drying technology for the production of pure drug particles and drug-loaded polymeric carriers. Adv. Colloid Interf. Sci. 2015; 223, 40–54. https://doi.org/10.1016/j.cis.2015.05.003.
- Sonvico F, Clementino A, Buttini F, Colombo G, Pescina S, Stanisçuaski Guterres S, Raffin Pohlmann A, Nicoli S. Surface-modified nanocarriers for nose-to-brain delivery: from bioadhesion to targeting. Pharmaceutics. 2018 Mar 15;10(1). pii: E34. doi: 10.3390/pharmaceutics10010034.
- Sood S, Jain K, Gowthamarajan K. Intranasal therapeutic strategies for management of Alzheimer's disease. J Drug Target. 2014;22(4):279-94. doi: 10.3109/1061186X.2013.876644.

- Stein MS, Scherer SC, Ladd KS, Harrison LCA. Randomized controlled trial of high-dose vitamin D2 followed by intranasal insulin in Alzheimer's disease. J Alzheimers Dis. 2011;26(3):477-484.
- Steiner DF, Peterson H, Tager S et al. Comparative Aspects of Proinsulin and Insulin Structure and Biosynthesis. Integr. Comp. Biol. 1973; 13: 591-604.
- Suryawanshi SR, Thakare NP, More DP, Thombre NA. Bioavailability enhancement of ondansetron after nasal administration of Caesalpinia pulcherrima-based microspheres. Drug Deliv. 2015; 22, 894–902. https://doi.org/10.3109/10717544. 2013.860205.
- Tariot PN, Farlow MR, Grossberg GT, et al. Memantine treatment in patients with moderate to severe Alzheimer disease already receiving donepezil: a randomized controlled trial. JAMA. 2004;291(3): 317–324.
- Tepper D. Breath-Powered Intranasal Sumatriptan Dry Powder. Headache. 2016;56(4):817-8. doi: 10.1111/head.12814.
- Tepper SJ, Johnstone MR. Breath-powered sumatriptan dry nasal powder: an intranasal medication delivery system for acute treatment of migraine. Medical Devices (Auckland, NZ), 2018;11, 147.
- Testa B, van de Waterbeemd H, Folkers G, Guy R. Pharmacokinetic Optimization in Drug Research: Biological, Physicochemical, and Computational Strategies. 2007. ISBN:9783906390222. Publisher: Verlag Helvetica Chimica Acta, CH- Zürich.
- Tian W, Hu Q, Xu Y, Xu Y. Effect of soybean-lecithin as an enhancer of buccal mucosa absorption of insulin. Biomed Mater Eng. 2012;22(1-3):171-8. doi: 10.3233/BME-2012-0704.
- Tiozzo Fasiolo L, Manniello MD, Tratta E, Buttini F, Rossi A, Sonvico F, Bortolotti F, Russo P, Colombo G. Opportunity and challenges of nasal powders: Drug formulation and delivery. Eur J Pharm Sci. 2018, 113:2-17. doi: 10.1016/j.ejps.2017.09.027.
- Tsapis N, Bennett D, Jackson B. et al. Trojan particles: large porous carriers of nanoparticles for drug delivery. Proc Natl Acad Sci U S A. 2002, 99(19):12001-5.
- Tsuneji N, Yuji N, Naoki N, Yoshiki S, Kunio S. Powder dosage form of in- sulin for nasal administration. J. Control. Release 1984;1,15–22. https://doi.org/10.1016/0168-3659(84)90017-8.

- Ugwoke MI, Agu RU, Verbeke N, Kinget R. Nasal mucoadhesive drug delivery: background, applications, trends and future perspectives. Advanced drug delivery reviews, 2005; 57(11), 1640-1665.
- Ugwoke MI, Verbeke N, Kinget R. The biopharmaceutical aspects of nasal mucoadhesive drug delivery. J Pharm Pharmacol. 2001;53(1):3-21.
- Varshosaz J, Sadrai H, Alinagari R. Nasal delivery of insulin using chitosan microspheres. J. Microencapsul. 2004; 21, 761–774. https://doi.org/10.1080/02652040400015403.
- Vasa DM, Buckner IS, Cavanaugh JE, Wildfong PLD. Improved flux of levodopa via direct deposition of solid microparticles on nasal tissue. AAPS PharmSciTech 2017:18, 904–912. http://dx.doi.org/10.1208/s12249-016-0581-4.
- Vasa DM, O'Donnell LA, Wildfong PLD, O'Donnell LA, Wildfong PLD. Influence of dosage form, formulation, and delivery device on olfactory deposition and clearance: enhancement of nose-to-CNS uptake. J. Pharm. Innov. 2015;10, 200–210.http://dx.doi.org/10.1007/s12247-015-9222-9.
- Vehring R. Pharmaceutical particle engineering via spray drying. Pharm Res. 2008;25(5):999-1022.
- Vo, C.L.-N., Park, C., Lee, B.-J. Current trends and future perspectives of solid dispersions containing poorly water-soluble drugs. Eur. J. Pharm. Biopharm. 2013; 85, 799–813. https://doi.org/10.1016/j.ejpb.2013.09.007.
- Walters RH, Bhatnagar B, Tchessalov S, Izutsu KI, Tsumoto K, Ohtake S. Next generation drying technologies for pharmaceutical applications. J. Pharm. Sci. 2014; 103, 2673–2695. https://doi.org/10.1002/jps.23998.
- Wang J, Tabata Y, Morimoto K. Aminated gelatin microspheres as a nasal delivery system for peptide drugs: evaluation of in vitrorelease and in vivo insulin absorption in rats. J Control Release. 2006;113(1):31-7.
- Washington N, Steele RJ, Jackson SJ et al. Determination of baseline human nasal pH and the effect of intranasally administered buffers. Int J Pharm. 2000;198(2):139-46.
- Wilcock GK, Black SE, Hendrix SB, Zavitz KH, Swabb EA, Laughlin MA. Tarenflurbil Phase II Study investigators. Efficacy and safety of tarenflurbil in mild to moderate Alzheimer's disease: a randomised phase II trial. Lancet Neurol. 2008 Jun;7(6):483-93. doi: 10.1016/S1474-4422(08)70090-5.

- Willette AA, Bendlin BB, Starks EJ, Birdsill AC, Johnson SC, Christian BT, Okonkwo OC, La Rue A, Hermann BP, Koscik RL, Jonaitis EM, Sager MA, Asthana S. Association of insulin resistance with cerebral glucose uptake in late middle–aged adults at risk for Alzheimer disease. JAMA Neurol. 2015;72(9):1013-20. doi: 10.1001/jamaneurol.2015.0613.
- Wioland MA, Fleury-Feith J, Corlieu P, Commo F, Monceaux G, Lacau-St-Guily J, Bernaudin JF. CFTR, MDR1, and MRP1 immunolocalization in normal human nasal respiratory mucosa. J. Histochem. Cytochem. 2000; 48:1215Y1222.
- Wyss-Coray T, Rogers J. Inflammation in Alzheimer disease-a brief review of the basic science and clinical literature. Cold Spring Harb Perspect Med. 2012;2(1):a006346. doi: 10.1101/cshperspect.a006346.
- Xi J, Kim J, Si XA, Corley RA, Zhou Y. Modeling of inertial deposition in scaled models of rat and human nasal airways: Towards in vitro regional dosimetry in small animals. J Aerosol Sci, 2016;99, 78-93.
- Zbicinski I. Modeling and Scaling Up of Industrial Spray Dryers: A Review. Journal of Chemical Engineering of Japan, 2017; 50(10), 757-767.
- Zeng XM, Martin GP, Marriott C. Particulate Interactions in Dry Powder Formulation for Inhalation. CRC Press. 2003
- Zhang C, Wang Y, Wang D, Zhang J, Zhang F. NSAID Exposure and Risk of Alzheimer's Disease: An Updated Meta-Analysis From Cohort Studies. Front Aging Neurosci. 2018;10:83. doi: 10.3389/fnagi.2018.00083.
- Zhao Y, Brown MB, Khengar RH, Traynor MJ, Barata P, Jones SA. Pharmacokinetic evaluation of intranasally administered vinyl polymer-coated lorazepam microparticles in rabbits. AAPS J. 2012; 14, 218–224. https://doi.org/10.1208/s12248-012-9325-x.
- Zheng D, Shuai X, Li Y, Zhou P, Gong T, Sun X, Zhang Z. Novel flurbiprofen derivatives with improved brain delivery: synthesis, in vitro and in vivo evaluations. Drug Deliv. 2016;23(7):2183-2192.

- https://www.alzdiscovery.org/news-room/announcements/innovative-alzheimers-combination-therapy-trial-supported-by-new-joint-fund
- https://www.alzdiscovery.org/news-room/blog/combination-therapy-the-right-approach-for-alzheimers
- https://clinicaltrials.gov/ct2/show/NCT01767909

- https://pubchem.ncbi.nlm.nih.gov/compound/3394#section=Experimental-Properties
- http://www.namzaric.com
- https://www.nature.com/articles/nm.4426